

AD/A-000 285

A SURFACE FORMULATION FOR CHARACTERISTIC  
MODES OF MATERIAL BODIES

Yu Chang, et al

Syracuse University

Prepared for:

Office of Naval Research

October 1974

DISTRIBUTED BY:

**NTIS**

National Technical Information Service  
U. S. DEPARTMENT OF COMMERCE

UNCLASSIFIED

SECURITY CLASSIFICATION OF THIS PAGE (When Data Entered)

REPORT DOCUMENTATION PAGE		READ INSTRUCTIONS BEFORE COMPLETING FORM
1. REPORT NUMBER TR-74-7	2. GOVT ACCESSION NO.	3. RECIPIENT'S CATALOG NUMBER <b>AD/A-000 285</b>
4. TITLE (and Subtitle) A SURFACE FORMULATION FOR CHARACTERISTIC MODES OF MATERIAL BODIES	5. TYPE OF REPORT & PERIOD COVERED Technical Report No. 2	
	6. PERFORMING ORG. REPORT NUMBER	
7. AUTHOR(s) Yu Chang Roger F. Harrington	8. CONTRACT OR GRANT NUMBER(s) N00014-67-A-0378-0006	
9. PERFORMING ORGANIZATION NAME AND ADDRESS Dept. of Electrical and Computer Engineering Syracuse University Syracuse, New York 13210	10. PROGRAM ELEMENT, PROJECT, TASK AREA & WORK UNIT NUMBERS NR-371-885	
11. CONTROLLING OFFICE NAME AND ADDRESS Department of the Navy Office of Naval Research Arlington, Virginia 22217	12. REPORT DATE October 1974	
	13. NUMBER OF PAGES	
14. MONITORING AGENCY NAME & ADDRESS (if different from Controlling Office)	15. SECURITY CLASS. (of this report) Unclassified	
	15a. DECLASSIFICATION/DOWNGRADING SCHEDULE	
16. DISTRIBUTION STATEMENT (of this Report) Approved for public release; distribution unlimited.		
17. DISTRIBUTION STATEMENT (of the abstract entered in Block 20, if different from Report)		
18. SUPPLEMENTARY NOTES Reproduced by NATIONAL TECHNICAL INFORMATION SERVICE U S Department of Commerce Springfield VA 22151		
19. KEY WORDS (Continue on reverse side if necessary and identify by block number) Characteristic Modes Computer Programs Electromagnetic Scattering Material Bodies Two-dimensional Fields		
20. ABSTRACT (Continue on reverse side if necessary and identify by block number) A theory of characteristic modes for material bodies is developed using equivalent surface currents. This is in contrast to the alternative approach using induced volume currents. The mode currents form a weighted orthogonal set over the material body surface, and the mode fields form an orthogonal set over the sphere at infinity. The characteristic modes of material bodies		

DD FORM 1473  
1 JAN 73EDITION OF 1 NOV 68 IS OBSOLETE  
S/N 0102-014-6601

UNCLASSIFIED

SECURITY CLASSIFICATION OF THIS PAGE (When Data Entered)

UNCLASSIFIED

SECURITY CLASSIFICATION OF THIS PAGE(When Data Entered)

have most of the properties of those for perfectly conducting bodies. Formulas for the use of these modes in electromagnetic scattering problems are given. A procedure for computing the characteristic modes is developed, and applied to two-dimensional bodies. Illustrative examples of the computation of characteristic currents and scattering cross sections are given for cylinders of different material constants.

UNCLASSIFIED

SECURITY CLASSIFICATION OF THIS PAGE(When Data Entered)

## ABSTRACT

A theory of characteristic modes for material bodies is developed using equivalent surface currents. This is in contrast to the alternative approach using induced volume currents. The mode currents form a weighted orthogonal set over the material body surface, and the mode fields form an orthogonal set over the sphere at infinity. The characteristic modes of material bodies have most of the properties of those for perfectly conducting bodies. Formulas for the use of these modes in electromagnetic scattering problems are given. A procedure for computing the characteristic modes is developed, and applied to two-dimensional bodies. Illustrative examples of the computation of characteristic currents and scattering cross sections are given for cylinders of different material constants.

## CONTENTS

	Page
ABSTRACT-----	iii
CHAPTER 1 INTRODUCTION-----	1
1.1 Background-----	1
1.2 The Fundamental Operator Equation-----	2
1.3 Format-----	7
CHAPTER 2 MATRIX FORMULATION-----	9
2.1 Method of Moments-----	9
2.2 Expansion Functions and the Evaluation of [Z] Matrix Elements-----	13
2.3 Evaluations of [B] and [C] Matrix Elements-----	24
2.4 Evaluation of [Y] Matrix Elements-----	31
2.5 Excitation Matrix, Measurement Matrix, and Scattering Cross Sections-----	34
CHAPTER 3 CHARACTERISTIC MODES - A SURFACE FORMULATION-----	42
3.1 Theoretical Development-----	42
3.2 Characteristic Equation and Modal Representation-----	46
3.3 Linear Measurement-----	49
3.4 Characteristic Fields and Scattering Cross Sections-----	50
3.5 Computational Considerations-----	53
CHAPTER 4 COMPUTATIONAL RESULTS-----	60
CHAPTER 5 DISCUSSION-----	103
APPENDIX A MATRIX ELEMENTS FOR PARALLEL POLARIZATION-----	106
APPENDIX B COMPUTER PROGRAMS-----	108
REFERENCES-----	118

CHAPTER 1  
INTRODUCTION

1.1 Background

Characteristic modes have long been used in the analysis of radiation and scattering by dielectric and/or magnetic bodies whose surfaces coincide with coordinate surfaces in coordinate systems for which the Helmholtz equation is separable. From consideration of the scattering matrix, Garbacz [1] has shown that similar modes must exist for any material body. An extensive theory for perfectly conducting bodies was given in reference [1], but the dielectric and magnetic body case was not developed. An alternative treatment of the characteristic modes for perfectly conducting bodies, starting from the impedance operator for the conducting surface, has been given by Harrington and Mautz [2]. The computation of such modes has also been considered by Harrington and Mautz [3]. A theory of characteristic modes for dielectric bodies, magnetic bodies, and for bodies both dielectric and magnetic, has been developed by Harrington, Mautz, and Chang [4]. In this work, a theory of characteristic modes for material bodies is developed using equivalent surface currents. This is in contrast to the approach used in [4], which used the induced volume currents.

The modes are defined by a weighted eigenvalue equation in such a way that both the generalized network matrix [5] and the scattering matrix [1], [2] for the body are diagonalized. The presentation given in this work leads to explicit formulas for determining the mode currents and fields of two-dimensional objects. The formulas remain the same for dielectric bodies, magnetic bodies, and

for bodies both dielectric and magnetic. In particular, the scattering problem of a two dimensional material cylinder will be presented. This formulation of the problem is applicable to any general material body. Details are worked out only for two-dimensional problems.

### 1-2 The Fundamental Operator Equation

Let the material body be represented as in Figure 1-1.

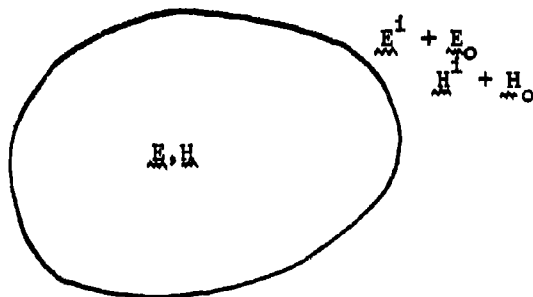


Figure 1-1. A general material body.

$\underline{H}^i, \underline{E}^i$  = incident fields (Wavy underline denotes vector quantities.)  
 $\underline{E}, \underline{H}$  = inside fields  
 $\underline{E}_0, \underline{H}_0$  = outside fields

The problem of Figure 1-1 can be viewed as a linear superposition of two cases,

- (I) zero field inside
- (II) zero field outside.

These two cases are illustrated in Figure 1-2.

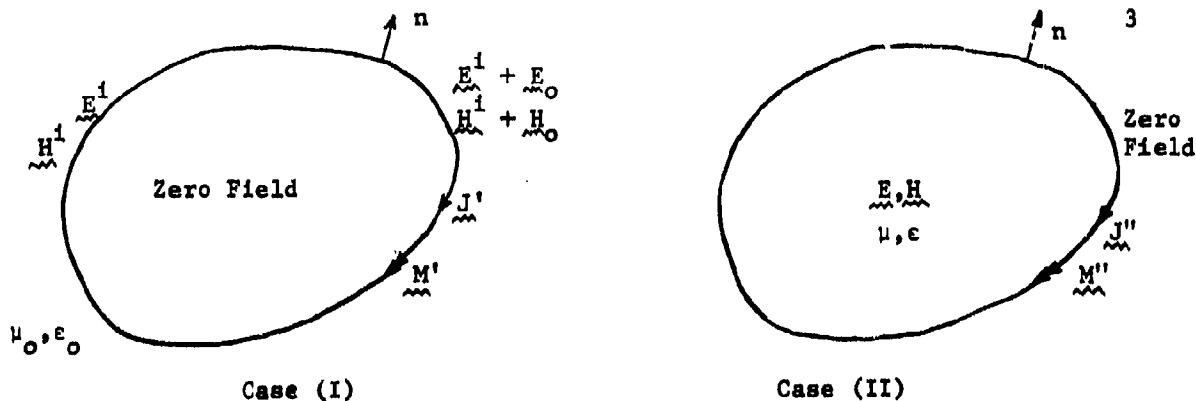


Figure 1-2. A decomposition of the original problem.

In case (I), let  $\mu_0, \epsilon_0$  be the material constants in the zero-field region, and similarly in case (II), let  $\mu, \epsilon$  be the material constants in the zero-field region. Having done so, radiation formulas [6] for unbounded space can be employed. The  $\underline{J}$  and  $\underline{M}$  are equivalent surface currents [6]. Since there are no actual surface currents, the following conditions should be satisfied by the equivalent currents

$$\underline{J}' + \underline{J}'' = 0 \quad (1-1)$$

$$\underline{M}' + \underline{M}'' = 0 \quad (1-2)$$

Equations (1-1) and (1-2) come from the fact that tangential components of fields are continuous across the interface in the original problem. Note that

$$\underline{E}_0 = -j\omega \underline{A}' - \nabla \phi_e' - \frac{1}{\epsilon_0} \nabla \times \underline{F}' + \underline{E}^i \quad (1-3)$$

$$\underline{H}_0 = -j\omega \underline{F}' - \nabla \phi_m' + \frac{1}{\mu_0} \nabla \times \underline{A}' + \underline{H}^i \quad (1-4)$$

and



$$\underline{E} = -j\omega \underline{A}'' - \nabla \phi_e'' - \frac{1}{\epsilon} \nabla \times \underline{F}'' \quad (1-5)$$

$$\underline{H} = -j\omega \underline{F}'' - \nabla \phi_m'' + \frac{1}{\mu} \nabla \times \underline{A}'' \quad (1-6)$$

and

$$\underline{E}^S = -j\omega \underline{A}' - \nabla \phi_e' - \frac{1}{\epsilon_0} \nabla \times \underline{F}' \quad (1-7)$$

$$\underline{H}^S = -j\omega \underline{F}' - \nabla \phi_m' + \frac{1}{\mu_0} \nabla \times \underline{A}' \quad (1-8)$$

where  $\underline{E}^S$  and  $\underline{H}^S$  are scattered fields, and

$\underline{A}$  = vector potential due to electric current

$\underline{F}$  = vector potential due to magnetic current

$\phi_e$  = scalar potential due to electric charge

$\phi_m$  = scalar potential due to magnetic charge

Primed quantities refer to case (I)

doubly primed quantities refer to case (II)

In terms of general operator notations, the following equations are obtained

$$\begin{bmatrix} L'_{11} & L'_{12} \\ L'_{21} & L'_{22} \end{bmatrix} \begin{bmatrix} \underline{J}' \\ \underline{M}' \end{bmatrix} = \begin{bmatrix} \underline{E}^S \\ \underline{H}^S \end{bmatrix} \quad (1-9)$$

$$\begin{bmatrix} L''_{11} & L''_{12} \\ L''_{21} & L''_{22} \end{bmatrix} \begin{bmatrix} \underline{J}'' \\ \underline{M}'' \end{bmatrix} = \begin{bmatrix} \underline{E} \\ \underline{H} \end{bmatrix} \quad (1-10)$$

where the definitions of the operators are obvious when comparing equations (1-9) and (1-10) with (1-5) to (1-8). Note that the tangential fields are continuous at the boundary surface, i.e.

$$\underline{n} \times (\underline{E}^S + \underline{E}^I - \underline{E}) = 0 \quad (1-11)$$

$$\underline{n} \times (\underline{H}^S + \underline{H}^I - \underline{H}) = 0 \quad (1-12)$$

where  $\underline{n}$  = unit normal pointing outward, or

$$-\underline{n} \times \underline{E}^S + \underline{n} \times \underline{E} = \underline{n} \times \underline{E}^I \quad (1-13)$$

$$-\underline{n} \times \underline{H}^S + \underline{n} \times \underline{H} = \underline{n} \times \underline{H}^I \quad (1-14)$$

The following equations are obtained by substituting equations (1-9) and (1-10) into (1-13) and (1-14).

$$-\underline{n} \times L_{11}^I(J') - \underline{n} \times L_{12}^I(M') + \underline{n} \times L_{11}^{II}(J'') + \underline{n} \times L_{12}^{II}(M'') = \underline{n} \times \underline{E}^I \quad (1-15)$$

$$-\underline{n} \times L_{21}^I(J') - \underline{n} \times L_{22}^I(M') + \underline{n} \times L_{21}^{II}(J'') + \underline{n} \times L_{22}^{II}(M'') = \underline{n} \times \underline{H}^I \quad (1-16)$$

By equations (1-1) and (1-2), it follows that

$$-\underline{n} \times [(L_{11}^I + L_{11}^{II})J'] - \underline{n} \times [(L_{12}^I + L_{12}^{II})M'] = \underline{n} \times \underline{E}^I \quad (1-17)$$

$$-\underline{n} \times [(L_{21}^I + L_{21}^{II})J'] - \underline{n} \times [(L_{22}^I + L_{22}^{II})M'] = \underline{n} \times \underline{H}^I \quad (1-18)$$

Define all the operators to be tangential operators; the above two equations can be put into standard matrix form as:

$$\begin{bmatrix} -(L'_{11} + L''_{11}) & -(L'_{12} + L''_{12}) \\ -(L'_{21} + L''_{21}) & -(L'_{22} + L''_{22}) \end{bmatrix} \begin{bmatrix} \underline{J'} \\ \underline{M'} \end{bmatrix}_{\tan} = \begin{bmatrix} \underline{E^1} \\ \underline{H^1} \end{bmatrix}_{\tan} \quad (1-19)$$

The  $[ ]_{\tan}$  means the tangential components of the bracketed quantity on the boundary surface. Let

$$L_e' = -L'_{11}, \quad L_e'' = -L''_{11}, \quad L_m' = -L'_{22}, \quad L_m'' = -L''_{22}$$

and define

$$-C'(\underline{M'}) = -\frac{1}{\epsilon_0} \nabla \times \underline{F'} = L'_{12}(\underline{M'})$$

$$-C''(\underline{M'}) = -\frac{1}{\epsilon} \nabla \times \underline{F''} = L''_{12}(\underline{M'})$$

$$C'(\underline{J'}) = \frac{1}{\mu_0} \nabla \times \underline{A'} = L'_{21}(\underline{J'})$$

$$C''(\underline{J'}) = \frac{1}{\mu} \nabla \times \underline{A''} = L''_{21}(\underline{J'})$$

Hence equation (1-19) becomes

$$\begin{bmatrix} L_e' + L_e'' & C' + C'' \\ -(C' + C'') & L_m' + L_m'' \end{bmatrix} \begin{bmatrix} \underline{J'} \\ \underline{M'} \end{bmatrix}_{\tan} = \begin{bmatrix} \underline{E^1} \\ \underline{H^1} \end{bmatrix}_{\tan} \quad (1-20)$$

It is convenient to rearrange equation (1-20) into the form

$$\begin{bmatrix} L_e & -jC \\ -jC & L_m \end{bmatrix} \begin{bmatrix} \underline{J} \\ \underline{jM} \end{bmatrix} = \begin{bmatrix} \underline{E}^i \\ \underline{jH}^i \end{bmatrix} \quad (1-21)$$

where

$$\begin{aligned} L_e &= L_e' + L_e'' & \underline{J} &= \underline{J}' \\ L_m &= L_m' + L_m'' & \underline{M} &= \underline{M}' \\ C &= C' + C'' \end{aligned}$$

and the subscript "tan" has been dropped for brevity. Equation (1-21) is simply the familiar operator equation expressed below.

$$\underline{L}(\underline{f}) = \underline{g} \quad (1-22)$$

$\underline{L}$  is a tangential operator on the surface of the material body, and

$$\underline{L} = \begin{bmatrix} L_e & -jC \\ -jC & L_m \end{bmatrix} ; \quad \underline{f} = \begin{bmatrix} \underline{J} \\ \underline{jM} \end{bmatrix} ; \quad \underline{g} = \begin{bmatrix} -\underline{E}^i \\ \underline{jH}^i \end{bmatrix}$$

### 1-3 Format

In this work the impressed magnetic field is assumed to be axially-directed (perpendicular polarization). The derivation of all the formulas for an impressed axially-directed electric field (parallel polarization) will not be given in the main body of this work, in order to conserve space, however, explicit formulas will be provided in Appendix A. A list of computer programs will be given in Appendix B.

The content of this work is as follows. In Chapter 2, the operator equation is reduced to a matrix equation suitable for numerical computation.

The reduction is accomplished by using the method of moments for perpendicular polarization. The equivalent surface currents can be obtained by matrix inversion. A concise theory of characteristic modes for material bodies, based on the surface formulation, and explicit formulas for obtaining the modal solutions are given in Chapter 3. Chapter 4 is a presentation of calculations made for cylinders of different material constants using both the matrix inversion method and the modal method. Chapter 5 is a discussion of the results. The computations presented in this work were performed on an IBM System 370, Model 155 digital computer. The computer programs are written in FORTRAN IV.

CHAPTER 2  
MATRIX FORMULATION

The determination of equivalent surface currents requires the solution of the following inhomogeneous equation

$$\underline{L}(\underline{f}) = \underline{g} \quad (2-1)$$

where  $L$  is the matrix of operators

$$L = \begin{bmatrix} L_e & -jC \\ -jC & L_m \end{bmatrix} \quad (2-2)$$

and

$$\underline{f} = \begin{bmatrix} \underline{J} \\ \underline{jM} \end{bmatrix} \quad \underline{g} = \begin{bmatrix} \underline{E}^i \\ \underline{jH}^i \end{bmatrix} \quad (2-3)$$

This chapter presents the reduction of equation (2-1) to matrix form by the method of moments.

### 2.1 Method of Moments

To apply the method of moments, an appropriate inner product for the problem is ( $\sim$  indicates transpose)

$$\begin{aligned} \langle \underline{f}, \underline{g} \rangle &= \iint_S \underline{\tilde{f}} \underline{g} \, ds \\ &= \iint_S (\underline{J} \cdot \underline{E} - \underline{H} \cdot \underline{M}) \, ds \end{aligned} \quad (2-4)$$

A solution by the method of moments is obtained as follows. Define electric expansion and testing functions as

$$\underline{f}_n^e = \begin{bmatrix} J_n \\ \underline{\quad} \\ 0 \end{bmatrix} \quad \underline{W}_n^e = \begin{bmatrix} W_n^e \\ \underline{\quad} \\ 0 \end{bmatrix} \quad (2-5)$$

and magnetic expansion and testing functions as

$$\underline{f}_n^m = \begin{bmatrix} 0 \\ \underline{\quad} \\ M_n \end{bmatrix} \quad \underline{W}_n^m = \begin{bmatrix} 0 \\ \underline{\quad} \\ W_n^m \end{bmatrix} \quad (2-6)$$

The expansion for  $f$  is then of the form

$$f = \sum_n (I_n \underline{f}_n^e + V_n \underline{f}_n^m) \quad (2-7)$$

where the  $I_n$  and  $V_n$  are constants to be determined.

The inner product of each  $\{\underline{W}_m^e\}$  with equation (2-1) yields

$$\langle \underline{W}_m^e, L(\underline{f}_n^e) \rangle = \langle \underline{W}_m^e, g \rangle \quad (2-8)$$

where

$$\begin{aligned} \langle \underline{W}_m^e, L(\underline{f}_n^e) \rangle &= \langle \underline{W}_m^e, \sum_n (I_n L(\underline{f}_n^e) + V_n L(\underline{f}_n^m)) \rangle \\ &= \sum_n I_n \langle \underline{W}_m^e, L(\underline{f}_n^e) \rangle \\ &\quad + \sum_n V_n \langle \underline{W}_m^e, L(\underline{f}_n^m) \rangle \\ &= \sum_n I_n \iint_s \underline{W}_m^e \cdot \underline{L}e(J_n) ds + \sum_n V_n \iint_s \underline{W}_m^e \cdot (-jC)(M_n) ds \quad (2-9) \end{aligned}$$

and

$$\langle \underline{W}_m^e, g \rangle = \iint_s \underline{W}_m^e \cdot \underline{E}^1 ds \quad (2-10)$$

Similarly, the inner product of each  $\{W_m^n\}$  with equation (2-1) yields

$$\langle \underbrace{W_m^n}, \underbrace{L(f_n)} \rangle = \langle \underbrace{W_m^n}, \underbrace{g} \rangle \quad (2-11)$$

and

$$\begin{aligned} \langle \underbrace{W_m^n}, \underbrace{L(f_n)} \rangle &= \sum_n I_n \iint_S \underbrace{W_m^n} \cdot (-jC) \underbrace{(J_n)} ds \\ &+ \sum_n V_n \iint_S \underbrace{W_m^n} \cdot \underbrace{L_m(M_n)} ds \end{aligned} \quad (2-12)$$

$$\langle \underbrace{W_m^n}, \underbrace{g} \rangle = \iint_S \underbrace{W_m^n} \cdot \underbrace{jH^i} ds \quad (2-13)$$

Equation (2-8) and Equation (2-11) can be placed in matrix form

$$\begin{bmatrix} [Z] & [B] \\ [C] & [Y] \end{bmatrix} \begin{bmatrix} [I] \\ [V] \end{bmatrix} = \begin{bmatrix} [V^i] \\ [I^i] \end{bmatrix} \quad (2-14)$$

where

$$Z_{mn} = \iint_S \underbrace{W_m^n} \cdot \underbrace{Le(J_n)} ds \quad (2-15)$$

$$B_{mn} = \iint_S \underbrace{W_m^n} \cdot (-jC) \underbrace{(M_n)} ds \quad (2-16)$$

$$C_{mn} = \iint_S \underbrace{W_m^n} \cdot (-jC) \underbrace{(J_n)} ds \quad (2-17)$$

$$Y_{mn} = \iint_S \underbrace{W_m^n} \cdot \underbrace{L_m(M_n)} ds \quad (2-18)$$



$$V_m^i = \iint_s \underbrace{W_m^e} \cdot \underbrace{E^i} ds \quad (2-19)$$

$$I_m^i = \iint_s \underbrace{W_m^m} \cdot \underbrace{jH^i} ds \quad (2-20)$$

Choose  $\underbrace{J_n} = \underbrace{W_n^e}$ . Note that [Z] is obviously symmetric, already shown by Harrington and Mautz. With the choice  $\underbrace{M_n} = \underbrace{W_n^m}$ , [Y] is the dual of [Z], magnetic instead of electric, so the symmetric nature of [Y] can be easily established. It is known that  $C(\underbrace{M_n})$  gives rise to an electric field and  $C(\underbrace{J_n})$  will produce a magnetic field. Observe that by reciprocity

$$\iint_s (\underbrace{E^a} \cdot \underbrace{J^b} - \underbrace{H^a} \cdot \underbrace{M^b}) = \iint_s (\underbrace{E^b} \cdot \underbrace{J^a} - \underbrace{H^b} \cdot \underbrace{M^a}) ds \quad (2-21)$$

Now, consider

- (i) In situation "a" only electric sources
- (ii) In situation "b" only magnetic sources.

It follows that

$$\iint_s (\underbrace{-H^a} \cdot \underbrace{M^b}) ds = \iint_s (\underbrace{E^b} \cdot \underbrace{J^a}) ds \quad (2-22)$$

Hence

$$B_{mn} = C_{nm} \quad (2-23)$$

Consequently, [C] is the transpose of [B], or

$$[B] = \widetilde{[C]} \quad \text{with} \quad \underbrace{J_n} = \underbrace{W_n^e} \quad (2-24)$$

$$\underbrace{M_n} = \underbrace{W_n^m}$$

To this point the matrix formulation is completely general and has been achieved without reference to specific excitation, expansion functions, and testing functions. Note that every one of the operators  $L_e$ ,  $C$ , and  $L_m$  is composed of two parts as indicated by equation (1-21), and consequently every matrix element in  $[Z]$ ,  $[B]$ ,  $[C]$  and  $[Y]$  has two parts; one is due to the primed operator, and the other is due to the doubly primed operator.

## 2.2 Expansion Functions and the Evaluation of $[Z]$ Matrix Element

In this section, the incident field is the axially directed magnetic field,  $H_z^i$ . Before going into any specific excitation for the scattering problem, some general considerations about the evaluation of different types of matrix elements will be presented as follows.

Note that the original problem, the scattering from material bodies, has been decomposed into two cases, and their associated operators are of the same functional form. For instance, the expression for  $L_e''(J)$  will be identical to  $L_e'(J)$  except for the constitutive constants,  $\mu$  and  $\epsilon$ . For the sake of brevity, only  $L_e'$  will be considered. Once  $L_e'(J)$  is known,  $L_e''(J)$  is obtained by replacing  $\epsilon_0$  and  $\mu_0$  by  $\epsilon$  and  $\mu$ , respectively.

By equation (2-15)

$$Z_{mn} = \int \underbrace{W_m}_{\text{m}} \cdot (\underbrace{j\omega A_n}_{\text{n}} + \underbrace{\nabla\phi_n}_{\text{n}}) d\ell \quad (2-25)$$

where

$\underbrace{A_n}_{\text{n}}$  = magnetic vector potential due to  $\underbrace{J_n}_{\text{n}}$   
 $\underbrace{\phi_n}_{\text{n}}$  = scalar potential due to  $\underbrace{\sigma_n}_{\text{n}}$ , surface charge

Applying the one dimensional divergence theorem to the vector  $\phi_n \underline{W}_m$ , and noting that

$$\nabla \cdot \phi_n \underline{W}_m = \phi_n \nabla \cdot \underline{W}_m + \underline{W}_m \cdot \nabla \phi_n \quad (2-26)$$

the following relationship is obtained

$$\int_c \nabla \phi_n \cdot \underline{W}_m d\ell = - \int_c \phi_n \nabla \cdot \underline{W}_m d\ell \quad (2-27)$$

Define  $\sigma_m$  such that

$$\sigma_m = - \frac{1}{j\omega} \nabla \cdot \underline{W}_m \quad (2-28)$$

Observe that equation (2-28) has the form of the continuity equation if  $\underline{W}_m$  and  $\sigma_m$  are interpreted as current and charge, respectively. An alternative form for the [Z] matrix element can be obtained by substituting equations (2-27) and (2-28) into equation (2-25). The new form is computationally more attractive.

$$Z_{mn} = j\omega \int (\underline{W}_m \cdot \underline{A}_n + \sigma_m \phi_n) d\ell \quad (2-29)$$

Define the two-dimensional Green's function  $G(r, r')$ .

$$G(r, r') = \frac{1}{4j} H_0^{(2)}(k|r - r'|) \quad (2-30)$$

and

$$\underline{A}(r) = \mu \int \underline{J}(r') G(r, r') d\ell' \quad (2-31)$$

$$\phi(r) = \frac{1}{c} \int q(r') G(r, r') d\ell' \quad (2-32)$$

where  $q$  is related to  $\underline{J}$  by the equation of continuity

$$\nabla \cdot \underline{J} = -j\omega q \quad (2-33)$$

After substituting equations (2-31), (2-32), and (2-33) into equation (2-29), the expression for  $Z_{mn}$  becomes

$$\begin{aligned} Z_{mn} &= j\omega \int_C \left\{ \int_C [\underline{W}_m \cdot \mu \underline{J}_n(r') + \frac{\sigma_m}{\epsilon} q_n(r')] G(r, r') dl' \right\} dl \\ &= \int_C \int_C [j\omega \mu \underline{W}_m \cdot \underline{J}_n + \frac{1}{j\omega \epsilon} (\nabla \cdot \underline{W}_m) (\nabla' \cdot \underline{J}_n)] G(r, r') dl' dl \quad (2-34) \end{aligned}$$

Note that the primed symbols refer to source location variation, while the unprimed symbols relate to variation in field point location.

The specific formulation proceeds by dividing the contour  $C$  into  $N$  segments, not necessarily equal in length. There are  $N$  segments and  $N+1$  points,

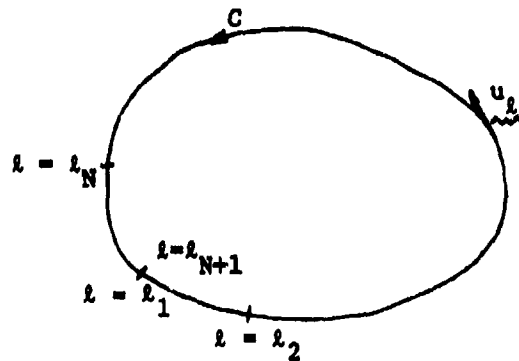


Fig. 2-1. A cross sectional contour.

and  $l$  is the path length proceeding counterclockwise around contour  $C$ .

The sets of expansion and testing functions are chosen as triangle functions for both electric and magnetic surface currents.

$$\underline{w}_k = T(l - l_k) \underline{u}_k \quad k=1,2,\dots,N \quad (2-35)$$

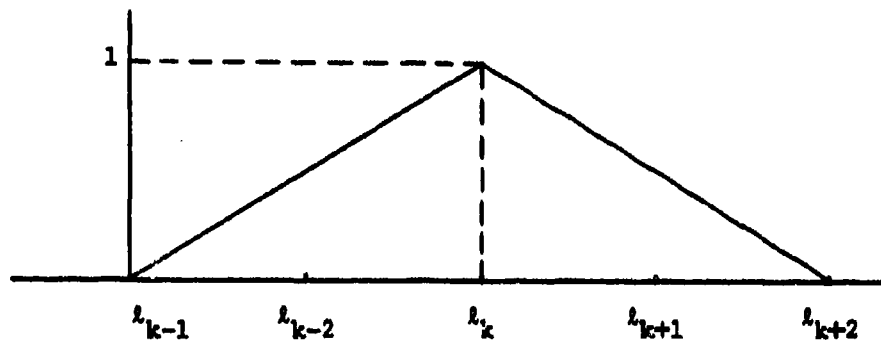


Fig. 2-2. A triangle function.

where  $\underline{u}_k$  is the unit vector tangent to  $C$  path length value  $l$ , and  $T$  is the triangle function defined by

$$T(l - l_k) = \begin{cases} 1 - \frac{l - l_k}{l_{k+2} - l_k} & l_k \leq l \leq l_{k+2} \\ 1 + \frac{l - l_k}{l_k - l_{k-2}} & l_{k-2} \leq l \leq l_k \\ 0 & l \geq l_{k+2} \\ 0 & l_{k-2} \geq l \end{cases} \quad (2-36)$$

or

$$T(l - l_k) = \begin{cases} 1 - \frac{l - l_k}{l_{k+2} - l_k} & 0 \leq l - l_k \leq l_{k+2} - l_k \\ 1 + \frac{l - l_k}{l_k - l_{k-2}} & -(l_k - l_{k-2}) \leq l - l_k \leq 0 \\ 0 & l - l_k \geq l_{k+2} - l_k \\ 0 & -(l_k - l_{k-2}) \geq l - l_k \end{cases} \quad (2-37)$$

Let  $\Delta l_k = l_{k+1} - l_k$  then

$$T(l - l_k) = \begin{cases} 1 - \frac{l - l_k}{\Delta l_k + \Delta l_{k+1}} & \sigma \leq l - l_k \leq \Delta l_k + \Delta l_{k+1} \\ 1 + \frac{l - l_k}{\Delta l_{k-2} + \Delta l_{k-1}} & -(\Delta l_{k-2} + \Delta l_{k-1}) \leq l - l_k \leq 0 \\ 0 & l - l_k \geq \Delta l_k + \Delta l_{k+1} \\ 0 & -(\Delta l_{k-2} + \Delta l_{k-1}) \geq l - l_k \end{cases} \quad (2-38)$$

and

$$\Delta l_0 = \Delta l_N$$

Now,  $Z_{mn}$  can be written as

$$\begin{aligned}
 Z_{mn} &= \iint [j\omega\mu \underline{W}_m \cdot \underline{J}_n + \frac{1}{j\omega\epsilon} (\nabla \cdot \underline{W}_m)(\nabla' \cdot \underline{J}_n)] G \, dl' \, dl \\
 &= \int_{l_{n-2}}^{l_{n+2}} \int_{l_{m-2}}^{l_{m+2}} [j\omega\mu T(l-l_m) T(l'-l_n) (\underline{u}_l \cdot \underline{u}'_l)] \\
 &\quad + \frac{1}{j\omega\epsilon} T'(l'-l_n) T'(l-l_m)] G \, dl' \, dl \tag{2-39}
 \end{aligned}$$

The subscript  $m$  indicates the  $m$ th triangle testing function and the subscript  $n$  indicates the  $n$ th triangle expansion function.  $T'$  is the derivative of the triangle function.

$$T'(l-l_k) = \begin{cases} -\frac{1}{l_{k+2} - l_k} & l_k \leq l \leq l_{k+2} \\ \frac{1}{l_k - l_{k-2}} & l > l_{k+2} \\ 0 & l < l_{k+2} \\ 0 & l_{k-2} \geq l \end{cases} \tag{2-40}$$

or

$$T'(l-l_k) = \begin{cases} \frac{1}{\Delta l_k + \Delta l_{k+1}} & 0 \leq l-l_k \leq \Delta l_k + \Delta l_{k+1} \\ \frac{1}{\Delta l_{k-2} + \Delta l_{k-1}} & -(\Delta l_{k-2} + \Delta l_{k-1}) \leq l-l_k \leq 0 \\ 0 & l-l_k \geq \Delta l_k + \Delta l_{k+1} \\ 0 & -(\Delta l_{k-2} + \Delta l_{k-1}) \geq l-l_k \end{cases} \tag{2-41}$$

The triangle function is approximated by four pulses with amplitudes

$h_{k-2}$ ,  $h_{k-1}$ ,  $h_k$ , and  $h_{k+1}$  as shown below

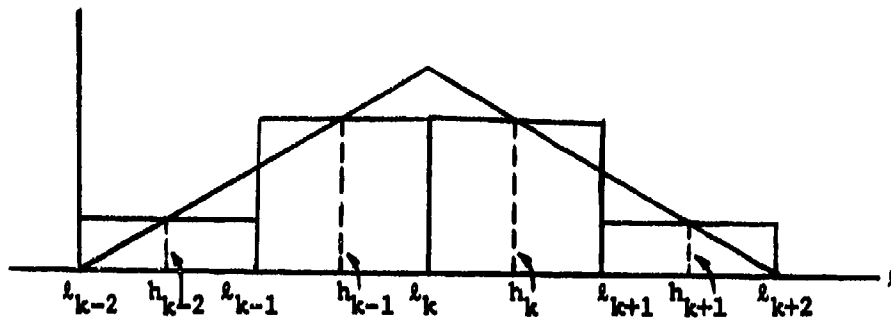


Fig. 2-3. A four-pulse approximation

where

$$\begin{aligned}
 h_{k-2} &= \frac{\frac{1}{2} \Delta l_{k-2}}{\Delta l_{k-2} + \Delta l_{k-1}} & h_{k-1} &= \frac{\Delta l_{k-2} + \frac{1}{2} \Delta l_{k-1}}{\Delta l_{k-2} + \Delta l_{k-1}} \\
 h_k &= \frac{\frac{1}{2} \Delta l_k + \Delta l_{k+1}}{\Delta l_k + \Delta l_{k+1}} & h_{k+1} &= \frac{\frac{1}{2} \Delta l_{k+1}}{\Delta l_k + \Delta l_{k+1}}
 \end{aligned} \tag{2-42}$$

The derivative  $T'$  of the Triangle function can be represented graphically as



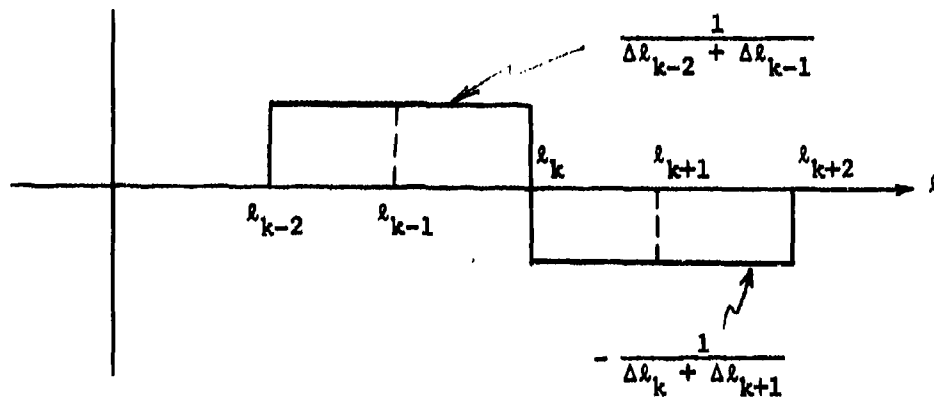


Fig. 2-4. The derivative of a triangle function.

Consider the contour interval spanned by the expansion or testing triangle function as shown in Fig. 2-5.

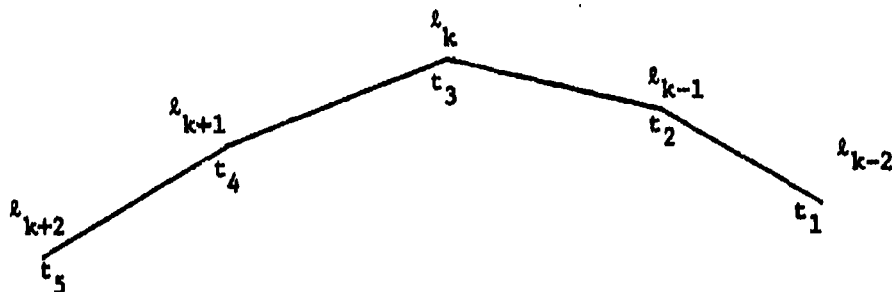


Fig. 2-5. Straight line representation of the contour.

To evaluate the integrals in equation (2-39) each such portion of the contour is replaced by straight line segments drawn between the points on the actual contour defined by  $l_1, l_2, \dots, l_{N+1}$ . The integration variables in equation (2-39) are taken along these straight line segments. For the  $n$ th expansion function, the index  $p=1,2,3,4$  is associated with the four pulse intervals for increasing path length. Similarly, the index  $q=1,2,3,4$  is defined for the  $m$ th testing function. Equation (2-39) can be put in the following form

$$Z_{mn} = \sum_{q=1}^4 \sum_{p=1}^4 \int_{t_q}^{t_{q+1}} \int_{t_p}^{t_{p+1}} [j\omega\mu T_p T_q (u_p \cdot u_q) + \frac{1}{j\omega\epsilon} T'_q T'_p] G d\lambda_p d\lambda_q \quad (2-43)$$

Note that  $T_p$  and  $T_q$  are the amplitudes of the  $p$ th and  $q$ th pulses, respectively. The unit vectors  $u_p$  and  $u_q$  are parallel to the straight lines of the  $p$ th and  $q$ th intervals in the direction of increasing path length. Observe that each of the sixteen terms on the right hand side of equation (2-43) results from one of two situations. Either the  $p$ th and  $q$ th intervals coincide, or they do not. These two situations will be considered separately.

(i) Noncoincident intervals

In this situation each integral in equation (2-44) is approximated by the product of its integrand evaluated at the interval midpoint times the interval length. Hence equation (2-44) becomes

$$Z_{mn} = \sum_{q=1}^4 \sum_{p=1}^4 \Delta t_p \Delta t_q [j\omega \mu T_p T_q (\underline{u}_p \cdot \underline{u}_q) + \frac{1}{j\omega \epsilon} T'_p T'_q] \frac{H_o^{(2)}(kR_{pq})}{4j} \quad (2-44)$$

$\Delta t_p$  and  $\Delta t_q$  are determined by

$$\Delta t_k = t_{k+1} - t_k \quad (k = 1, 2, 3, 4)$$

and  $R_{pq}$  is the distance between the midpoints of the pth and qth pulses.

(ii) Coincident intervals

For coincident pth and qth intervals the integral evaluations proceed as follows. The q integral is approximated by the product of the integrand, sampled at the midpoint of the interval, times the interval length. The p integral is then evaluated as an improper integral.

The small argument approximation for  $H_o^{(2)}(kR)$  is

$$H_o^{(2)}(kR) \approx 1 - j \frac{2}{\pi} \log \left( \frac{\gamma kR}{2} \right) \quad (2-46)$$

where  $\log \gamma$  is Euler's constant. Then for coincident pulse intervals

$$\begin{aligned} & \int_{t_q}^{t_{q+1}} \int_{t_p}^{t_{p+1}} [j\omega \mu T_p T_q (\underline{u}_p \cdot \underline{u}_q) + \frac{1}{j\omega \epsilon} T'_p T'_q] \frac{H_o^{(2)}(kR)}{4} d\ell_p d\ell_q \\ &= \frac{1}{4} \Delta t_q [j\omega \mu T_p T_q + \frac{1}{j\omega \epsilon} T'_p T'_q] \int_{t_p}^{t_{p+1}} H_o^{(2)}(kR) d\ell_p \end{aligned} \quad (2-47)$$

Note that the integrand is singular at the midpoint. The improper integral can be treated as:

$$\begin{aligned}
 \int_{t_p}^{t_{p+1}} H_o^{(2)}(kR) dx &= \int_{-\Delta t_p/2}^{\Delta t_p/2} \left[ 1 - j \frac{2}{\pi} \log \left( \frac{\gamma k |x|}{2} \right) \right] dx \\
 &= \lim_{\epsilon \rightarrow 0} \int_{-\Delta t_p/2}^{-\epsilon} \left[ 1 - j \frac{2}{\pi} \log \left( -\frac{\gamma k x}{2} \right) \right] dx \\
 &\quad + \lim_{\epsilon \rightarrow 0} \int_{\epsilon}^{\Delta t_p/2} \left[ 1 - j \frac{2}{\pi} \log \left( \frac{\gamma k x}{2} \right) \right] dx \\
 &= \Delta t_p \left[ 1 - j \frac{2}{\pi} \log \frac{\gamma k \Delta t_p}{4e} \right] \tag{2-48}
 \end{aligned}$$

Therefore  $Z_{mn}$  can be expressed as

$$Z_{mn} = \frac{1}{4} \sum_{q=1}^4 \sum_{p=1}^4 \Delta t_p \Delta t_q [\omega \mu T_p T_q (u_p \cdot u_q) - \frac{1}{\omega \epsilon} T_p' T_q'] Z \tag{2-49}$$

where

$$Z = \begin{cases} H_o^{(2)}(kR_{pq}) & \text{noncoincident intervals} \\ 1 - j \frac{2}{\pi} \log \frac{\gamma k \Delta t_p}{4e} & \text{coincident intervals} \end{cases}$$

Equation (2-49) is used to compute the two parts of each matrix element, with  $\epsilon_o$ ,  $\mu_o$ , and  $k_o$  in one part and  $\epsilon$ ,  $\mu$ , and  $k$  in the other. It can be readily observed that the use of equation (2-49) will lead to a symmetric [Z] matrix.

### 2.3 Evaluation of [B] and [C] Matrix Elements

Matrix elements for [B] are expressed by equation (2-16)

$$B_{mn} = \int_C \underbrace{W_m^e} \cdot (-jC) \underbrace{(M_n)} d\ell \quad (2-50)$$

Because of the discontinuity of the curl operator at the boundary, care should be exercised in evaluating equation (2-50). The Green's function is singular, and a simple interchange of differentiation and integration is not always possible. Note that the operator C consists of two kinds of operators, namely, C' and C''. C' is for the outside field, and C'' for the inside field, with respect to the material body. In the following development, the symbol C can be either C' or C'' unless stated otherwise. Since the incident field,  $H^1$  in the present case, is considered to be axially directed, there will be a circumferentially directed electric current and an axially directed magnetic current.

Let

$$\underbrace{W_m^e} = T(\ell - \ell_k) \underbrace{u_\ell} \quad (2-51)$$

and

$$\underbrace{M_n} = T(\ell - \ell_k) \underbrace{u_z}$$

Hence, equation (2-51) takes the form

$$\begin{aligned} B_{mn} &= -\frac{1}{4} \int \underbrace{T(\ell - \ell_m)} \underbrace{u_\ell} \cdot \nabla \times \underbrace{u_z} \int \underbrace{T(\ell' - \ell_n)} H_o^{(2)}(kR) d\ell' d\ell \\ &= -\frac{1}{4} \sum_{q=1}^4 \sum_{p=1}^4 \int_{t_q}^{t_{q+1}} \underbrace{T_q u_\ell} \cdot \nabla \times \underbrace{u_z} \int_{t_p}^{t_{p+1}} \underbrace{T_p H_o^{(2)}}(kR) d\ell' d\ell \quad (2-52) \end{aligned}$$

Since  $T_p$  and  $T_q$  are constant between  $t_p$  and  $t_{p+1}$ ,  $t_q$  and  $t_{q+1}$ , respectively, hence they can be taken outside the integral signs, so

$$B_{mn} = -\frac{1}{4} \sum_{q=1}^4 \sum_{p=1}^4 T_p T_q \int_{t_q}^{t_{q+1}} \underbrace{u_\ell} \cdot \underbrace{\nabla \times u_z}_{\underbrace{\quad}} \int_{t_p}^{t_{p+1}} H_o^{(2)}(kR) dl' dl \quad (2-53)$$

Again, two situations will be treated separately.

(1) Non-coincident p and q intervals

The Hankel function is continuous and differentiable. After performing the indicated curl operation in equation (2-53), and noting that  $u_\ell$  refers to q coordinates, then

$$B_{mn} = -\frac{1}{4} \sum_{q=1}^4 \sum_{p=1}^4 \Delta t_p \left\{ \frac{\partial H_o^{(2)}(kR_{pq})}{\partial y_q} \Delta x_q - \frac{\partial H_o^{(2)}(kR_{pq})}{\partial x_q} \Delta y_q \right\} T_p T_q \quad (2-54)$$

where

$$R_{pq} = [(x_q - x_p)^2 + (y_q - y_p)^2]^{1/2} \quad (2-55)$$

and

$$\frac{\partial H_o^{(2)}(kR)}{\partial x} = -kH_1^{(2)}(kR) \frac{x - x_p}{R} \quad (2-56)$$

$$\frac{\partial H_o^{(2)}(kR)}{\partial y} = -kH_1^{(2)}(kR) \frac{y - y_p}{R} \quad (2-57)$$

Hence

$$B_{mn} = -\frac{1}{4} \sum_{q=1}^4 \sum_{p=1}^4 \Delta t_p \frac{-T_p T_q kH_1^{(2)}(kR)}{R} [-(y_p - y_q)\Delta x_q + (x_p - x_q)\Delta y_q] \quad (2-58)$$

Equation (2-58) is obtained through the application of triangle expansion and testing function employing a four-pulse approximation to the triangle, and the integrand was evaluated at the midpoint of each pulse interval.

(ii) Coincident  $p$  and  $q$

Note that in this case, the method used in evaluating the improper integral for [2] can not be applied here because the curl operator is not continuous across the boundary, for instance

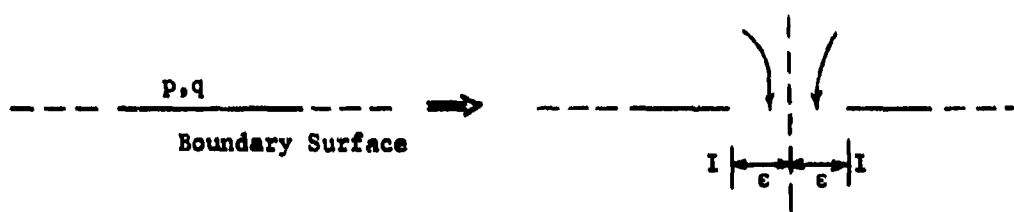


Fig. 2-6 Boundary Surface

By visualizing a current sheet that flows into the paper as shown in Fig. 2-6, it is evident that the tangential field component will decidedly be zero as  $\epsilon \rightarrow 0$ .

A better way is to find the field at a point above the boundary surface, then find the limit as it approaches the boundary surface from above. Before performing the limiting process, the integrals in equation (2-53) becomes

$$\int_{t_q}^{t_{q+1}} \underbrace{u_l}_{\sim} \cdot \nabla \times \underbrace{u_g}_{\sim} \int_{t_p}^{t_{p+1}} H_o^{(2)}(kR) dl' dl$$

$$= \Delta t_p \int_{t_q}^{t_{q+1}} \left[ \underbrace{u_x}_{\sim} \frac{\partial H_o^{(2)}(kR)}{\partial y_q} - \underbrace{u_y}_{\sim} \frac{\partial H_o^{(2)}(kR)}{\partial x_q} \right] \cdot \left[ \underbrace{u_x dx_q}_{\sim} + \underbrace{u_y dy_q}_{\sim} \right]$$

Note that in equation (2-58)  $\underbrace{u_l}_{\sim}$  refers to the q-coordinates and the p-integral is evaluated as the product of the integrand sampled at the midpoint of the p-interval times the interval length.

A local coordinate system is constructed for the evaluation of the improper integral as  $R \rightarrow 0$ . A local coordinate system is shown in Fig. 2-7.

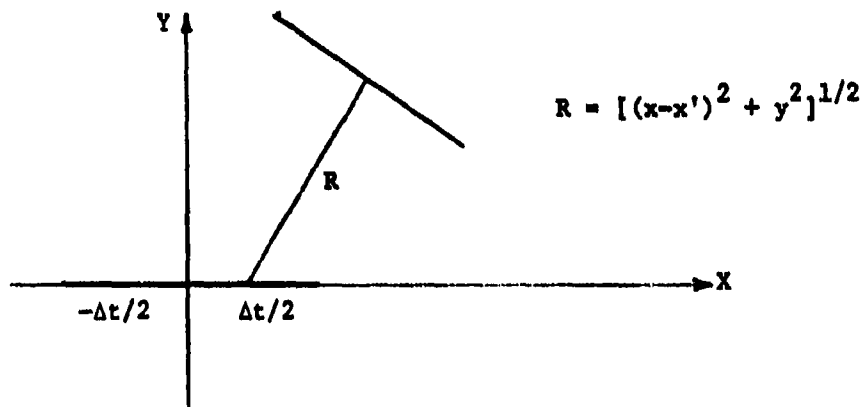


Fig. 2-7. A local coordinate system.



Next, consider the term

$$\int_{-\Delta t/2}^{\Delta t/2} \frac{\partial H_0^{(2)}(kR)}{\partial y} dx' \quad (2-59)$$

and noting that

$$\frac{\partial H_0^{(2)}(kR)}{\partial y} = -kH_1^{(2)}(kR) \frac{\partial R}{\partial y} \quad (2-60)$$

By using small argument approximation for  $H_1^{(2)}(kR)$

$$\begin{aligned} H_1^{(2)}(kR) &= J_1(kR) - jN_1(kR) \\ &\approx \frac{kR}{2} + j \frac{2}{\pi} \frac{1}{kR} \end{aligned} \quad (2-61)$$

equation (2-59) becomes

$$\begin{aligned} \int_{-\Delta t/2}^{\Delta t/2} \frac{\partial H_0^{(2)}(kR)}{\partial y} dx' &= -k \int_{-\Delta t/2}^{\Delta t/2} \left[ \frac{kR}{2} + j \frac{2}{\pi kR} \right] \frac{\partial R}{\partial y} dx' \\ &= -\frac{k^2}{2} y \Delta t - j \frac{2}{\pi} \left[ \tan^{-1} \left( \frac{\Delta t}{2} - \frac{x}{y} \right) - \tan^{-1} \left( -\frac{\Delta t}{2} - \frac{x}{y} \right) \right] \end{aligned} \quad (2-62)$$

Note that as  $x \rightarrow 0$ ,  $y \rightarrow 0$ , the improper integral approaches  $-j2$ .

Finally the expression for  $B_{mn}$  can be stated as follows.

$$B_{mn} = -\frac{1}{4} \sum_{q=1}^4 \sum_{p=1}^4 \Delta t T_p T_q B \quad (2-63)$$

where

$$B = - \frac{kH_1^{(2)} (kR_{pq})}{R_{pq}} [- (y_p - y_q) \Delta x_q + (x_p - x_q) \Delta y_q]$$

(non-coincident)

$$B = - j2$$

(coincident)

Equation (2-63) is used to compute the two parts of each [B] matrix element, R in one part (due to primed operator) and k in the other (due to doubly primed operator). Since C' is an outside operator and C'' is an inside operator, the values of B for the coincidental case will have opposite signs. Hence the coincidental-pulse-interval situation contributes nothing to the values of the matrix elements.

In spite of the fact that  $[C] = \widetilde{[B]}$ , it is advantageous to evaluate  $C_{mn}$  explicitly. The procedures involved will be essentially the same as in evaluating  $B_{mn}$ . Recall equation (2-17), and it can be expressed in greater detail as

$$C_{mn} = \int_C \underbrace{W_m^n} \cdot (-jC) \underbrace{(J_n)} dl$$

A specific form, suitable for computational purposes is developed in a manner similar to that used for  $B_{mn}$ . Considerations governing the choices of expansion and testing functions are the same as those discussed at the beginning of this section. Note that the electric surface current, in the present case, is circumferentially directed.

$$\underbrace{W_m^n} = T(\ell - \ell_k) \underbrace{u_z}$$

(2-65)

$$\underbrace{J_n} = T(\ell - \ell_k) \underbrace{u_\ell}$$

where  $T$  is defined by equation (2-38) and  $\underline{u}_z$  is the unit vector in the direction of the axis;  $\underline{u}_\ell$  is the unit vector along the cross-sectional contour.  $C_{mn}$  can be expressed as

$$C_{mn} = -\frac{1}{4} \sum_{q=1}^4 \sum_{p=1}^4 \int_{t_q}^{t_{q+1}} \int_{t_p}^{t_{p+1}} T_q \underline{u}_z \cdot \nabla \times \underline{u}_\ell T_p H_o^{(2)}(kR) d\ell' d\ell \quad (2-66)$$

The evaluation of the integrals appearing in equation (2-66) is facilitated by approximating the triangle function by four pulses. The index  $p = 1, 2, 3, 4$  is associated with each pulse, respectively, for the  $n$ th expansion function, while the index  $q = 1, 2, 3, 4$  is similarly defined for the  $m$ th testing function. Since  $T_p$  is constant between  $t_p$  and  $t_{p+1}$  and  $T_q$  is constant between  $t_q$  and  $t_{q+1}$ , they can be taken outside the integral signs.  $\underline{u}_\ell$  is the unit vector along the contour with respect to  $p$  coordinates. Hence

$$\begin{aligned} C_{mn} &= -\frac{1}{4} \sum_{q=1}^4 \sum_{p=1}^4 T_p T_q \Delta t_q \int_{t_p}^{t_{p+1}} \underline{u}_z \cdot \nabla \times [ \underline{u}_x dx_p H_o^{(2)}(kR) \\ &\quad + \underline{u}_y dy_p H_o^{(2)}(kR) ] \\ &= -\frac{1}{4} \sum_{q=1}^4 \sum_{p=1}^4 T_p T_q \Delta t_q \int_{t_p}^{t_{p+1}} \left[ -\frac{\partial H_o^{(2)}(kR)}{\partial x_q} dy_p - \frac{\partial H_o^{(2)}(kR)}{\partial y_q} dx_p \right] \end{aligned} \quad (2-67)$$

Note that the integral

$$\int_{t_p}^{t_{p+1}} \left[ -\frac{\partial H_o^{(2)}(kR)}{\partial x_q} dy_p - \frac{\partial H_o^{(2)}(kR)}{\partial y_q} dx_p \right] \quad (2-68)$$

can be evaluated just like in the previous  $B_{mn}$  case. It follows that equation (2-68) becomes

$$-kH_1^{(2)}(kR_{pq}) \left[ -\frac{x_p - x_q}{R_{pq}} \Delta y_p + \frac{y_p - y_q}{R_{pq}} \Delta x_p \right] \quad (2-69)$$

For coincident p-pulse and q-pulse intervals, the evaluation of the improper integral is identical to that developed for  $B_{mn}$ . To this point, the matrix elements for [C] can be conveniently specified as

$$C_{mn} = -\frac{1}{4} \sum_{q=1}^4 \sum_{p=1}^4 \Delta t_q T_p^T C \quad (2-70)$$

where

$$C = -\frac{kH_1^{(2)}(kR)}{R_{pq}} \left[ -(x_p - x_q) \Delta y_p + (y_p - y_q) \Delta x_p \right]$$

(noncoincident intervals)

$$C = -j2 \quad (\text{coincident intervals})$$

Equation (2-70) is used to compute the two parts of each [C] matrix elements; one part is due to the outside operator  $C'$ , and the other is due to the inside operator  $C''$ . Again, for the coincidental-pulse-interval situation, the net contribution, to the value of each matrix element, is zero, because the two values of C in equation (2-70) have opposite signs.

#### 2.4 Evaluation of [Y] Matrix Elements

The only expression left to be developed is that for the [Y] matrix elements. By equation (2-18)

$$Y_{mn} = \int_C \underbrace{W_m^m} \cdot \underbrace{L_m(M_n)} d\ell$$

$$= \int \underbrace{W_m^m} \cdot \left( \underbrace{j\omega F_n} + \underbrace{\nabla \phi_n^m} \right) d\ell \quad (2-71)$$

The superscript, m, indicates magnetic quantities. By equations (2-26) to (2-28), the following is obtained

$$Y_{mn} = j\omega \int_C (\underline{W}_m \cdot \underline{F}_n + \sigma_m \phi_n^m) dl \quad (2-72)$$

In this case all the currents are axially directed. The expansion and testing functions are chosen as

$$\underline{W}_k = \underline{M}_k = T(l - l_k) \underline{u}_z \quad (2-73)$$

where T is the triangle function defined by equation (2-38), and  $\underline{u}_z$  is the unit vector in the axial direction. The continuity equation in this case is

$$\sigma_n = -\frac{1}{j\omega} \nabla \cdot \underline{M}_n \quad (2-74)$$

Note that  $\underline{M}_n$  is  $\underline{u}_z$  directed, so

$$\nabla \cdot \underline{M}_n = 0 \quad (2-75)$$

and it follows that

$$\sigma_n = 0 \quad \text{and} \quad \phi_n^m = 0 \quad (2-76)$$

Therefore

$$\begin{aligned} Y_{mn} &= j\omega \int_C \underline{W}_m^m \cdot \underline{A}_n^m dl \\ &= \frac{\omega\epsilon}{4} \int_C \int_C (\underline{W}_m \cdot \underline{M}_n) H_0^{(2)}(kR) dl' dl \end{aligned} \quad (2-77)$$

where the unprimed integration is taken over field points and the primed integration over the source points. A specific form is developed in a manner similar to that used for  $Z_{mn}$ . Equation (2-77) can be expressed

in greater detail as

$$Y_{mn} = \frac{\omega \epsilon}{4} \int_{l_{m-2}}^{l_{m+2}} \int_{l_{n-2}}^{l_{n+2}} [T(l-l_m) T(l'-l'_m) H_o^{(2)}(kR)] dl' dl \quad (2-78)$$

The evaluation of the integrals appearing in equation (2-78) is carried out by approximating the triangle function by four pulses as shown in Fig. 2-3.

Equation (2-78) can be written as

$$Y_{mn} = \frac{\omega \epsilon}{4} \sum_{q=1}^4 \sum_{p=1}^4 \int_{t_q}^{t_{q+1}} \int_{t_p}^{t_{p+1}} T_p T_q H_o^{(2)}(kR) dl' dl \quad (2-79)$$

The indices  $p$  and  $q$  have the usual meaning.  $T_p$  and  $T_q$  have already been defined by equation (2-42). Each of the sixteen terms contributing to  $Y_{mn}$  falls into one of two categories. Either the  $p$ -pulse and  $q$ -pulse intervals coincide, or they do not. If the latter is true, each integral is approximated by the product of its integrand sampled at the interval midpoint times the interval length. The expression for  $Y_{mn}$  becomes

$$Y_{mn} = \frac{\omega \epsilon}{4} \sum_{q=1}^4 \sum_{p=1}^4 T_p T_q \Delta t_p \Delta t_q H_o^{(2)}(kR_{pq}) \quad (2-80)$$

As previously stated,  $\Delta t_p$  and  $\Delta t_q$  are defined by equation (2-45) and  $R_{pq}$  is the distance between the midpoints of the  $p$ -pulse and  $q$ -pulse intervals. For coincident  $p$ -pulse and  $q$ -pulse intervals, the improper integral and its evaluation are the same as those in  $Z_{mn}$ . Hence

$$\int_{t_q}^{t_{q+1}} \int_{t_p}^{t_{p+1}} T_p T_q H_o^{(2)}(kR) dl' dl$$

$$= T_p T_q \Delta t_p \Delta t_q \left[ 1 - j \frac{2}{\pi} \log \left( \frac{\gamma k \Delta t_p}{4e} \right) \right] \quad (2-81)$$

where  $\log \gamma =$  Euler's constant

$$e = 2.718 \dots$$

The final expression for  $Y_{mn}$  is

$$Y_{mn} = \frac{\omega \epsilon}{4} \sum_{q=1}^4 \sum_{p=1}^4 T_p T_q \Delta t_p \Delta t_q Y \quad (2-82)$$

where

$$Y = H_o^{(2)}(kR_{pq}) \quad (\text{non-coincident intervals})$$

$$= \left[ 1 - j \frac{2}{\pi} \log \left( \frac{\gamma k \Delta t_p}{4e} \right) \right] \quad (\text{coincident intervals})$$

## 2.5 Excitation Matrix, Measurement Matrix, and Scattering Cross Section

The matrix elements of the excitation matrix are represented by two expressions, equations (2-19) and (2-20). It is important to realize that the transformation of (2-19) and (2-20) into computable forms depends on the type and polarization of the impressed field. In the case under consideration, the excitation is assumed to be a z-directed magnetic field of unit magnitude. The incident field is given by

$$\underline{H}_z^i(\rho) = e^{-jk \cdot \underline{\rho}} \quad (2-83)$$

The wave number vector  $k$  points in the direction of travel of the incident wave. A coordinate system for the evaluation of the excitation matrix

elements is shown in Fig. 2-8.

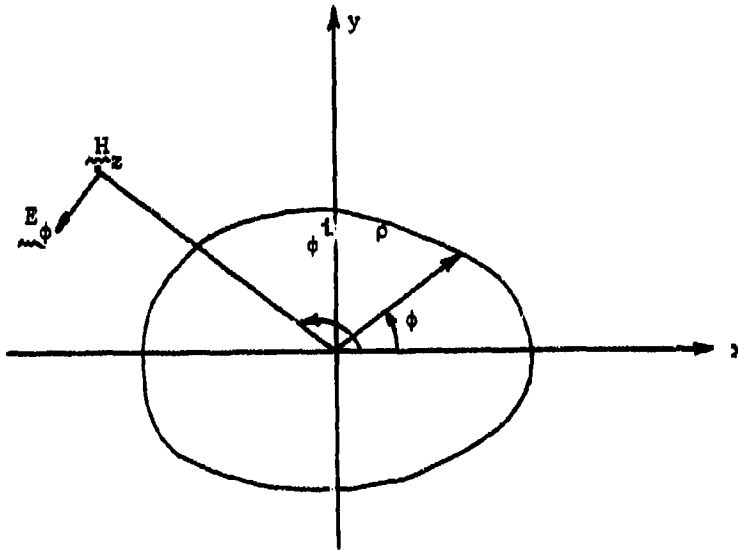


Fig. 2-8. Incident field.

Equation (2-19) will be considered first. The testing function is

$$\underline{W}_m^s = T(\underline{l} - \underline{l}_k) \underline{u}_\phi \quad (2-84)$$

For plane wave excitation the  $\phi$ -directed electric field, associated with the  $z$ -directed magnetic field defined by equation (2-83), is

$$\begin{aligned} \underline{E}^i &= -\eta \underline{u}_\phi e^{-jk \cdot \underline{r}} \\ &= -\eta (-\underline{u}_x \sin \phi^i + \underline{u}_y \cos \phi^i) e^{jk(x_{mp} \cos \phi^i + y_{mp} \sin \phi^i)} \end{aligned} \quad (2-85)$$

where

- $\underline{u}_\phi$  =  $\phi$ -directed unit vector
- $\underline{u}_x$  =  $x$ -directed unit vector
- $\underline{u}_y$  =  $y$ -directed unit vector



$\phi^i$  = incident angle

$x_{mp}, y_{mp}$  = midpoint coordinates of each straight line segment

$\eta$  = intrinsic wave impedance

By using four-pulse approximations for the triangle testing functions, equation (2-19) can be expressed as

$$V_m^i = \sum_{p=1}^4 \int_{t_p}^{t_{p+1}} \underbrace{u_z}_{T_p} \cdot E^i(\rho) dt \quad (2-86)$$

Note that the excitation matrix element  $V_m^i$  is given as the component of  $E^i(\rho)$  tangent to the contour for the  $m$ th triangle. The integral in equation (2-86) is evaluated as the tangential field component of  $E^i$  sampled at the midpoint of each  $p$ -pulse interval. Hence

$$V_m^i = -\eta \sum_{p=1}^4 T_p \{ e^{jk(x_{mp} \cos \phi^i + y_{mp} \sin \phi^i)} [-\Delta x \sin \phi^i + \Delta y \cos \phi^i] \} \quad (2-87)$$

where  $\Delta x$  and  $\Delta y$  are the rectangular components of the pulse interval. A portion of the contour is shown in Fig. 2-9 which illustrates how equation (2-87) is obtained.

Equation (2-20) can be evaluated in a similar manner. The testing functions are triangle functions, and each triangle function is represented by equation (2-39) and chosen to be  $z$ -directed.

$$\underbrace{W_k}_{z} = T(l - l_k) \underbrace{u_z}_{z} \quad (2-88)$$

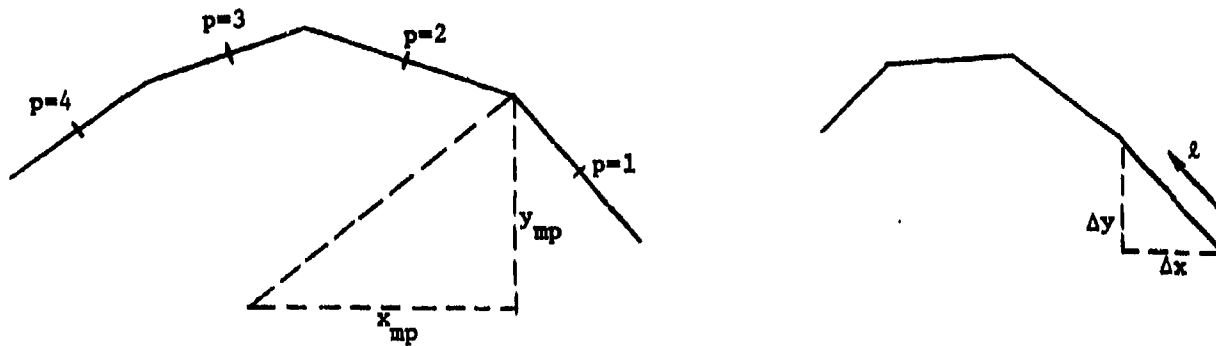


Fig. 2-9. A partial contour.

The evaluation of (2-20) is quite straightforward and the procedures are identical to those used in the evaluation of  $V_m^i$ . Hence

$$I_m^i = j \sum_{p=1}^4 T_p \Delta t_p e^{jk(x_{mp} \cos \phi^i + y_{mp} \sin \phi^i)} \quad (2-89)$$

The distant scattered field can be evaluated by reciprocity. A z-directed magnetic current filament at  $\rho_0$  of strength  $M_p$  is adjusted to produce the unit plane wave incident on the material body

$$\underline{H}^i = \underline{u}_z e^{jk(x_n \cos \phi^s + y_n \sin \phi^s)} \quad (2-90)$$

Note that  $M_p$  produces a  $\phi$ -directed  $\underline{E}^i$  and a z-directed  $\underline{H}^i$

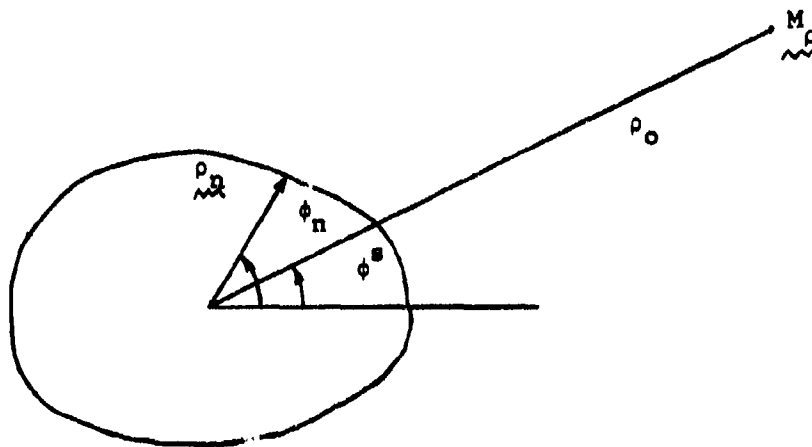


Fig. 2-10. A two-dimensional contour and z-directed magnetic current filament.

By reciprocity it is evident that

$$-H_{\rho} = \frac{1}{M} \int_C (\underline{E}^i \cdot \underline{J} - \underline{H}^i \cdot \underline{M}) d\ell \quad (2-91)$$

or

$$-H_{\rho} = \frac{1}{M_{\rho}} \int_C \underline{f} \begin{bmatrix} \underline{E}^i \\ \underline{J} \\ \underline{H}^i \\ \underline{M} \end{bmatrix} d\ell \quad (2-92)$$

where

$$\underline{f} = \begin{bmatrix} \underline{J} \\ \underline{M} \end{bmatrix}$$

Equation (2-7) can be expressed in matrix form as

$$\underline{f} = \begin{bmatrix} [\underline{I}_n] & [\underline{J}_n] \\ [\underline{V}_n] & [\underline{M}_n] \end{bmatrix} \quad (2-93)$$

With the help of equation (2-93), a new form for equation (2-92) is

$$-H_p = \frac{1}{M_p} [D] \begin{bmatrix} [I_n] \\ [V_n] \end{bmatrix} \quad (2-94)$$

Note that  $[I_n]$  and  $[V_n]$  are column matrices, and the matrix  $[D]$  is

$$[D] = \left[ \left[ \int_C \underline{\underline{E}}^i \cdot \underline{\underline{J}}_n^i d\ell \right] \left[ \int_C \underline{\underline{M}}_n^i \cdot \underline{\underline{j}}_n^i d\ell \right] \right] \quad (2-95)$$

The values of  $I_n$  and  $V_n$  can be obtained from equation (2-14) by matrix inversion. The constant  $1/M_p$  is that needed to produce a plane wave of unit amplitude at the origin, which is

$$\begin{aligned} \frac{1}{M_p} &= -\frac{k^2}{4\omega\mu} H_o^{(2)}(k\rho_o) \\ &= -\frac{\omega E}{4} H_o^{(2)}(k\rho_o) \end{aligned} \quad (2-96)$$

Redefine equation (2-95) as

$$[D] = ([D^e] [D^m]) \quad (2-97)$$

where

$$D_n^e = \int_C \underline{\underline{E}}^i \cdot \underline{\underline{J}}_n^i d\ell \quad (2-98)$$

$$D_n^m = \int_C \underline{\underline{j}}_n^i \cdot \underline{\underline{M}}_n^i d\ell \quad (2-99)$$

The evaluation of the integrals in equation (2-98) and (2-99) is straightforward, and the procedures involved are completely analogous to

those used in the evaluation of  $V_m^1$  and  $I_m^1$ . Only the results will be given here

$$D_n^e = -\eta \sum_{p=1}^4 T_p e^{jk(x_{np} \cos \phi^s + y_{np} \sin \phi^s)} [-\Delta x \sin \phi^s + \Delta y \cos \phi^s] \quad (2-100)$$

$$D_n^m = j \sum_{p=1}^4 T_p \Delta t_p e^{jk(x_{np} \cos \phi^s + y_{np} \sin \phi^s)} \quad (2-101)$$

The scattered field can be expressed as

$$H_\rho = \frac{\omega \epsilon}{4} H_o^{(2)}(k\rho_o) [[D_n^e][D_n^m]] \begin{bmatrix} [I_n] \\ [V_n] \end{bmatrix} \quad (2-102)$$

or

$$H_\rho = \frac{\omega \epsilon}{4} H_o^{(2)}(k\rho_o) [[D_n^e][D_n^m]] \begin{bmatrix} [Z] & [B] \\ [C] & [Y] \end{bmatrix}^{-1} \begin{bmatrix} [V_n^i] \\ [I_n^i] \end{bmatrix} \quad (2-103)$$

In the scattering problem, the bistatic scattering cross section  $\sigma$  is a parameter of interest. It is defined as the width for which the incident wave carries sufficient power to produce the field  $E_\rho, H_\rho$  by omnidirectional radiation. It may be expressed as

$$\sigma(\phi^s) = 2\pi \rho_o \lim_{\rho_o \rightarrow \infty} = \left| \frac{E_\rho(\phi^s)}{\eta} \right|^2$$

or

$$= 2\pi \rho_o \lim_{\rho_o \rightarrow \infty} = \left| H_\rho(\phi^s) \right|^2 \quad (2-104)$$

The large argument approximation for  $H_0^{(2)}(kR)$  is

$$H_0^{(2)}(x) \xrightarrow{x \rightarrow \infty} \sqrt{\frac{2j}{\pi x}} e^{-jx} \quad (2-107)$$

The expression for the scattering cross section can be stated as

$$\begin{aligned} \sigma &= \lim_{\rho_0 \rightarrow \infty} 2\pi\rho_0 \left| \frac{\omega\epsilon}{4} \sqrt{\frac{2}{\pi k\rho_0}} h \right|^2 \\ &= \frac{k}{4\eta^2} |h|^2 \end{aligned} \quad (2-106)$$

where

$$h = \left| [D] \begin{bmatrix} [Z] & [B] \\ [C] & [Y] \end{bmatrix}^{-1} \begin{bmatrix} [V_n^i] \\ [I_n^i] \end{bmatrix} \right|$$

## CHAPTER 3

## CHARACTERISTIC MODES - A SURFACE FORMULATION

3.1 Theoretical Development

The treatment of characteristic modes for perfectly conducting bodies, starting from the impedance operator for the conducting surface, has been given by Harrington and Mautz [2]. In terms of the polarization current and the magnetization current, a volume formulation of the characteristic mode theory for dielectric and magnetic bodies has also been treated [4]. In this chapter a theory of characteristic modes for material bodies (dielectric, magnetic, or both) based on a surface formulation is developed. The appropriate operator formulation of the problem is

$$\begin{bmatrix} L_e & N \\ N & L_m \end{bmatrix} \begin{bmatrix} \underline{J} \\ \underline{jM} \end{bmatrix} = \begin{bmatrix} \underline{E}^i \\ \underline{jH}^i \end{bmatrix} \quad (3-1)$$

To emphasize the symmetric nature of the matrix of operators, the off-diagonal operators are denoted by a single symbol,  $N$ . Define the following rise vectors

$$\underline{f} = \begin{bmatrix} \underline{J} \\ \underline{jM} \end{bmatrix}, \quad \underline{g} = \begin{bmatrix} \underline{E} \\ \underline{jH} \end{bmatrix} \quad (3-2)$$

and the matrix of operators

$$T = \begin{bmatrix} L_e & N \\ N & L_m \end{bmatrix} \quad (3-3)$$

where  $N = -jC$ .

Equation (3-1) can then be written as

$$\underline{Tf} = \underline{g}^i$$

Define the symmetric product

$$\begin{aligned} \langle \underline{f}, \underline{g} \rangle &= \iint_{\underline{S}} \underline{\tilde{f}} \underline{g} \, ds \\ &= \iint_{\underline{S}} (\underline{J} \cdot \underline{E} - \underline{M} \cdot \underline{H}) \, ds \end{aligned} \quad (3-4)$$

which, for  $f$  a source quantity and  $g$  a field quantity, is reaction. The product

$$\begin{aligned} \langle \underline{f}^*, \underline{g} \rangle &= \iint_{\underline{S}} \underline{\tilde{f}}^* \underline{g} \, ds \\ &= \iint_{\underline{S}} (\underline{J}^* \cdot \underline{E} + \underline{M}^* \cdot \underline{H}) \, ds \end{aligned} \quad (3-5)$$

is a suitable inner product for the Hilbert space of functions  $f, g$  in  $S$ .

If  $f$  is a source quantity and  $g$  a field quantity, the real part of (3-5) is time average power, but the imaginary part of (3-5) differs from the usual imaginary power. It is easy to show that  $T$  is symmetric, that is,

$\langle \underline{f}_1, \underline{Tf}_2 \rangle = \langle \underline{f}_2, \underline{Tf}_1 \rangle$  by reciprocity. The operator  $T$  can be expressed in terms of its Hermitian parts as  $T = T_1 + jT_2$  where

$$T_1 = \frac{1}{2} (T + T^*) = \begin{bmatrix} R & N_1 \\ N_1 & G \end{bmatrix} \quad (3-6)$$

$$T_2 = \frac{1}{2j} (T - T^*) = \begin{bmatrix} X & N_2 \\ N_2 & B \end{bmatrix} \quad (3-7)$$



Here  $N_1$  and  $N_2$  are the Hermitian parts of  $N$ ,  $R$  and  $X$  are the Hermitian parts of  $Z$ ,  $G$  and  $B$  are the Hermitian parts of  $Y$ .

By equation (1-9), the fields due to  $J$  and  $M$  can be expressed as

$$L' \begin{bmatrix} J \\ jM \end{bmatrix} = - \begin{bmatrix} E \\ jH \end{bmatrix} ; \quad L' = \begin{bmatrix} L_e' & -jC' \\ -jC' & L_m' \end{bmatrix} \quad (3-8)$$

As far as radiation is concerned, the contribution due to the doubly primed operators is zero. The power radiated by any  $J$  and  $M$  on  $S$  is given by

$$\begin{aligned} \text{Re}(P_s) &= - \text{Re} \iint (\underbrace{E \cdot J^*}_{\text{}} + \underbrace{M \cdot H^*}_{\text{}}) ds \\ &= - \text{Re} \iint (\underbrace{E \cdot J^*}_{\text{}} + \underbrace{M^* \cdot H}_{\text{}}) ds \\ &= \text{Re} \{ \underbrace{\langle f^*, Tf \rangle}_{\text{}} \} \end{aligned} \quad (3-9)$$

Hence the time average power delivered by a source  $f$  is

$$\text{Re}(P_s) = \text{Re} \{ \underbrace{\langle f^*, Tf \rangle}_{\text{}} \} \quad (3-10)$$

The imaginary part of  $\langle f^*, Tf \rangle$  is not simply related to reactive power.

Using six-vector notation, we formulate a theory of characteristic modes which parallels that of the volume formulation [4]. The eigenvalue equation defining the modes is

$$T_2(\underbrace{f_n}_{\text{}}) = \lambda_n T_1(\underbrace{f_n}_{\text{}}) \quad (3-11)$$

where  $T_1$  and  $T_2$  are real symmetric operators. Hence, all eigenvalues  $\lambda_n$  are real and all characteristic sources  $\underbrace{f_n}_{\text{}}$  may be chosen real. In expanded form

$$\underline{f}_n = \begin{bmatrix} J_n \\ jM_n \end{bmatrix} \quad (3-12)$$

which, for characteristic sources, implies that  $M_n$  is imaginary and  $J_n$  is real. The characteristic sources can be normalized to radiate unit power, and the usual orthogonality relationships expressed as

$$\begin{aligned} \langle \underline{f}_m^*, T_1 \underline{f}_n \rangle &= \langle \underline{f}_m, T_1 \underline{f}_n \rangle = \delta_{mn} \\ \langle \underline{f}_m^*, T_2 \underline{f}_n \rangle &= \langle \underline{f}_m, T_2 \underline{f}_n \rangle = \lambda_n \delta_{mn} \\ \langle \underline{f}_m^*, T \underline{f}_n \rangle &= \langle \underline{f}_m, T \underline{f}_n \rangle = (1 + j\lambda_n) \delta_{mn} \end{aligned} \quad (3-13)$$

where  $\delta_{mn}$  is the Kronecker delta. The field

$$\underline{g}_n = \begin{bmatrix} E_n \\ jH_n \end{bmatrix} \quad (3-14)$$

due to a source  $\underline{f}_n$  is called a characteristic field. In the radiation zone the characteristic field is of the form of an outward traveling wave, and it is completely characterized by either  $E_n$  or  $H_n$ .

Let  $\underline{f}_n$  and  $\underline{f}_m$  be two characteristic sources. By equation (3-13), the following expression is true.

$$\begin{aligned} \langle \underline{f}_m, T \underline{f}_n \rangle &= \left\langle \begin{bmatrix} J_n & jM_n \\ N & Lm \end{bmatrix} \begin{bmatrix} L_e & N \\ N & Lm \end{bmatrix} \begin{bmatrix} J_n \\ jM_n \end{bmatrix} \right\rangle \\ &= 0 \quad \text{for } m \neq n \end{aligned} \quad (3-15)$$

Equation (3-13) is essentially

$$\iint (\underline{J}_m \cdot \underline{E}_n - \underline{H}_n \cdot \underline{M}_m) ds = 0 \quad (3-16)$$

where  $\underline{E}_n$  and  $\underline{H}_n$  are produced by  $\underline{f}_n$ . Because  $\underline{J}_m$  is real and  $\underline{M}_m$  is imaginary, we have

$$\iint (\underline{J}_m^* \cdot \underline{E}_n + \underline{H}_n \cdot \underline{M}_m^*) ds = 0 \quad (3-17)$$

It follows that

$$\text{Re} \iint (\underline{E}_n \cdot \underline{J}_m^* + \underline{H}_n^* \cdot \underline{M}_m) ds = 0 \quad (3-18)$$

which means that the real part of the cross power is zero. In the radiation zone the characteristic waves are of the form of outward traveling wave, i.e.

$$\underline{E}_n = \eta \underline{H}_n \times \underline{n} \quad (3-19)$$

where  $\underline{n}$  is the unit radial vector on  $S_n$ . The real part of the cross power can be expressed as

$$\text{Re} \iint \underline{E}_m \times \underline{H}_n^* \cdot ds = \text{Re} \iint \frac{\underline{E}_m \cdot \underline{E}_n^*}{\eta} ds = 0 \quad (3-20)$$

The real part of the cross power between  $j(\underline{E}_n, \underline{H}_n)$  and  $(\underline{E}_m, \underline{H}_m)$  is also zero. Hence,

$$\frac{1}{\eta} \iint \underline{E}_m \cdot \underline{E}_n^* ds = \eta \iint \underline{H}_m \cdot \underline{H}_n^* ds = \delta_{mn} \quad (3-21)$$

### 3.2 Characteristic Equation and Modal Representation

In the preceding section, the analytical development was based on the interpretation of operators. The reduction of operator equations to matrix equations can be effected in the usual manner by the method of moments.

Let

$$\underline{f}_n = \left( \sum_j I_j \underline{f}_j^e + \sum_j V_j \underline{f}_j^m \right) \quad (3-22)$$

where

$$\underline{f}_j^e = \begin{bmatrix} W_j^e \\ \underline{w}_j \\ 0 \end{bmatrix}, \quad \underline{f}_j^m = \begin{bmatrix} 0 \\ \underline{w}_j \\ W_j^m \end{bmatrix} \quad (3-23)$$

After substituting equation (3-22) into equation (3-11), the following is obtained.

$$\left\{ \sum_j I_j T_2 \underline{f}_j^e + \sum_j V_j T_2 \underline{f}_j^m \right\} = \lambda_n \left\{ \sum_j I_j T_1 \underline{f}_j^e + \sum_j V_j T_1 \underline{f}_j^m \right\} \quad (3-24)$$

Perform inner product with electric testing function  $\underline{W}_1^e$ ,

$$\begin{aligned} \left\{ \sum_j I_j \langle \underline{W}_1^e, T_2 \underline{f}_j^e \rangle + \sum_j V_j \langle \underline{W}_1^e, T_2 \underline{f}_j^m \rangle \right\} \\ = \lambda_n \left\{ \sum_j I_j \langle \underline{W}_1^e, T_1 \underline{f}_j^e \rangle + \sum_j V_j \langle \underline{W}_1^e, T_1 \underline{f}_j^m \rangle \right\} \end{aligned} \quad (3-25)$$

and with magnetic testing function  $\underline{W}_1^m$ .

$$\begin{aligned} \left\{ \sum_j I_j \langle \underline{W}_1^m, T_2 \underline{f}_j^e \rangle + \sum_j V_j \langle \underline{W}_1^m, T_2 \underline{f}_j^m \rangle \right\} \\ = \lambda_n \left\{ \sum_j I_j \langle \underline{W}_1^m, T_1 \underline{f}_j^e \rangle + \sum_j V_j \langle \underline{W}_1^m, T_1 \underline{f}_j^m \rangle \right\} \end{aligned} \quad (3-26)$$

Equation (3-25) and equation (3-26) can be put into one matrix equation.

$$\begin{bmatrix} [X] & [N_2] \\ [N_2] & [B] \end{bmatrix} \begin{bmatrix} [I] \\ [V] \end{bmatrix}_n = \lambda_n \begin{bmatrix} [R] & [N_1] \\ [N_1] & [G] \end{bmatrix} \begin{bmatrix} [I] \\ [V] \end{bmatrix}_n \quad (3-27)$$

The definitions of  $[X]$ ,  $[N_2]$ ,  $[B]$ ,  $[R]$ ,  $[N_1]$ ,  $[G]$ ,  $[I]$ , and  $[V]$  are obvious by comparing equation (3-27) with equations (3-25) and (3-26).

Equation (3-27) is the eigenvalue equation which will be used in the actual computation of the modes. In abbreviated form, it becomes

$$[T_2] [f_n] = \lambda_n [T_1] [f_n] \quad (3-28)$$

Now, with the understanding that  $\lambda_n$  and  $f_n$  can be found, the modal solution for  $f$  can be expressed as

$$f = \sum_n \alpha_n f_n \quad (3-29)$$

Recall that

$$Tf = g^i \quad (3-30)$$

After substituting equation (3-29) into equation (3-30) and performing the inner product with  $f_m$ , the following equation results.

$$\sum_n \alpha_n \langle f_m, Tf_n \rangle = \langle f_m, g^i \rangle \quad (3-31)$$

Apply the orthogonality relationships given in equation (3-13). It follows that

$$\alpha_n = \frac{\langle f_m, g^i \rangle}{(1 + j \lambda_n) \langle f_m, Tf_n \rangle} \quad (3-32)$$

Explicitly,

$$\langle f_m, g^i \rangle = \sum_i I_i \langle f_i^a, g^i \rangle + \sum_i V_i \langle f_i^m, g^i \rangle \quad (3-33)$$

The matrix equivalents of the orthogonality relationships for the characteristic currents, equation (3-13), are also of interest.

For example, that for  $T_1$  is

$$\begin{aligned}
\langle \underbrace{f_m}_m, T_1 \underbrace{f_n}_n \rangle &= \langle \sum_i \{ I_i \underbrace{f_i^e}_i + V_i \underbrace{f_i^m}_i \}_m, T_1 \sum_j \{ I_j \underbrace{f_j^e}_j + V_j \underbrace{f_j^m}_j \}_n \rangle \\
&= \sum_i \sum_j \{ I_i I_j \langle \underbrace{f_i^e}_i, T_1 \underbrace{f_j^e}_j \rangle + I_i V_j \langle \underbrace{f_i^e}_i, T_1 \underbrace{f_j^m}_j \rangle \\
&\quad + V_i I_j \langle \underbrace{f_i^m}_i, T_1 \underbrace{f_j^e}_j \rangle + V_i V_j \langle \underbrace{f_i^m}_i, T_1 \underbrace{f_j^m}_j \rangle \} \\
&= [\widetilde{I}]_m [R] [I]_n + [\widetilde{I}]_m [N_1] [V]_n \\
&\quad + [\widetilde{V}]_m [\widetilde{N}_1] [I]_n + [\widetilde{V}]_m [G] [V]_n \\
&= [\widetilde{f}_m] [T_1] [\underbrace{f_n}_n] = \delta_{mn} \tag{3-34}
\end{aligned}$$

where  $\widetilde{\phantom{x}}$  denotes transpose. Similar derivations hold for  $T_2$  and  $T$ .

### 3.3 Linear Measurement

Any scalar  $\rho$  linearly related to the generalized current, i.e. a linear functional of the equivalent electric and magnetic currents, will be called a linear measurement of the current.

Any linear functional of  $\underbrace{f}_m$  can be expressed as

$$\rho = \langle \underbrace{g^m}_m, \underbrace{f}_m \rangle \tag{3-35}$$

where  $g^m$  is a vector function which consists of an electric field and a magnetic field. By equations (3-32) and (3-33), the linear measurement of  $f$  can be stated as

$$\rho = \sum_n \frac{\langle \underbrace{f}_n, \underbrace{g^1}_n \rangle}{(1 + j\lambda_n) \langle \underbrace{f}_n, T_1 \underbrace{f}_n \rangle} \langle \underbrace{g^m}_m, \underbrace{f}_n \rangle \tag{3-36}$$

where

$$\langle \underbrace{g^m}_n, \underbrace{f_n}_n \rangle = \sum \underbrace{I}_{i_n} \langle \underbrace{g^m}_n, \underbrace{f_i^s}_n \rangle = \sum \underbrace{V}_{i_n} \langle \underbrace{g^m}_n, \underbrace{f_i^m}_n \rangle \quad (3-37)$$

and define the following

$$K_n^m = \langle \underbrace{g^m}_n, \underbrace{f_n}_n \rangle = \text{modal measurement coefficient} \quad (3-38)$$

$$\langle \underbrace{g^i}_n, \underbrace{f_n}_n \rangle = \text{modal excitation coefficient} \quad (3-39)$$

Equation (3-36) is a symmetric bilinear functional of  $\underbrace{g^i}_n$  (the impressed field) and of  $\underbrace{g^m}_n$  (the measured field). The symmetry of (3-36) is a consequence of the symmetry of the original operator T. Equation (3-36) can be expressed as

$$\rho = \sum_n \frac{K_n^i K_n^m}{1 + j \lambda_n} \quad (3-40)$$

similarly, in terms of  $K_n^i$  equation (3-32) becomes

$$\alpha_n = \frac{K_n^i}{1 + j \lambda_n} \quad (3-41)$$

and equation (3-29) will take the form

$$\underbrace{f}_n = \sum_n \frac{K_n^i}{1 + j \lambda_n} \underbrace{f}_n \quad (3-42)$$

### 3.4 Characteristic Fields and Scattering Cross Section

The characteristic fields are linearly related to the characteristic currents,  $\underbrace{f}_n$ , and hence can also be expressed in modal form.

$$\underbrace{E}_n = \sum_n \frac{K_n^i}{1 + j \lambda_n} \underbrace{g}_n \quad (3-43)$$

When  $K_n^i$  and  $f_n$  are known, the field pattern can be obtained by employing equation (3-43). A convenient way is to evaluate the modal measurement coefficient first. In the two-dimensional case, consider a magnetic current filament,  $M = M u_m$  at  $(\rho, \phi)$  on  $S_m$ . See Fig. 3-1 below.

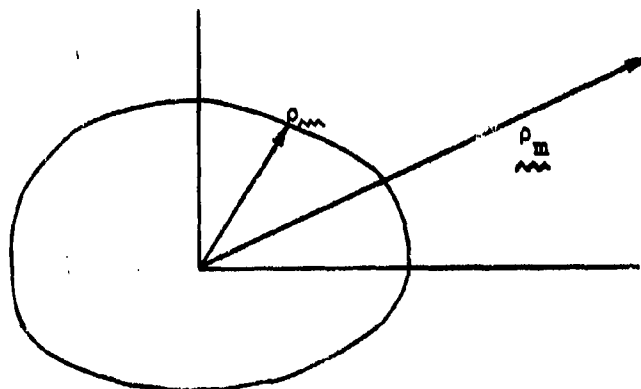


Fig. 3-1. A coordinate system for modal measurement coefficient

By reciprocity, it is readily seen that

$$- \int_{S_m} H_n \cdot M = \int_{S_m} (J_n \cdot E_m - M_n \cdot H_m) ds \quad (3-44)$$

where  $H_n$  is the characteristic field components produced by the mode current  $f_n$ .  $E_m$  and  $H_m$  are the fields due to the magnetic current filament,  $M$ . To simplify the analysis, the magnitude of the magnetic current,  $M$ , is adjusted to produce a plane wave on the material body, i.e.

$$H_m = u_m e^{-jk_m \cdot r_m} \quad (3-45)$$

$$E_m = \eta H_m \times u_{km} \quad (3-46)$$



where  $\eta$  is the wave impedance and  $\underline{u}_{km}$  is the unit vector in the direction of propagation. The right hand side of equation (3-44), in matrix form, is the modal measurement coefficient. Hence,

$$K_n^m = \int_c (\underline{J}_n \cdot \underline{E}_m - \underline{M}_n \cdot \underline{H}_m) dl \quad (3-47)$$

Explicitly, the electric field and the magnetic field can be extracted from equation (3-43) as

$$\underline{E} = \sum_n \frac{K_n^i}{1 + j \lambda_n} \underline{E}_n \quad (3-48)$$

$$\underline{H} = \sum_n \frac{K_n^i}{1 + j \lambda_n} \underline{H}_n \quad (3-49)$$

Since the magnetic field is currently under consideration, only equation (3-49) will be used. The component of the magnetic field on  $\underline{u}_m$  is

$$\begin{aligned} \underline{H} \cdot \underline{u}_m &= \sum_n \frac{K_n^i}{1 + j \lambda_n} \underline{H}_n \cdot \underline{u}_m \\ &= -\frac{1}{M} \sum_n \frac{K_n^i K_n^m}{1 + j \lambda_n} \\ &= -\frac{\omega \epsilon}{4} H_o^{(2)}(k\rho) \sum_n \frac{K_n^i K_n^m}{1 + j \lambda_n} \end{aligned} \quad (3-50)$$

Note that  $K_n^i$  is of the same functional form as  $K_n^m$ . Equation (2-98) has been used in deriving equation (3-50).

A commonly used parameter in plane wave scattering problems is the echo area. In two-dimensional problems the quantity "echo width" corresponds to the "echo area" of the three-dimensional problems.

The echo width is defined in equation (2-106).

$$\sigma = 2 \pi \rho_m \lim_{\rho_m \rightarrow \infty} \left| \sum_n \frac{K_n^i K_n^m}{1 + j \lambda_n} \right|^2 \quad (3-51)$$

By equations (3-50) and (2-106), the following expression for the scattering cross section is obtained.

$$\sigma = \frac{k}{4 \eta^2} \left| \sum_n \frac{K_n^i K_n^m}{1 + j \lambda_n} \right|^2 \quad (3-52)$$

### 3.5 Computational Considerations

The solution of the matrix eigenvalue problem, equation (3-28), will be discussed.

$$[T_2] [f] = \lambda [T_1] [f] \quad (3-53)$$

Note that the subscript  $n$  has been dropped for brevity. The conventional method for reducing (3-53) to a symmetric unweighted eigenvalue equation requires  $[T_2]$  to be positive definite. In theory  $[T_1]$  is positive semi-definite, but because of numerical inaccuracies it is actually indefinite, with some small negative eigenvalues. If the values of the matrix elements cover a very wide range, scaling will become desirable. The magnitude of the scale factor can be chosen as such that all scaled matrix elements will be brought, as close as possible, to the same order of magnitude. The conventional method will be modified as follows.

Let  $[D]$  be a diagonal matrix. After premultiplying by  $[D]$ , equation (3-47) becomes

$$[D][T_2][\underline{f}] = \lambda [D][T_1][\underline{f}] \quad (3-54)$$

Then observe that

$$\begin{aligned} [D][T_2][D]([D]^{-1}[\underline{f}]) \\ = \lambda [D][T_1][D]([D]^{-1}[\underline{f}]) \end{aligned} \quad (3-55)$$

The eigenvalue equation as given by (3-55) will have the same eigenvalues as the original unscaled equation, but the eigenvectors will be different. In other words the eigenvalues are not affected by the diagonal transformation. The original eigenvectors will be modified by [D] inverse. If the scale factor is s, [D] can be chosen as

$$[D] = \begin{bmatrix} 1/s & 0 \\ 0 & 1 \end{bmatrix} \quad (3-56)$$

By equations (3-27), (3-55), and (3-56), the scaled eigenvalue equation is

$$[T_2^s][\underline{f}^s] = \lambda [T_1^s][\underline{f}^s] \quad (3-57)$$

where

$$[T_2^s] = \begin{bmatrix} [X]/s^2 & [N_2]/s \\ [\widetilde{N}_2]/s & [B] \end{bmatrix} \quad (3-58)$$

$$[T_1^s] = \begin{bmatrix} [R]/s^2 & [N_1]/s \\ [\widetilde{N}_1]/s & [G] \end{bmatrix} \quad (3-59)$$

and

$$\underline{[f^s]} = \begin{bmatrix} s[ I ] \\ [ V ] \end{bmatrix} \quad (3-60)$$

Note that  $[I]$  and  $[V]$  ( $J$  and  $M$ ) should first be recovered from the scaled eigenvectors before computing the surface currents and the scattered fields.

Rewrite equation (3-57) below

$$\underline{[T_2]} \underline{[f]} = \lambda \underline{[T_1]} \underline{[f]} \quad (3-61)$$

Note that the superscripts have been dropped for brevity. An approximation will be used in finding the eigenvalues and eigenvectors. The eigenvalue equation

$$\underline{[T_1]} \underline{r} = \mu \underline{r} \quad (3-62)$$

is used to find a set of basis functions for the  $T_1$  vector space. An orthonormal set of vectors can be obtained by using the vectors  $\{r_i\}$ . Let  $\{U_i\}$  be the set of orthonormal vectors, and let  $[U]$  be the orthogonal matrix which diagonalizes  $[T_1]$  according to

$$\underline{[U]} \underline{[T_1]} \underline{[U]} = \begin{bmatrix} \mu_1 & 0 & 0 & 0 & \dots \\ 0 & \mu_2 & 0 & 0 & \dots \\ 0 & 0 & \mu_3 & 0 & \dots \\ 0 & 0 & 0 & \mu_4 & \dots \\ \dots & \dots & \dots & \dots & \dots \\ \dots & \dots & \dots & \dots & \dots \\ \dots & \dots & \dots & \dots & \dots \end{bmatrix} \quad (3-63)$$

where the  $\mu_i$  are the eigenvalues of  $[T_1]$  ordered  $\mu_1 \geq \mu_2 \geq \mu_3 \geq \mu_4 \geq \dots$ . Every column of  $[U]$  is in  $\{U_i\}$ . Only the larger  $\mu_i$  can be considered accurate. All  $\mu_i > M\mu_1$  are put in  $[\mu_1]$  where  $M$  is some small positive number set by the estimated accuracy of  $[T_1]$ . Usually  $M$  is anywhere between  $10^{-3}$  and  $10^{-6}$ . The diagonal matrix  $[\mu]$  is then partitioned as

$$[ \mu ] = \begin{bmatrix} [ \mu_1 ] & [ 0 ] \\ [ 0 ] & [ \mu_2 ] \end{bmatrix} \quad (3-64)$$

where

$$[ \mu_1 ] = \begin{bmatrix} \mu_1 & & & 0 \\ & \mu_2 & & \\ & & \ddots & \\ & 0 & & \mu_m \end{bmatrix} \quad (3-65)$$

$$[ \mu_2 ] = \begin{bmatrix} \mu_{m+1} & & & 0 \\ & \mu_{m+2} & & \\ & & \ddots & \\ & 0 & & \mu_n \end{bmatrix} \quad (3-66)$$

Now consider

$$f = \sum_{l=1}^n x_l U_l \quad (3-67)$$

where  $U_l$  is a column vector of  $[U]$ . This is a valid expansion because the  $\{ U_l \}$  vectors form a basis for  $T_1$  vector space. In matrix form equation (3-67) becomes

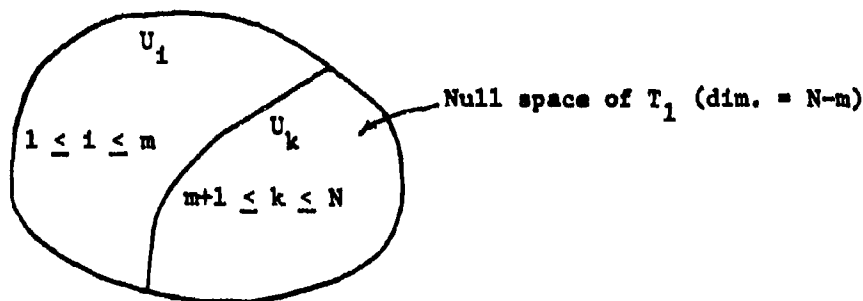
$$f = [U][x] \quad (3-68)$$

If  $[ \mu_2 ]$  is set to zero, it follows that all column vectors of  $[U]$  corresponding to all  $\mu_k \in [ \mu_2 ]$  are in the null space of  $T_1$ . This is illustrated in Fig. 3-2.

The expression for  $f$  as given in equation (3-67) can be written

as

$$f = \sum_{i=1}^m x_i U_i + \sum_{k=m+1}^n x_k U_k \quad (3-69)$$

Fig. 3-2.  $T_1$  vector space

The column vector  $\underline{x}$  in equation (3-68) can be partitioned as

$$\underline{x} = [\widetilde{U}][f] = \begin{bmatrix} \underline{x}_1 \\ \underline{x}_2 \end{bmatrix} \quad (3-70)$$

where  $\underline{x}_1$  and  $\underline{x}_2$  are column vectors, and they are obtained by partitioning  $\underline{x}$  according to equation (3-69). Premultiply equation (3-61) by  $[\widetilde{U}]$  and use equations (3-63) and (3-68). The result is

$$[\widetilde{U}][T_2][U]\underline{x} = \lambda[\mu]\underline{x} \quad (3-71)$$

Set  $[\mu_2]$  equal to zero and partition all other matrices conformably. The following two matrix equations are obtained.

$$[A_{11}]\underline{x}_1 + [A_{12}]\underline{x}_2 = \lambda[\mu_1]\underline{x}_1 \quad (3-72)$$

$$[\widetilde{A}_{12}]\underline{x}_1 + [A_{22}]\underline{x}_2 = 0 \quad (3-73)$$

Note that  $[A] = [U][T_2][U]$ . Equation (3-73) can be solved for  $\underline{x}_2$  and the result substituted into equation (3-72) to get

$$[A_{11} - A_{12}A_{22}^{-1}\widetilde{A}_{12}]\underline{x}_1 = \lambda[\mu_1]\underline{x}_1 \quad (3-74)$$

The brackets of submatrices have been dropped to conserve space.

Now  $[\mu_1]$  has only positive diagonal elements as defined by equation (3-65).

Observe that

$$[\mu_1] = [\mu_1^{1/2}] [\mu_1^{1/2}] \quad (3-75)$$

where

$$[\mu_1^{1/2}] = \begin{bmatrix} \mu_1^{1/2} & & & 0 \\ & \mu_2^{1/2} & & \\ & & \mu_3^{1/2} & \\ & & & \ddots \\ 0 & & & & \mu_m^{1/2} \end{bmatrix} \quad (3-76)$$

By equations (3-74) and (3-75) a new and unweighted eigenvalue equation is obtained.

$$[B][y] = \lambda[y] \quad (3-77)$$

where

$$[y] = [\mu_1^{1/2}][x_1] \quad (3-78)$$

$$[B] = [\mu_1^{-1/2}][A_{11} - A_{12}A_{22}^{-1}A_{12}] [\mu_1^{-1/2}] \quad (3-79)$$

The eigenvalues of equation (3-77) are the smaller eigenvalues of the original equation (3-61), and the eigenvectors of (3-77) give the corresponding eigenvectors of equation (3-61) according to

$$f = [U][x] = [U] \begin{bmatrix} [\delta] \\ [-A_{22}^{-1}A_{12}] \end{bmatrix} [\mu_1^{-1/2}][y] \quad (3-80)$$

where  $[\delta]$  is the identity matrix.

Once the eigenvalues and the eigencurrents are known, the equivalent surface currents and scattered fields can be obtained by employing appropriate formulas for those quantities.



## CHAPTER 4

## RESULTS

The results of far field scattering calculations for some material cylinders are presented in this chapter. Equations used are those developed in Chapter 2 and Chapter 3.

The far field scattering patterns of circular material cylinders have been computed and the results are shown in Figures 4-1 through 4-16, for perpendicular polarization (TE). Figures 4-17 through 4-22 give the results for parallel polarization (TM). All results are compared with exact harmonic series solutions [7]. Figures 4-1 to 4-5 are obtained by using 15 triangle expansion functions. Twenty expansion functions have been used in obtaining Figures 4-6 to 4-22. In all figures the computed scattering cross section are normalized by  $\pi a$ , where "a" is the radius of the cylinder.

The normalized scattering cross sections of square cylinders are shown in Figures 4-23 through 4-27. All computed results are normalized by  $\pi b$ , where "b" is one-half the width of the square cylinder under consideration. Twenty expansions have been used in all computations for square cylinders of different material constants.

Figures 4-28 through 4-30 show the characteristic currents (or mode currents) for circular cylinders of different material constants. Fifteen expansion functions have been used for the computation of mode currents.

For representative computations, consider a circular cylinder with  $ka = 0.7$  (where "a" is the radius of the cylinder,  $\epsilon_r = 9.5$ ,  $\mu_r = 1.0$ ). The contour is approximated by 32 straight line segments of equal length (the

line segments can be of different length), and 15 expansion functions are used for both electric and magnetic surface currents. Figure 4-28 shows the characteristic currents plotted vs. the contour length variable in terms of a sequence of triangle functions. All the mode currents are composite currents. The first 15 points represent the electric mode current, and the second the magnetic current.

Figure 4-29 shows the characteristic currents for a circular cylinder with  $\epsilon_r = 50.0$ ,  $\mu_r = 1.0$ , and  $ka = 0.7$ . Figure 4-30 shows the characteristic currents for a circular cylinder of  $\epsilon_r = 2.56$ . Note that every mode current is normalized by its maximum magnitude.

For perpendicular polarization (TE), the modal solution for the scattered field agrees extremely well with the scattered field computed directly from matrix inversion. The scattering cross sections using characteristic modes are almost identical to the matrix inversion solutions (the differences are less than 0.001 db).

To be specific, Fig. 4-1 shows the normalized scattering cross section of a circular cylinder with  $\epsilon_r = 9.5$ ,  $\mu_r = 1.0$ , and  $ka = 0.7$  for perpendicular polarization (TE). The computed scattering cross section is in good agreement with harmonic solution [7]. The maximum deviation is 0.65 db. Figure 4-2 gives the normalized scattering cross section of a circular cylinder with  $\epsilon_r = 20.0$ ,  $\mu_r = 1.0$ , and  $ka = 0.7$ , for perpendicular polarization (TE). The maximum deviation from exact harmonic series solution is 0.076 db. Figure 4-3 shows the normalized scattering cross section of a circular cylinder with  $\epsilon_r = 50.0$ ,  $\mu_r = 1.0$ , and  $ka = 0.7$ , for perpendicular polarization (TE). Maximum

deviation from exact harmonic solution is 0.485 db. The scattering cross section shown in Fig. 4-4 is for a circular cylinder with  $\epsilon_r = 100.0$ ,  $\mu_r = 0.01$ , and  $ka = 0.7$  for perpendicular polarization. The computed solution is in excellent agreement with the exact solution. Maximum deviation is 0.01 db. Figure 4-5 gives the normalized scattering cross section of a circular cylinder with  $\epsilon_r = 1000.0$ ,  $\mu_r = 0.001$ , and  $ka = 0.7$ , for perpendicular polarization. Note that the computed result is in excellent agreement with the calculations of a conducting cylinder. Maximum deviation is 0.01 db. The conducting cylinder problem can be viewed as a specialization of the more general material cylinder problem. This is expected to be true even for three-dimensional objects. Figure 4-6 shows the normalized scattering cross section of a circular cylinder with  $\epsilon_r = 9.0$ ,  $\mu_r = 1.0$ , and  $ka = 2.0$ , for perpendicular polarization (TE). Maximum deviation from exact harmonic solution is 1.79 db. Better agreement can be reached, if more expansion functions are used. The scattering cross section given in Fig. 4-7 is for a circular cylinder with  $\epsilon_r = 9.0$ ,  $\mu_r = 1.0$ , and  $ka = 1.0$ , for perpendicular polarization. The agreement with exact solution is excellent. Maximum deviation is 0.013 db. Figure 4-8 shows the normalized scattering cross section of a circular cylinder with  $\epsilon_r = 9.0$ ,  $\mu_r = 100.0$ , and  $ka = 0.7$ , for perpendicular polarization. Agreement with exact solution is very good. Maximum deviation is 0.01 db. Figure 4-9 shows the normalized scattering cross section of a circular cylinder with  $\epsilon_r = 9.0$ ,  $\mu_r = 5.0$ , and  $ka = 0.7$ , for perpendicular polarization. The computed result is in good agreement with exact

solution. Maximum deviation is 0.3 db. The computed scattering cross section of a circular cylinder with  $\epsilon_r = 0.001$ ,  $\mu_r = 1000.0$ , and  $ka = 0.7$ , for perpendicular polarization is shown in Fig. 4-10. Note that the cylinder is highly magnetic. Maximum deviation from exact harmonic solution is 0.001 db. The agreement is excellent. Figure 4-11 shows the normalized scattering cross section of a circular cylinder with  $\epsilon_r = 1.0$ ,  $\mu_r = 1000.0$ , and  $ka = 0.7$ , for perpendicular polarization. Maximum deviation from exact solution is 0.04 db. Figure 4-12 represents the computed scattering cross section of a circular cylinder with  $\epsilon_r = 1.0$ ,  $\mu_r = 10.0$ , and  $ka = 0.7$ , for perpendicular polarization. Maximum deviation from exact solution is 0.04 db. Figure 4-13 shows the computed scattering cross section of a circular cylinder with  $\epsilon_r = 1.0$ ,  $\mu_r = 300$ , and  $ka = 0.7$ , for perpendicular polarization. Maximum deviation from exact harmonic solution is 0.2 db. Figure 4-14 gives the normalized scattering cross section of a circular cylinder with  $\epsilon_r = 2.56$ ,  $\mu_r = 1.0$ , and  $ka = 0.7$ , for perpendicular polarization. Maximum deviation is 0.6 db. Figure 4-15 shows the computed scattering cross section of a circular cylinder with  $\epsilon_r = 1000.0$ ,  $\mu_r = 0.001$ , and  $ka = 0.7$ , for perpendicular polarization. The computed solution is in excellent agreement with exact solution. Maximum deviation is 0.01 db. The computed scattering cross sections of a circular cylinder with  $ka = 0.7$ , are given in Fig. 4-16 for three different sets of material constants; i)  $\epsilon_r = 1000.0$ ,  $\mu_r = 1.0$  ii)  $\epsilon_r = 10000.0$ ,  $\mu_r = 1.0$  iii)  $\epsilon_r = 5.0$ ,  $\mu_r = 10^{-6}$ . All are for perpendicular polarization. Figure 4-17 shows the normalized scattering cross section of a circular cylinder with  $\epsilon_r = 1000.0$ ,  $\mu_r = 0.001$ , and  $ka = 0.7$ , for parallel polarization (TM). The solution agrees excellently with conducting cylinder solution. Maximum deviation is 0.023 db. The normalized scattering

cross section of a circular cylinder with  $\epsilon_r = 2.56$ ,  $\mu_r = 1.0$ , and  $ka = 0.7$ , for parallel polarization is shown in Fig. 4-18. Maximum deviation from exact solution is 0.5 db. Figure 4-19 represents the computed scattering cross section of a circular cylinder with  $\epsilon_r = 20.0$ ,  $\mu_r = 1.0$ , and  $ka = 0.7$ , for parallel polarization. Maximum deviation from exact solution is 0.2 db. Figure 4-20 shows the computed scattering cross section of a circular cylinder with  $\epsilon_r = 50.0$ ,  $\mu_r = 1.0$ , and  $ka = 0.7$ , for parallel polarization. The computed solution is in excellent agreement with exact harmonic solution. Maximum deviation is 0.05 db. Figure 4-21 shows the computed scattering cross section of a circular cylinder with  $\epsilon_r = 4.0$ ,  $\mu_r = 1.0$ , and  $ka = 0.7$ , for parallel polarization. Maximum deviation from exact solution is 0.2 db. Figure 4-22 shows the computed scattering cross section of a circular cylinder with  $\epsilon_r = 9.5$ ,  $\mu_r = 1.0$ , and  $ka = 0.7$ , for parallel polarization. The computed solution is in excellent agreement with exact harmonic solution maximum deviation is 0.01 db. Figure 4-23 shows the computed scattering cross sections of a square cylinder with  $kb = 1.4$ , for two sets of material constants: i)  $\epsilon_r = 1000.0$ ,  $\mu_r = 0.001$  ii)  $\epsilon_r = 1000.0$ ,  $\mu_r = 1.0$ , all for perpendicular polarization. For square cylinders, there are no exact solutions. Figure 4-24 shows the computed scattering cross section of a square cylinder with  $\epsilon_r = 10000.0$ ,  $\mu_r = 0.0001$ , and  $kb = 1.4$ , for perpendicular polarization. The computed solution has been compared with the solution of a conducting square cylinder by using E-field formulation [13]. Maximum deviation is 0.1 db. Figure 4-25 shows the computed scattering cross section of a square cylinder with  $\epsilon_r = 9.0$ ,  $\mu_r = 1.0$ , and  $kb = 1.4$ , for perpendicular polarization. Figure 4-26 shows the computed scattering cross section of a square cylinder with  $\epsilon_r = 100.0$ ,  $\mu_r = 1.0$ , and  $kb = 1.4$ , for

parallel polarization. Figure 4-27 shows the scattering cross section of a square cylinder with  $\epsilon_r = 10000.0$ ,  $\mu_r = 0.0001$ , and  $kb = 1.4$ , for parallel polarization. The computed result is in excellent agreement with conducting square cylinder solution. Figure 4-28 shows the lowest order characteristic currents, plotted as a function of the contour variable. The currents are normalized by choosing their maximum amplitude to be unity. The characteristic currents are for a circular cylinder with  $\epsilon_r = 9.5$ ,  $\mu_r = 1.0$ , and  $ka = 0.7$ , for perpendicular polarization. The electric part of each characteristic current is circumferentially directed and the magnetic part is axially directed. The scattering cross section computed from modal solution is almost identical to that from matrix inversion. Figure 4-29 shows the normalized characteristic currents for a circular cylinder with  $\epsilon_r = 50.0$ ,  $\mu_r = 1.0$ , and  $ka = 0.7$ , for perpendicular polarization. Figure 4-30 gives the normalized characteristic currents for a circular cylinder with  $\epsilon_r = 2.56$ ,  $\mu_r = 1.0$ , and  $ka = 0.7$ , for perpendicular polarization.

The purpose of this work is to show the feasibility that a surface formulation for the theory characteristic modes can be applied to the solution of scattering from material objects. For large cylinders, more expansion functions are needed. No attempt has been made to treat large objects. It is expected that this is one of the important areas for future research. Many questions are still left unanswered in the interpretation and application of characteristic modes to material objects. It is hoped that this work will be of some value to future researchers in their effort to gain a complete understanding of the theory of characteristic modes.

The eigenvalue equation (3-61) is

$$[T_2][f] = \lambda [T_1][f] \quad (4-1)$$

and the expression for the Rayleigh quotient associated with equation (4-1) is

$$\lambda_1 = \frac{[\widetilde{f}_1][T_2][f_1]}{[\widetilde{f}_1][T_1][f_1]} \quad (4-2)$$

The computed eigenvalues and their corresponding eigenvectors should satisfy equation (4-2). The Rayleigh quotient check is important because it gives some verification to the approximations used in numerical computation.

The quadratic term  $[f_1][T_1][f_1]$  deserves some elaboration since it appears frequently in equations. Note that

$$\begin{aligned} [\widetilde{f}][T_1][f] &= [\widetilde{x}][\widetilde{U}][T_1][U][x] \\ &= [\widetilde{x}][\mu][x] \\ &= [\widetilde{x}_1][\mu_1][x_1] + [\widetilde{x}_2][\mu_2][x_2] \end{aligned} \quad (4-3)$$

It has already been pointed out in Chapter 3 that  $[x_2]$  is the component of an eigencurrent  $f$  that lies within the null space of  $T_1$ , in other words,  $[x_2]$  does not radiate. Since approximations are made in the computational procedures, the eigencurrents will not be absolutely exact. Consequently, the second quadratic term on the right hand side of equation (4-3) will differ from zero, but it should be much smaller than the first quadratic term. To a certain degree, this will give some indication of the accuracy of the computed eigencurrents. The first quadratic term at the right hand side of equation (4-3) can be further expressed as

$$\begin{aligned}
& \widetilde{[x_1]} \{u_1\} [x_1] \\
&= \widetilde{[u_1^{-1/2}]} [y] \{u_1\} [u_1^{-1/2}] [y] \\
&= \widetilde{[y]} \{u_1^{-1/2}\} \{u_1\} [u_1^{-1/2}] [y] \\
&= \widetilde{[y]} [y] \\
&= 1 \text{ (if } \{y_1\} \text{ are orthonormal)} \qquad (4-4)
\end{aligned}$$

In numerical computation, approximations are inevitable. Some special analytical manipulations such as those discussed above can often provide added insight to the correctness of the numerical results.



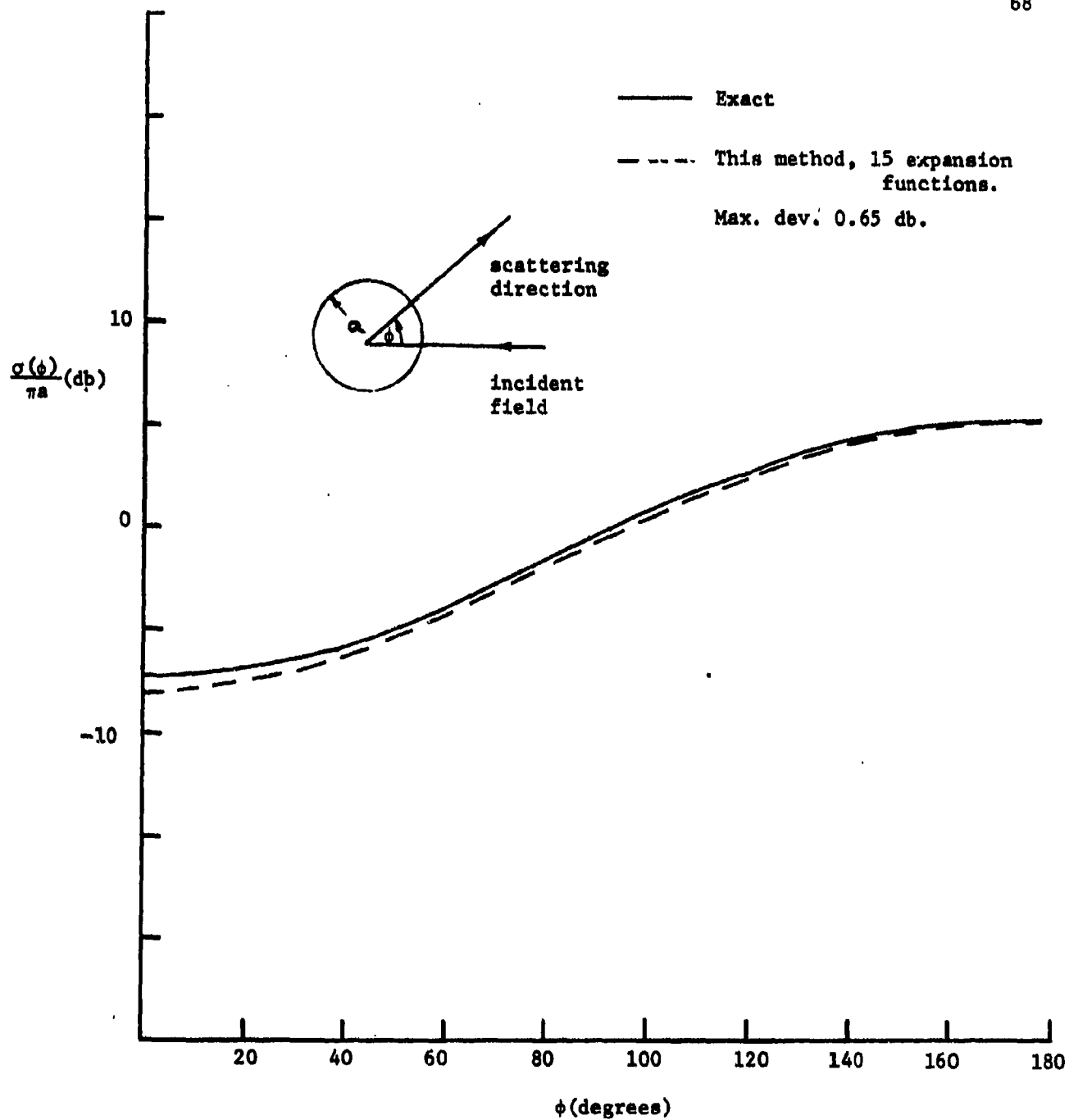


Fig. 4-1. Normalized scattering cross section of a circular cylinder with  $\epsilon_r = 9.5$ ,  $\mu_r = 1.0$ ,  $ka = 0.7$ , perpendicular polarization (TE).

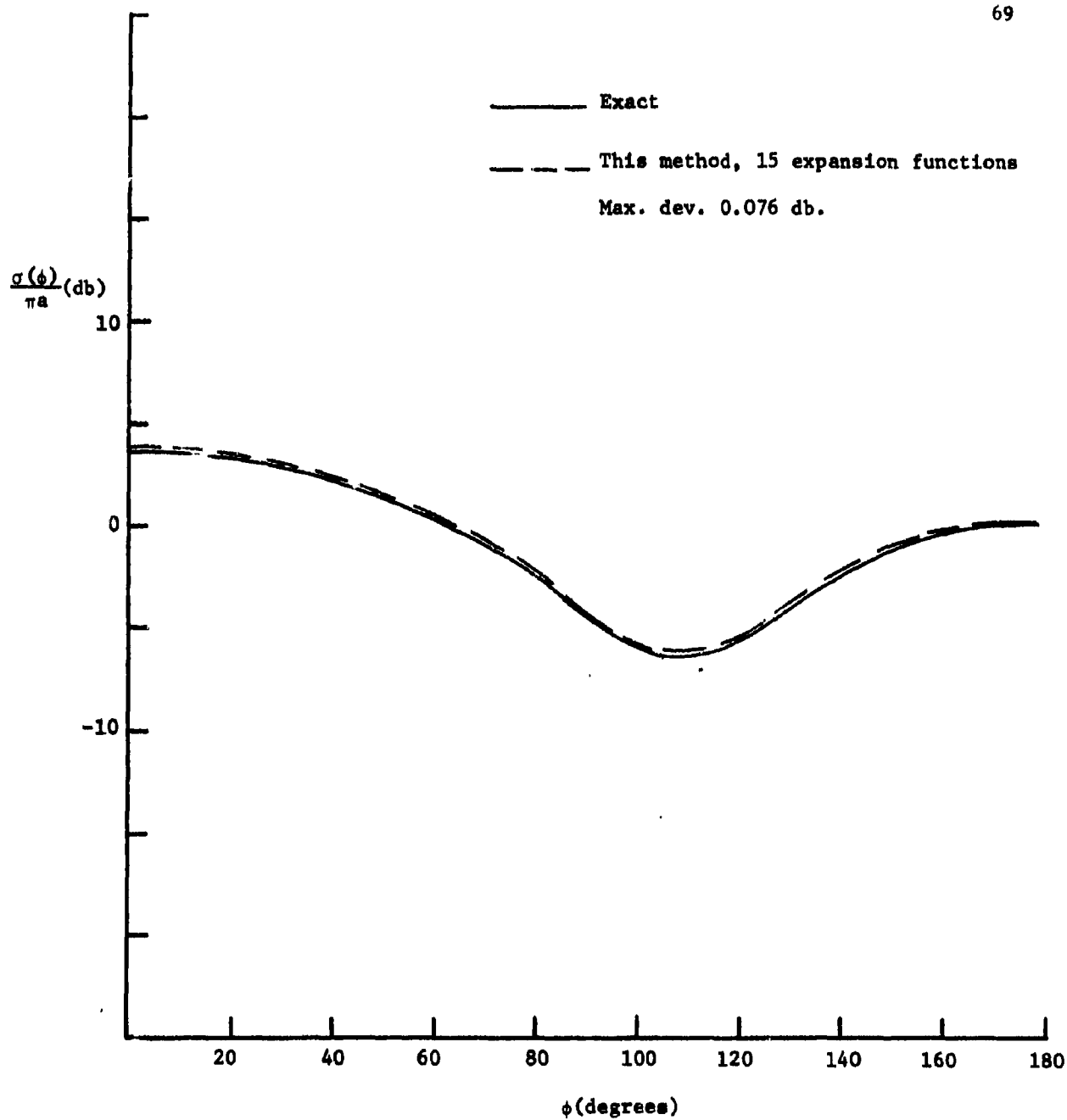


Fig. 4-2. Normalized scattering cross section of a circular cylinder with  $\epsilon_r = 20.0$ ,  $\mu_r = 1.0$ ,  $ka = 0.7$ , perpendicular polarization (TE).

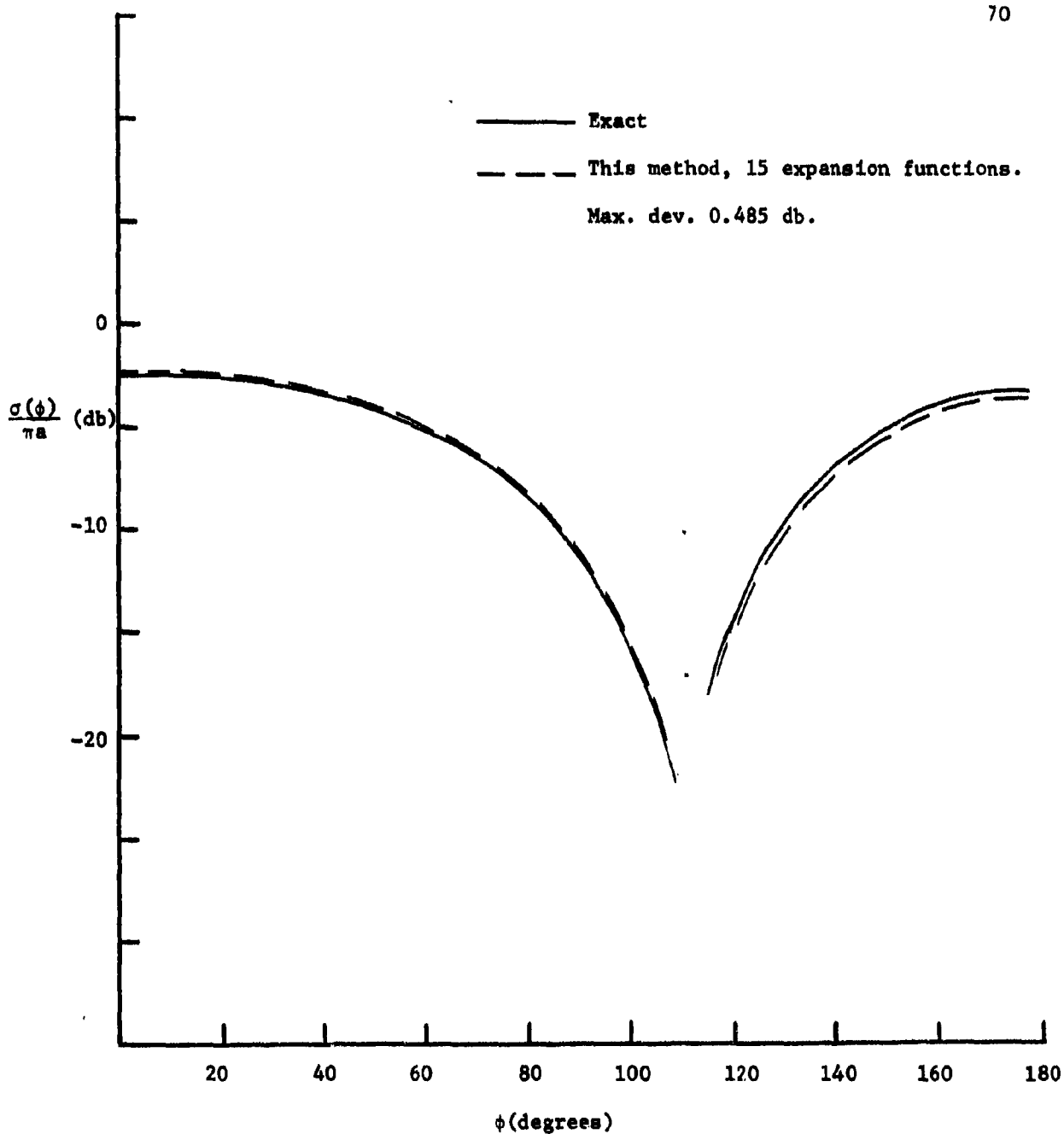


Fig. 4-3. Normalized scattering cross section of a circular cylinder with  $\epsilon_r = 50.0$ ,  $\mu_r = 1.0$ ,  $ka = 0.7$ , perpendicular polarization (TE).

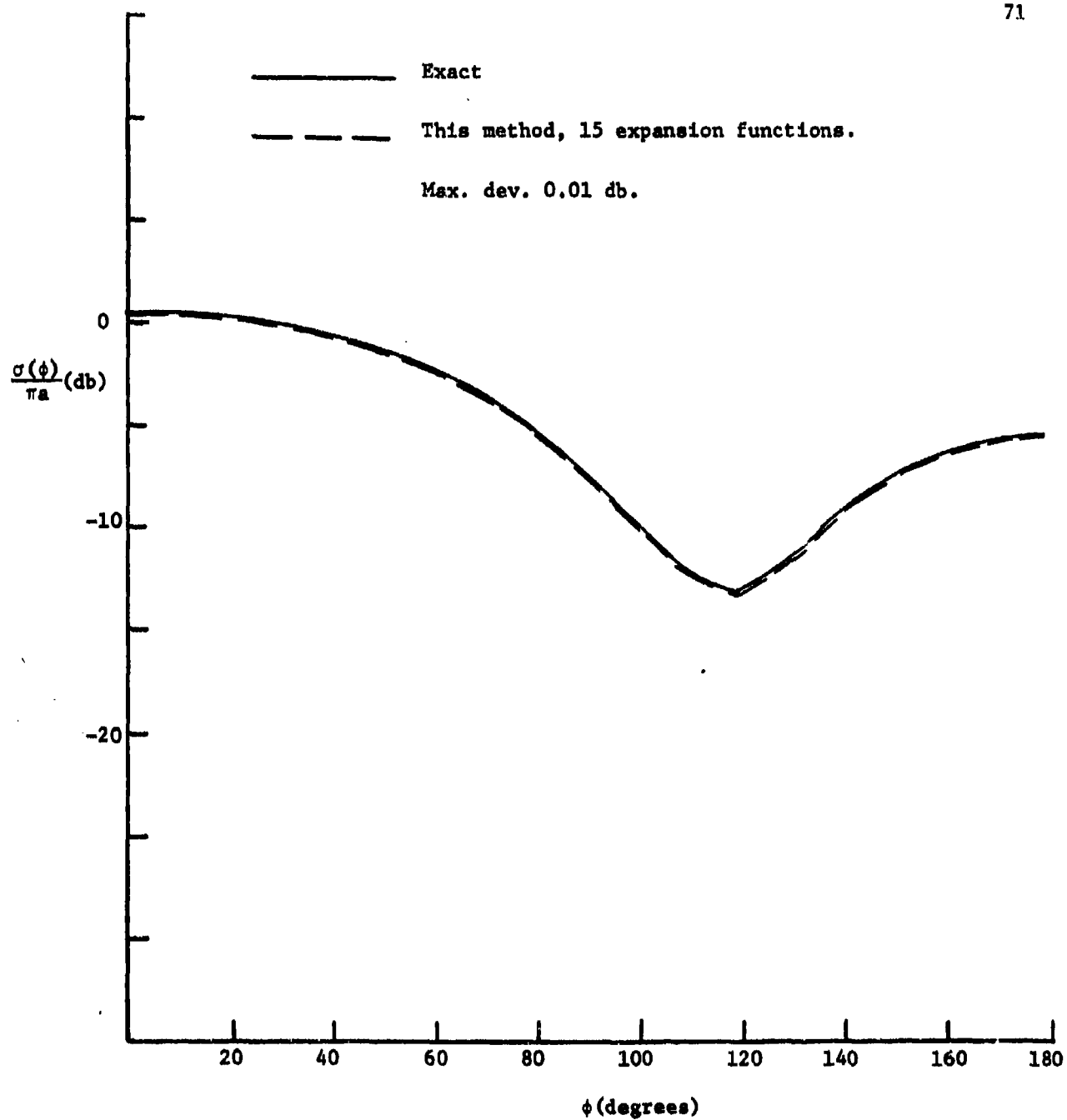


Fig. 4-4. Normalized scattering cross section of a circular cylinder with  $\epsilon_r = 100.0$ ,  $\mu_r = 0.01$ ,  $ka = 0.7$ , perpendicular polarization (TE).

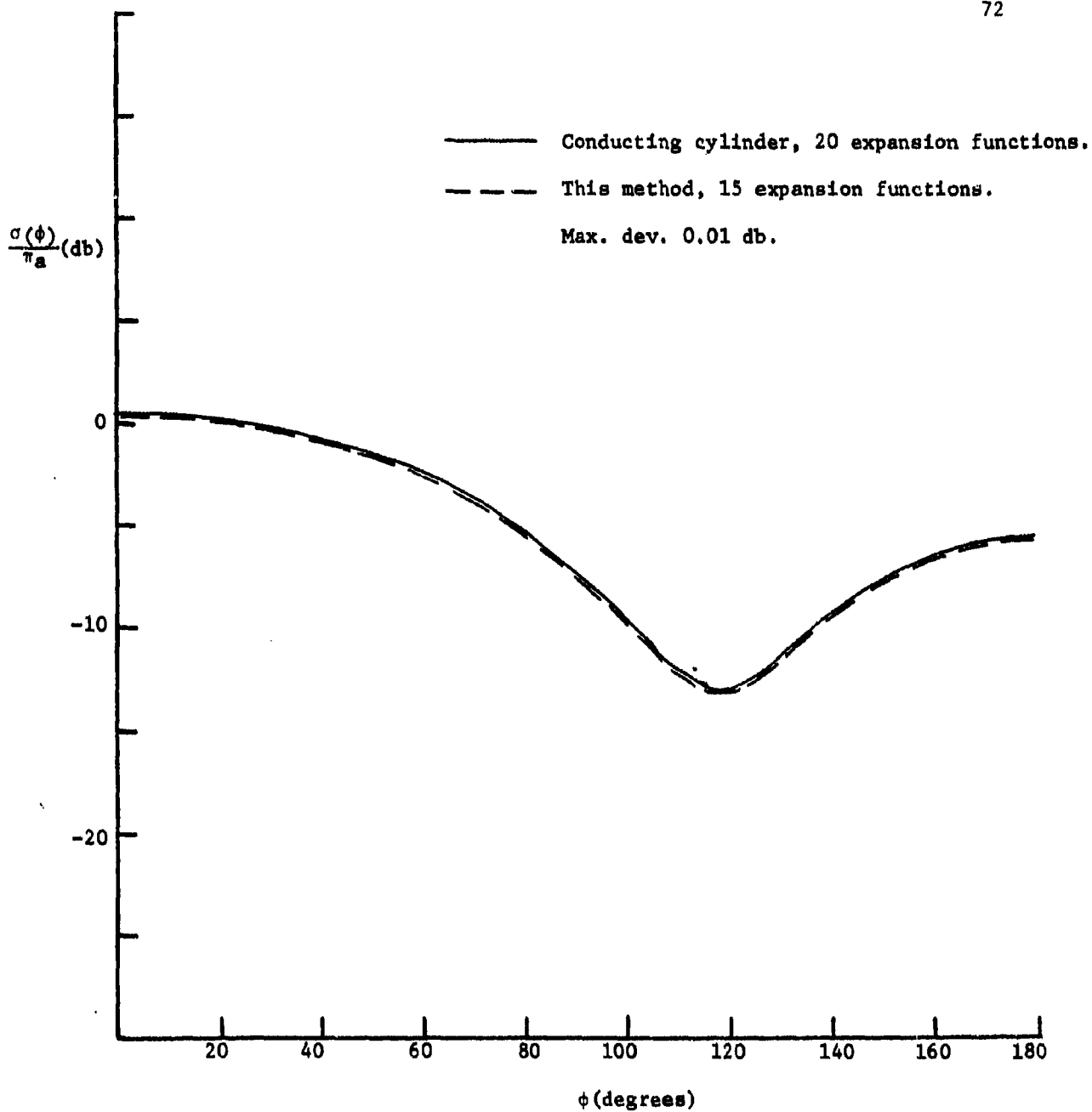


Fig. 4-5. Normalized scattering cross section of a circular cylinder with  $\epsilon_r = 1000.0$ ,  $\mu_r = 0.001$ ,  $ka = 0.7$ , perpendicular polarization (TE).

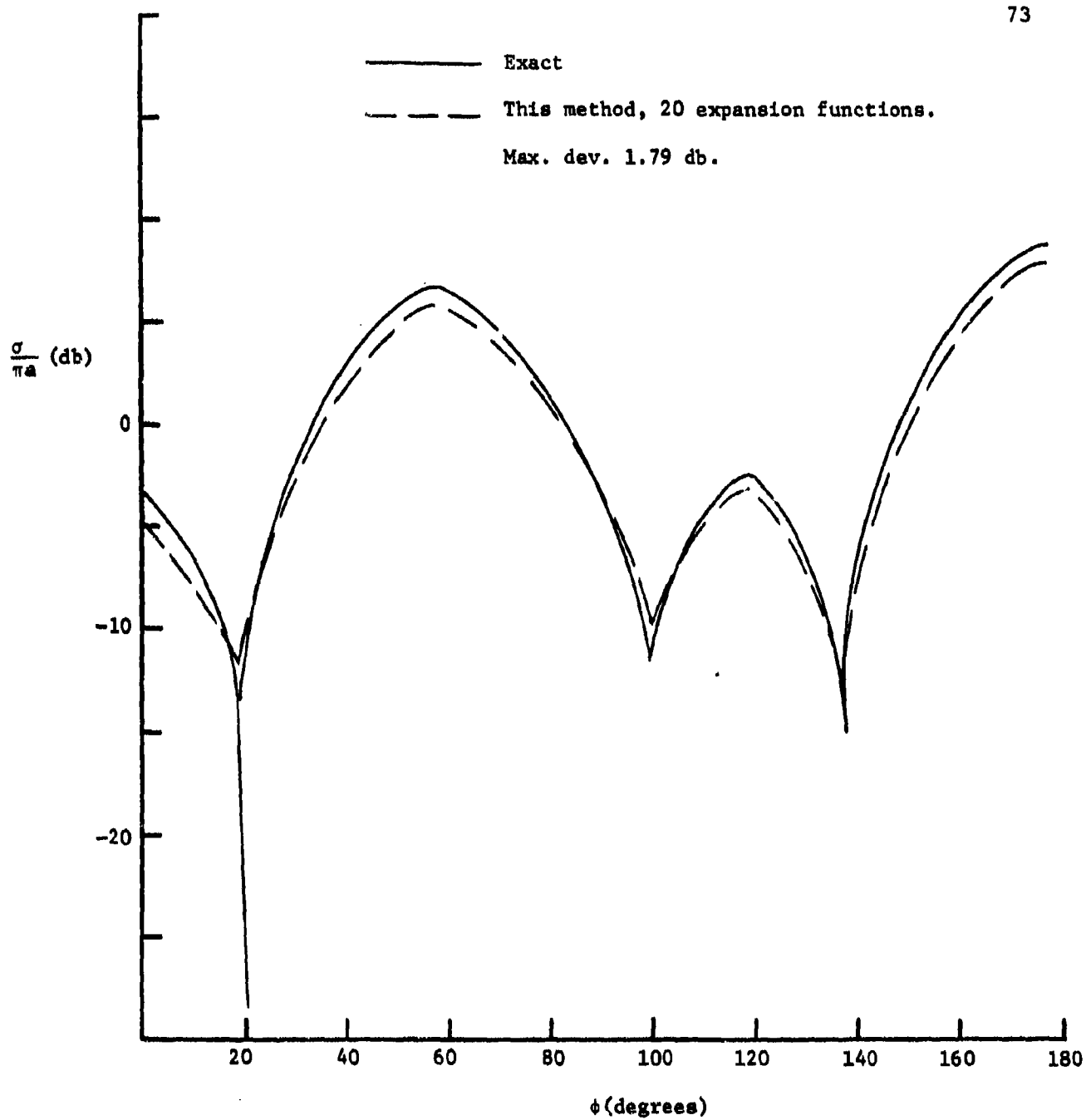


Fig. 4-6. Normalized scattering cross section of a circular cylinder with  $\epsilon_r = 9.0$ ,  $\mu_r = 1.0$ ,  $ka = 2.0$ , perpendicular polarization (TE).

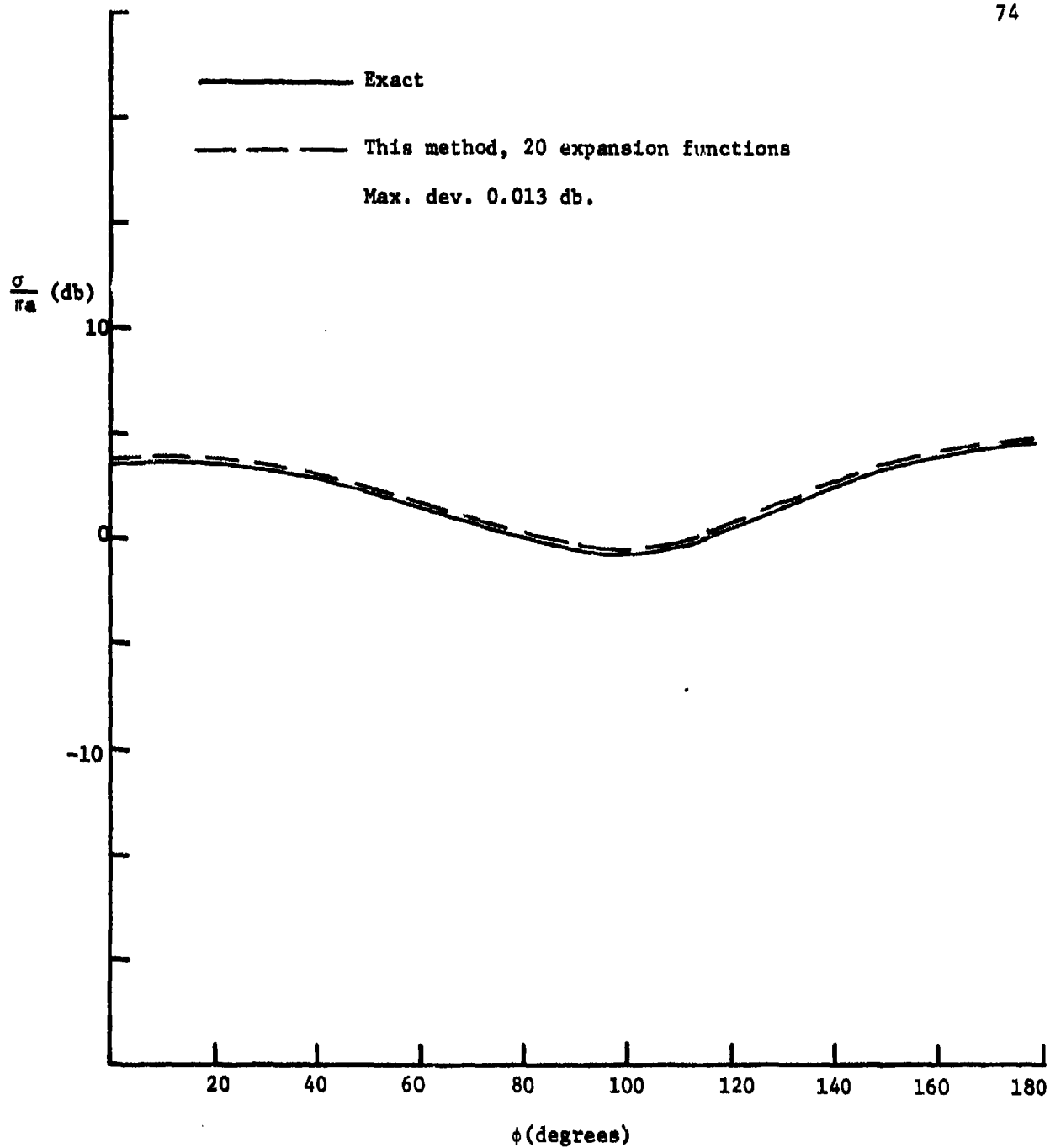


Fig. 4-7. Normalized scattering cross section of a circular cylinder with  $\epsilon_r = 9.0$ ,  $\mu_r = 1.0$ ,  $ka = 1.0$ , perpendicular polarization (TE).

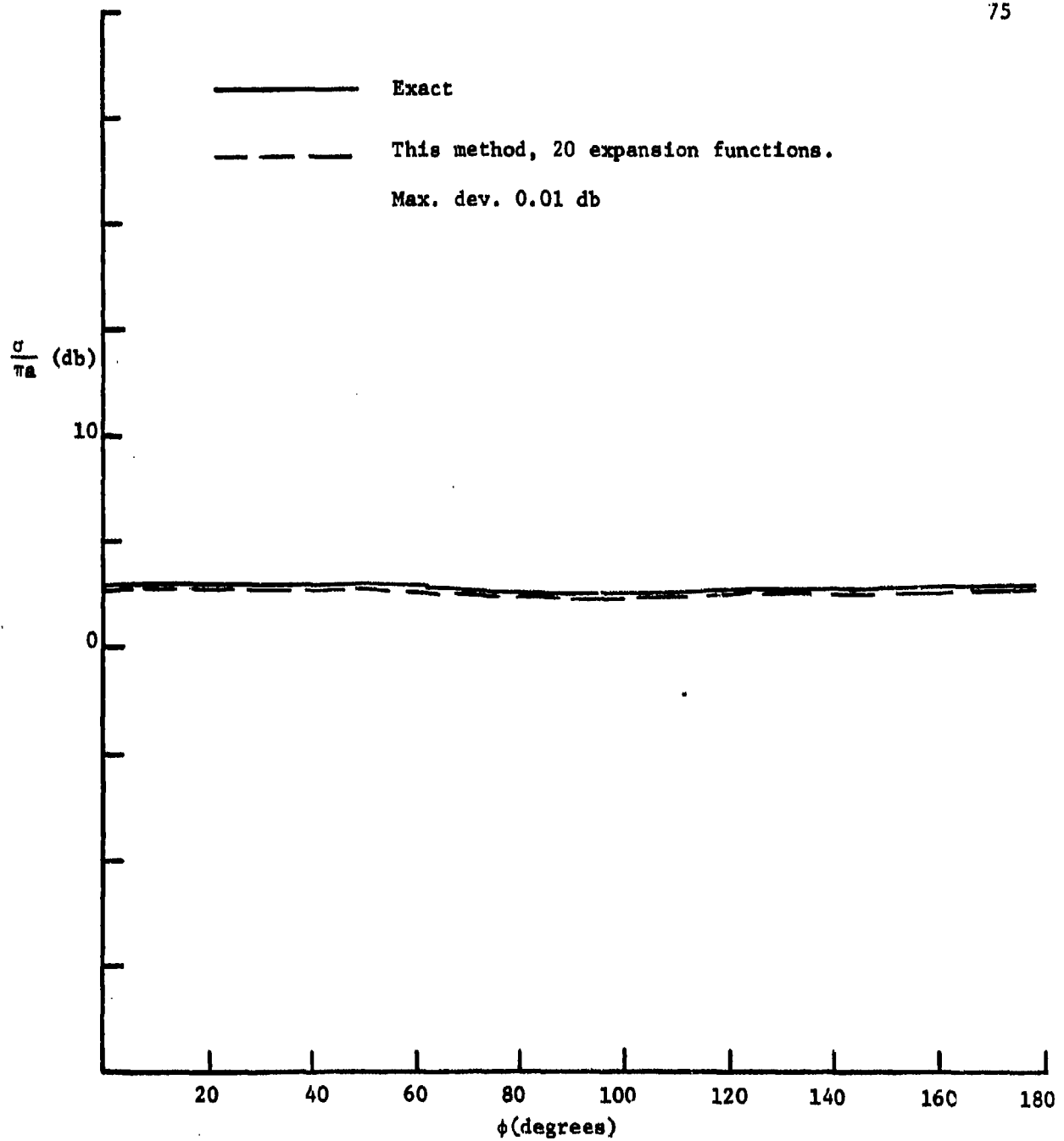


Fig. 4-8. Normalized scattering cross section of a circular cylinder with  $\epsilon_r = 9.0$ ,  $\mu_r = 100.0$ ,  $ka = 0.7$ , perpendicular polarization (TE).



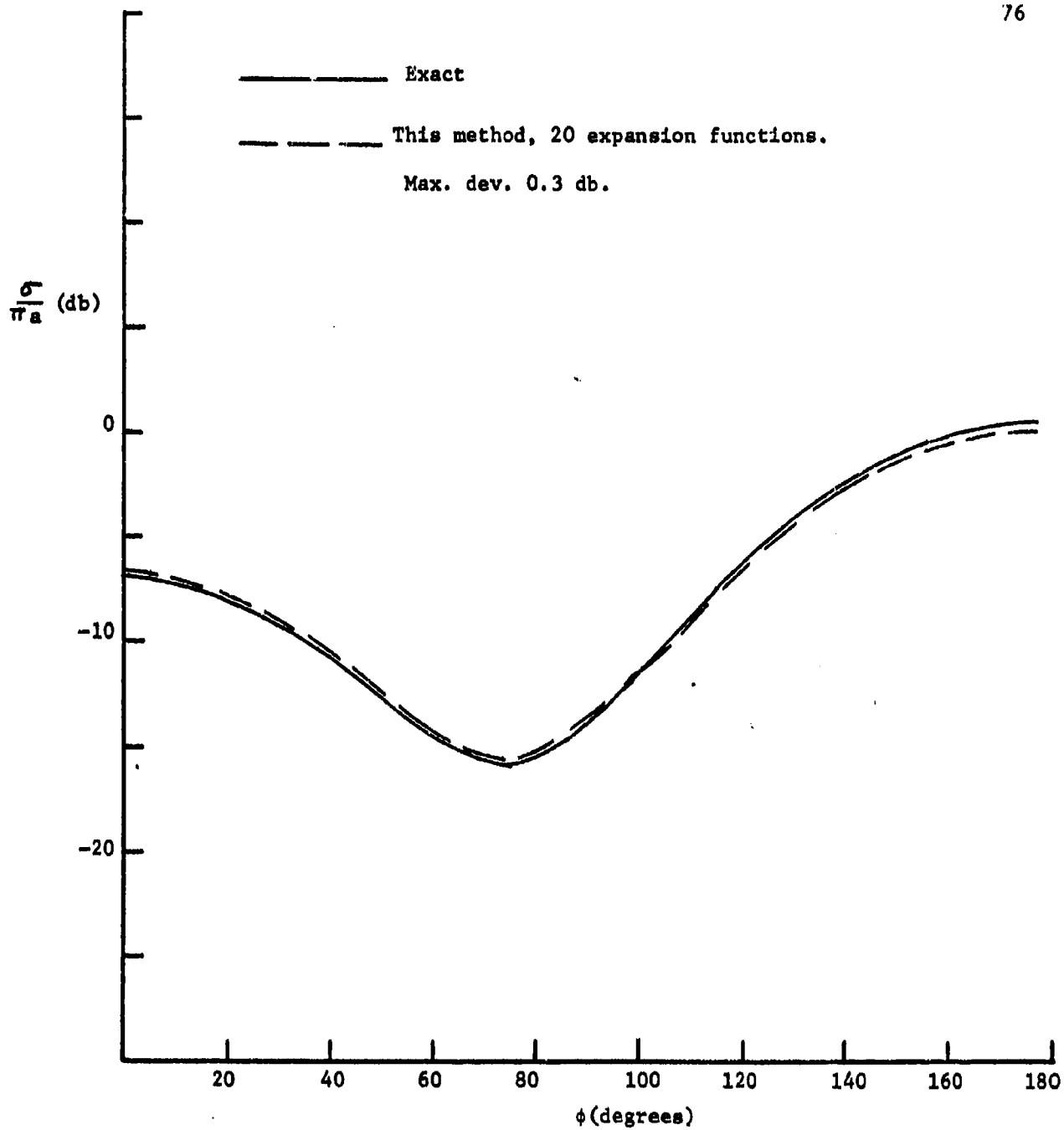


Fig. 4-9. Normalized scattering cross section of a circular cylinder with  $\epsilon_r = 9.0$ ,  $\mu_r = 5.0$ ,  $ka = 0.7$ , perpendicular polarization (TE).

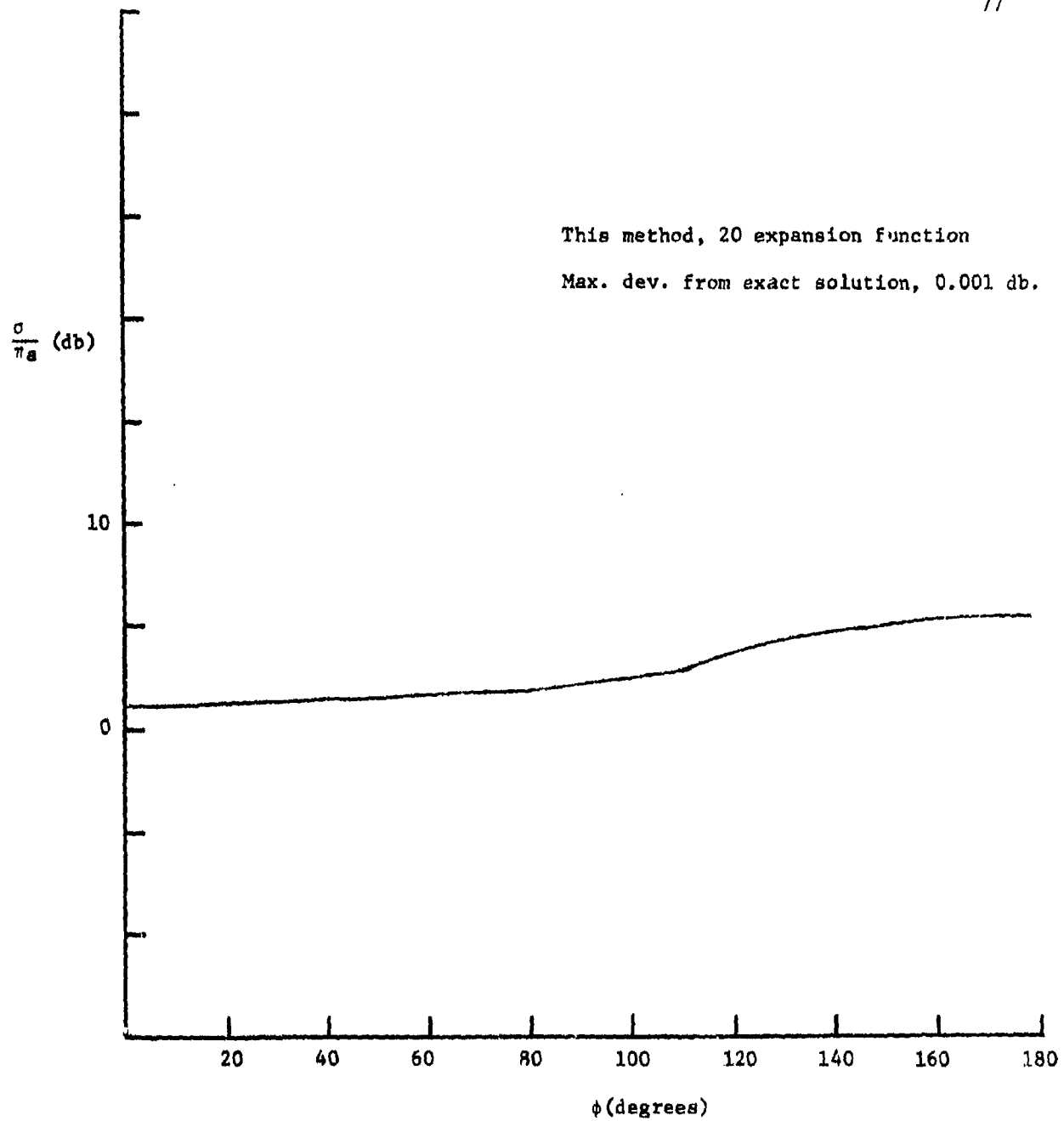


Fig. 4-10. Normalized scattering cross section of a circular cylinder with  $\epsilon_r = 0.001$ ,  $\mu_r = 1000.0$ ,  $ka = 0.7$ , perpendicular polarization (TE).

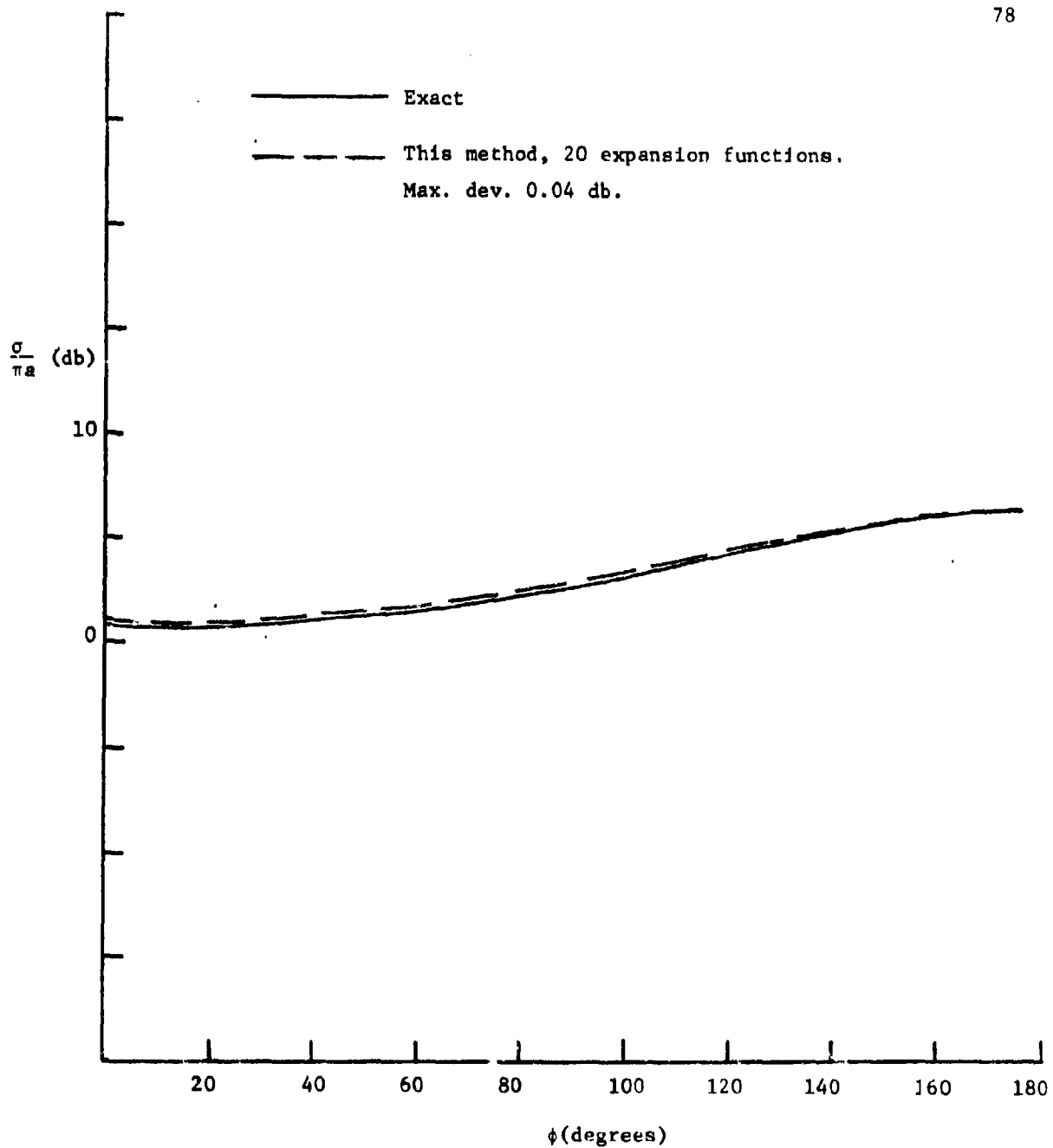


Fig. 4-11. Normalized scattering cross section of a circular cylinder with  $\epsilon_r = 1$ ,  $\mu_r = 1000$ ,  $ka = 0.7$ , perpendicular polarization (TE).

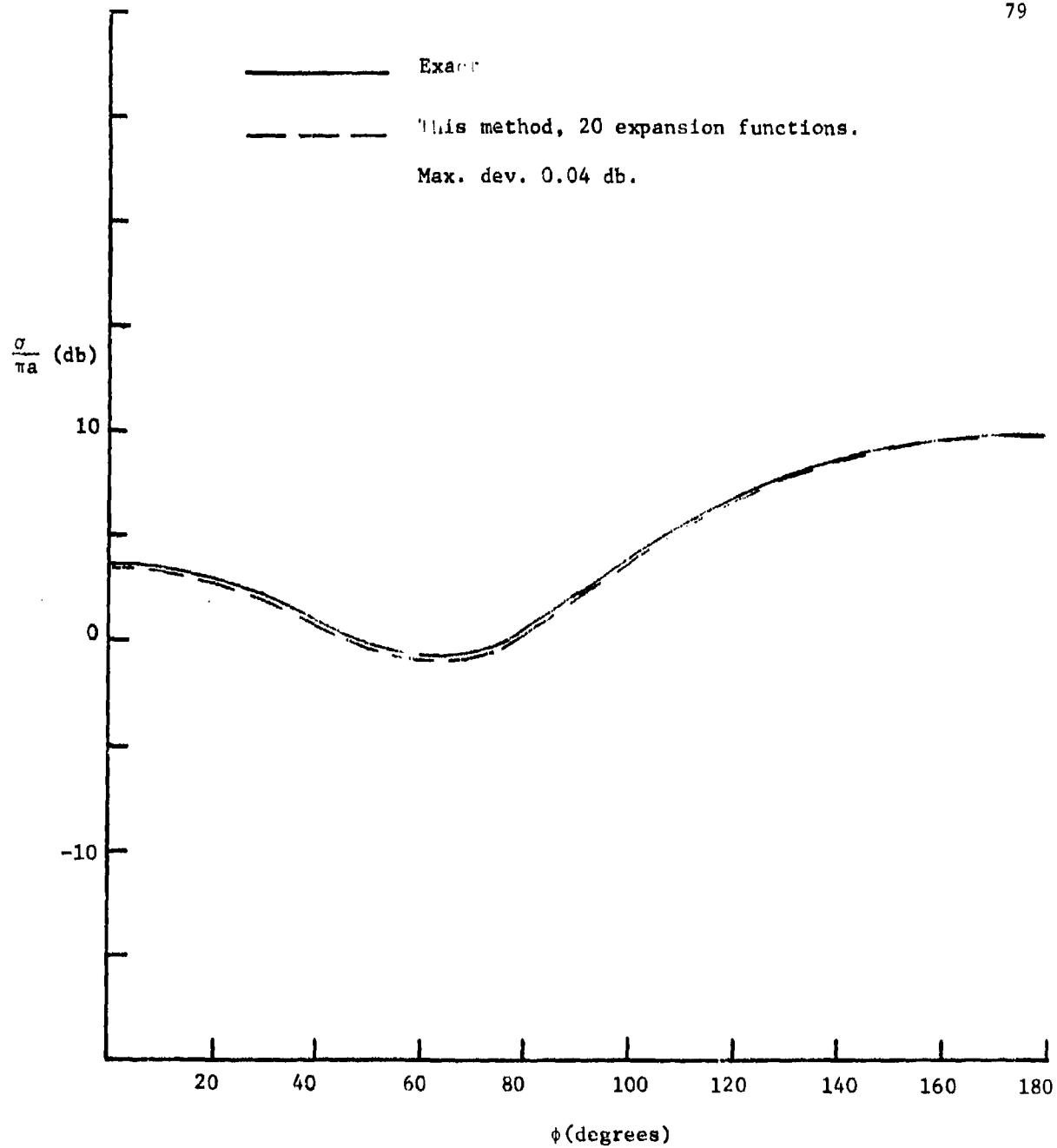


Fig. 4-12. Normalized scattering cross section of a circular cylinder with  $\epsilon_r = 1.0$ ,  $\mu_r = 10.0$ ,  $ka = 0.7$ , perpendicular polarization (TE).

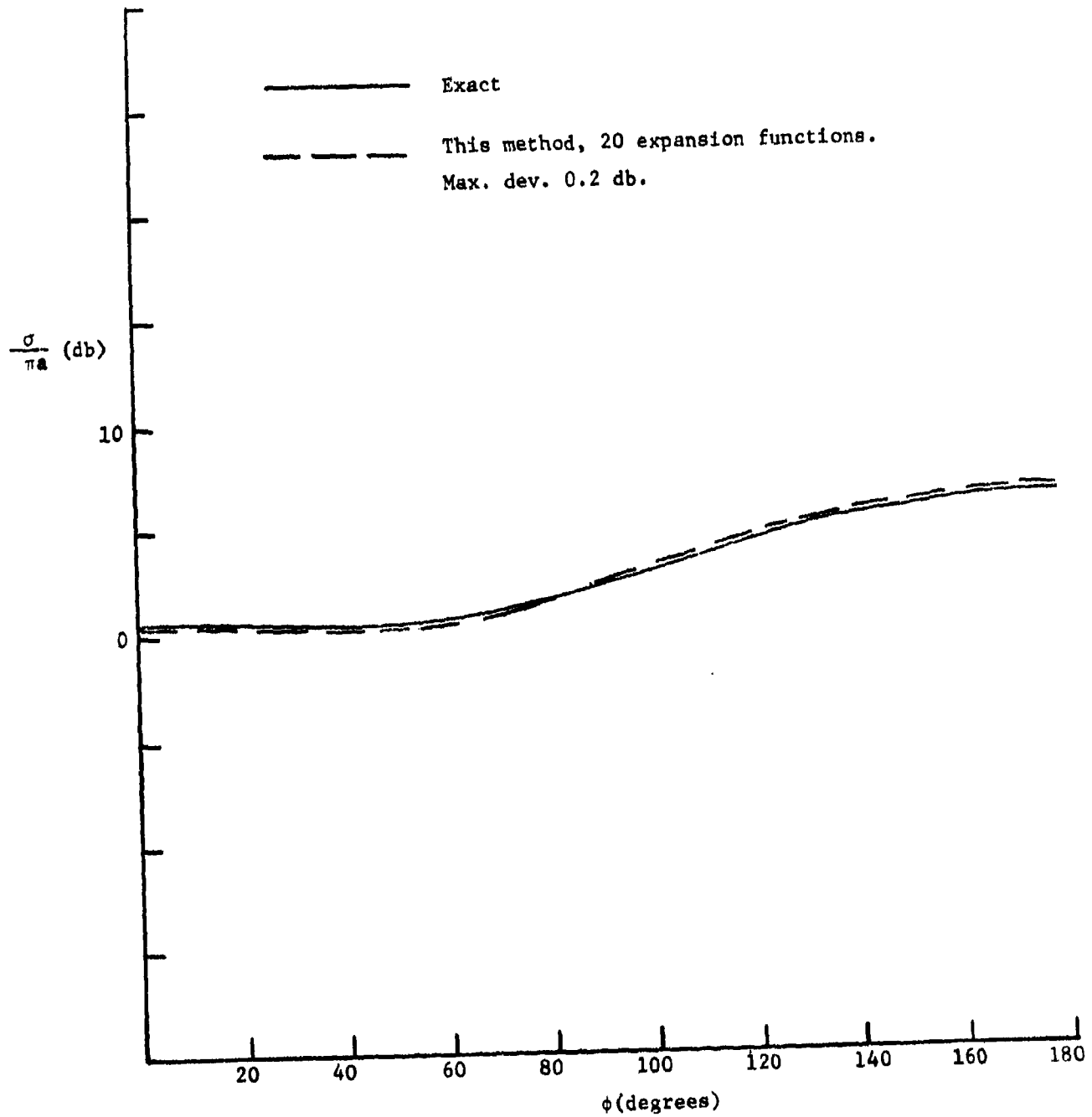


Fig. 4-13. Normalized scattering cross section of a circular cylinder with  $\epsilon_r = 1.0$ ,  $\mu_r = 300$ ,  $ka = 0.7$ , perpendicular polarization (TE).

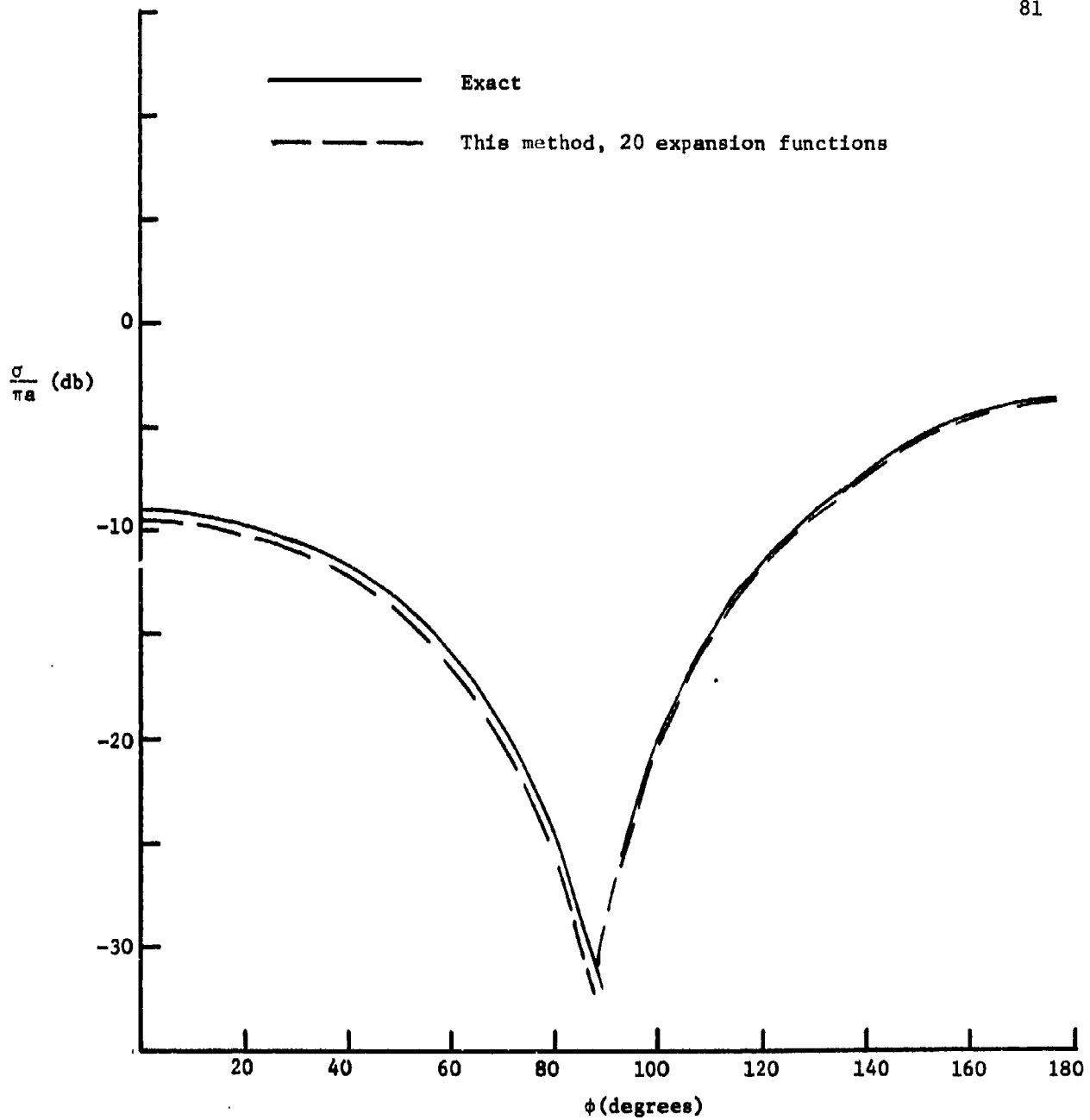


Fig. 4-14. Normalized scattering cross section of a circular cylinder with  $\epsilon_r = 2.56$ ,  $\mu_r = 1.0$ ,  $ka = 0.7$ , perpendicular polarization (TE).

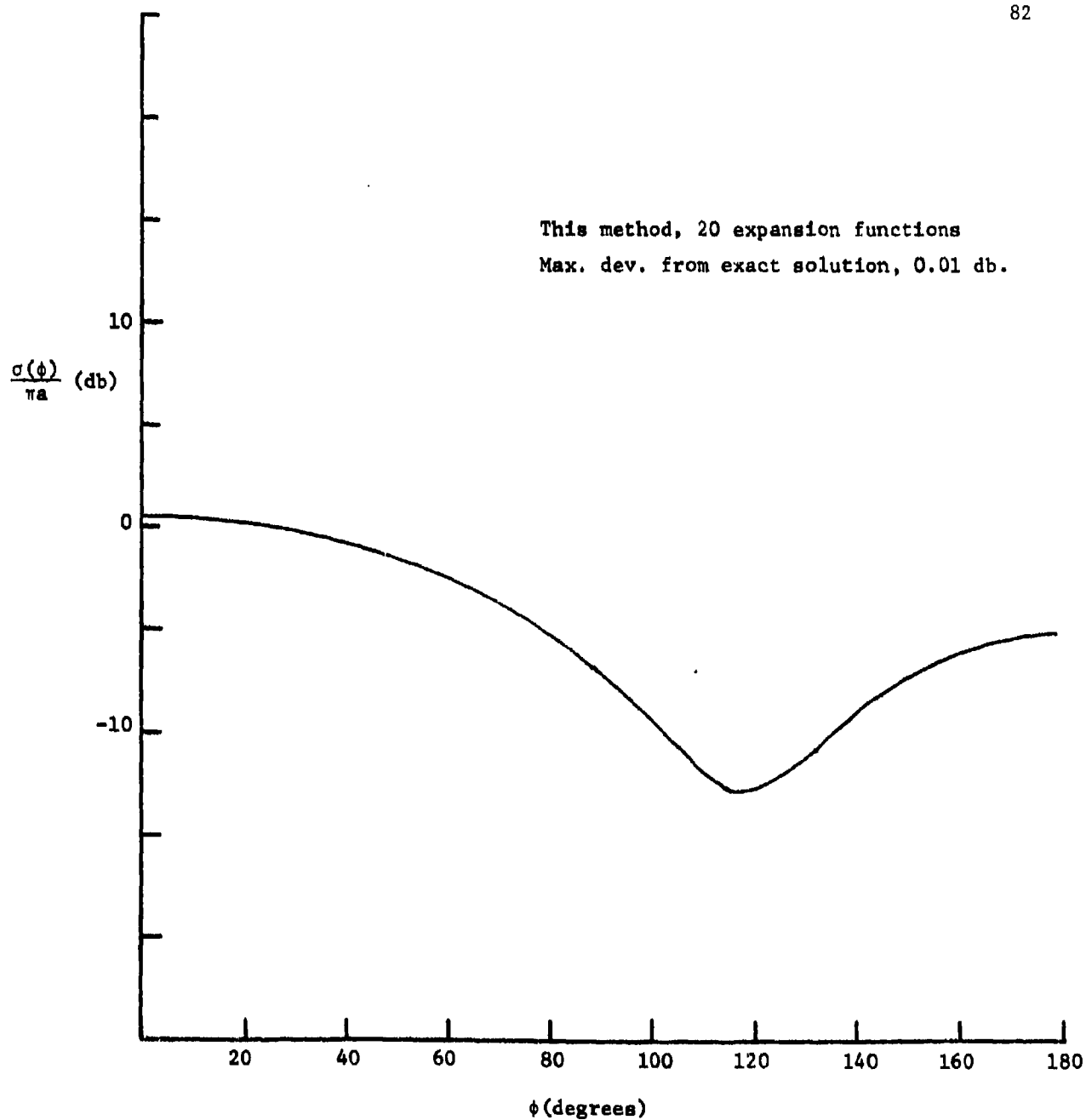


Fig. 4-15. Normalized scattering cross section of a circular cylinder with  $\epsilon_r = 1000.0$ ,  $\mu_r = 0.001$ ,  $ka = 0.7$ , perpendicular polarization (TE).

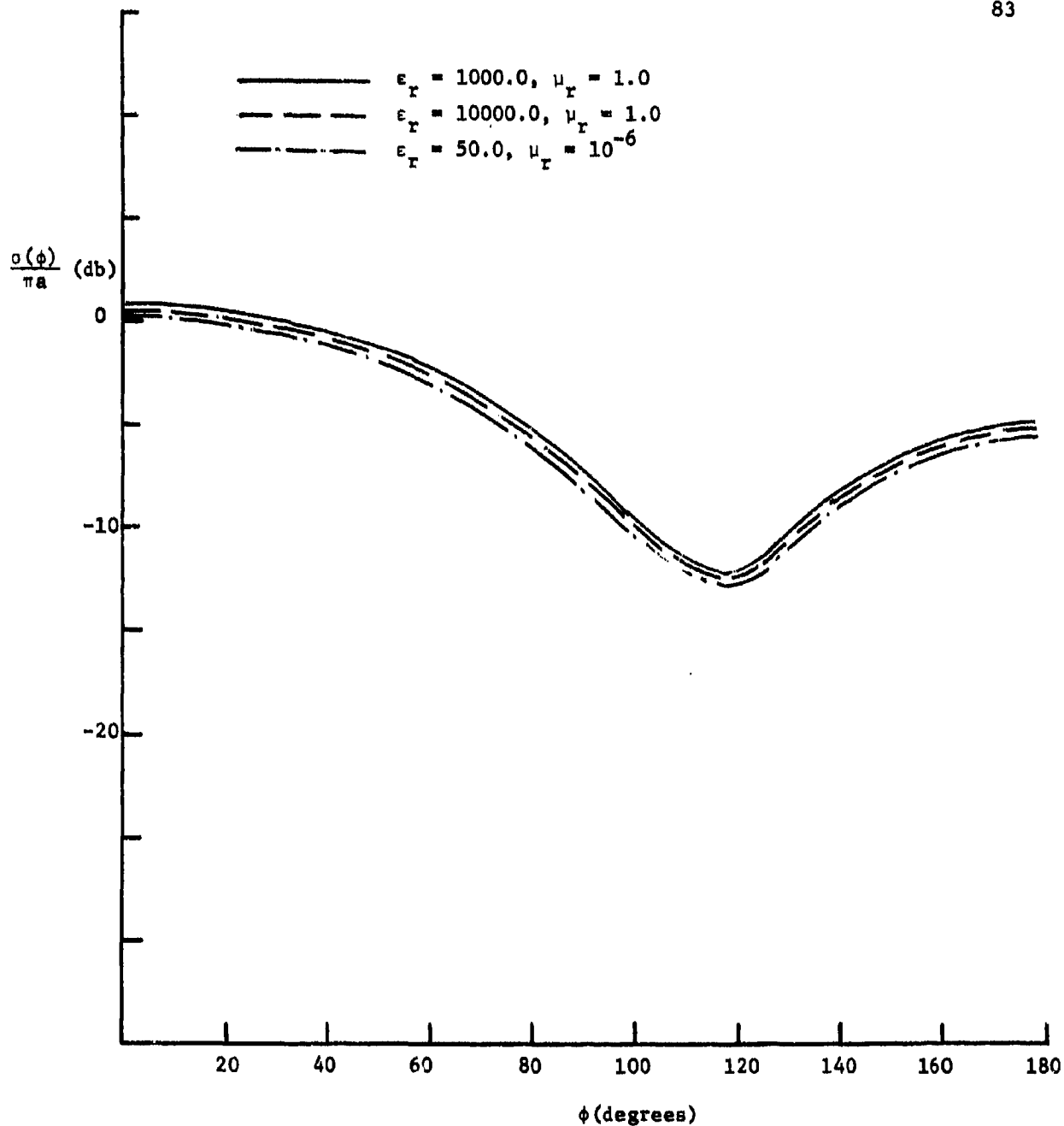


Fig. 4-16. Normalized scattering cross section of a circular cylinder with  $ka = 0.7$ , perpendicular polarization (TE).



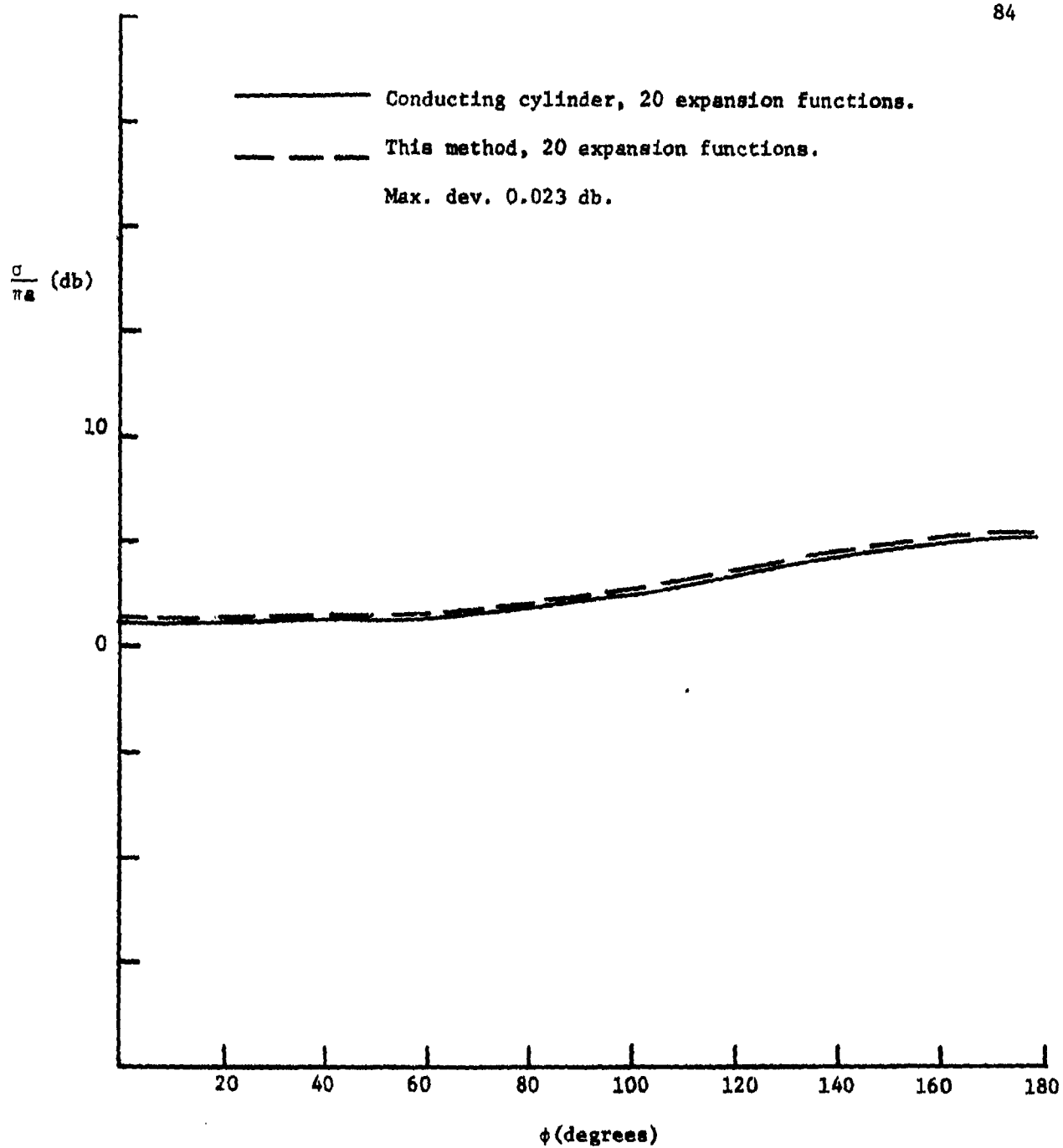


Fig. 4-17. Normalized scattering cross section of a circular cylinder with  $\epsilon_r = 1000.0$ ,  $\mu_r = 0.001$ ,  $ka = 0.7$ , parallel polarization (TM).

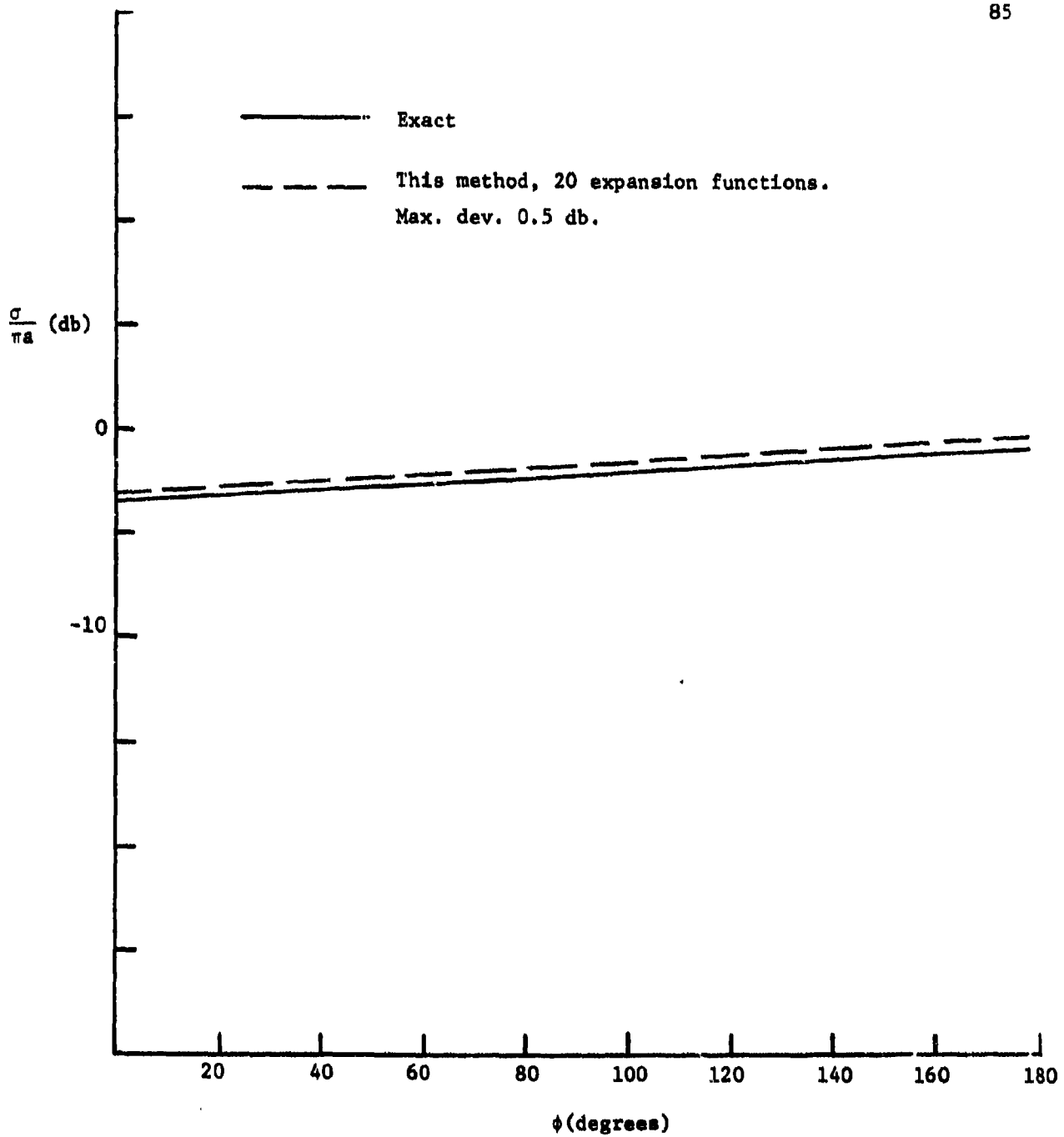


Fig. 4-18. Normalized scattering cross section of a circular cylinder with  $\epsilon_r = 2.56$ ,  $\mu_r = 1.0$ ,  $ka = 0.7$ , parallel polarization (TM).

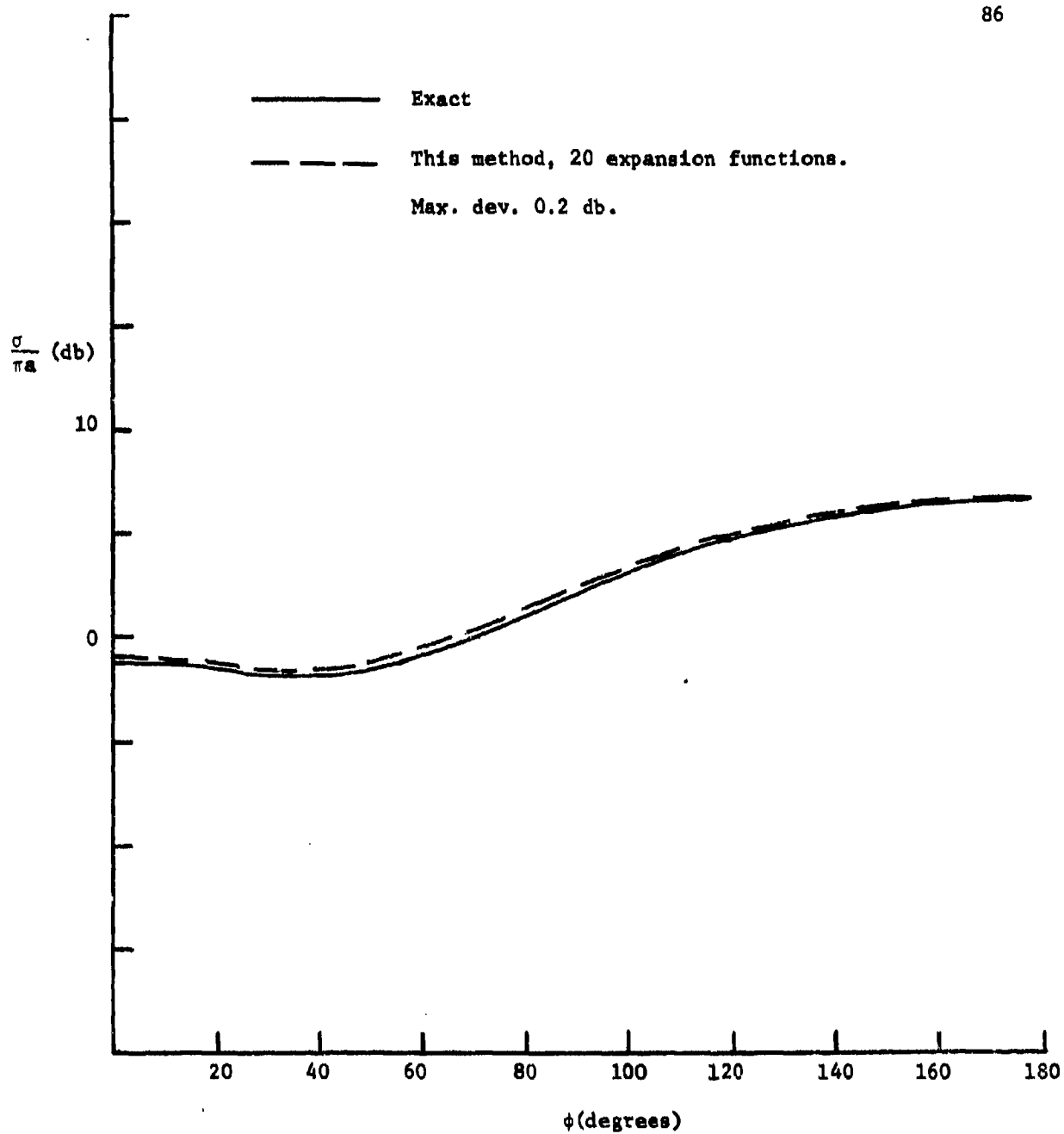


Fig. 4-19. Normalized scattering cross section of a circular cylinder with  $\epsilon_r = 20.0$ ,  $\mu_r = 1.0$ ,  $ka = 0.7$ , parallel polarization (TM).

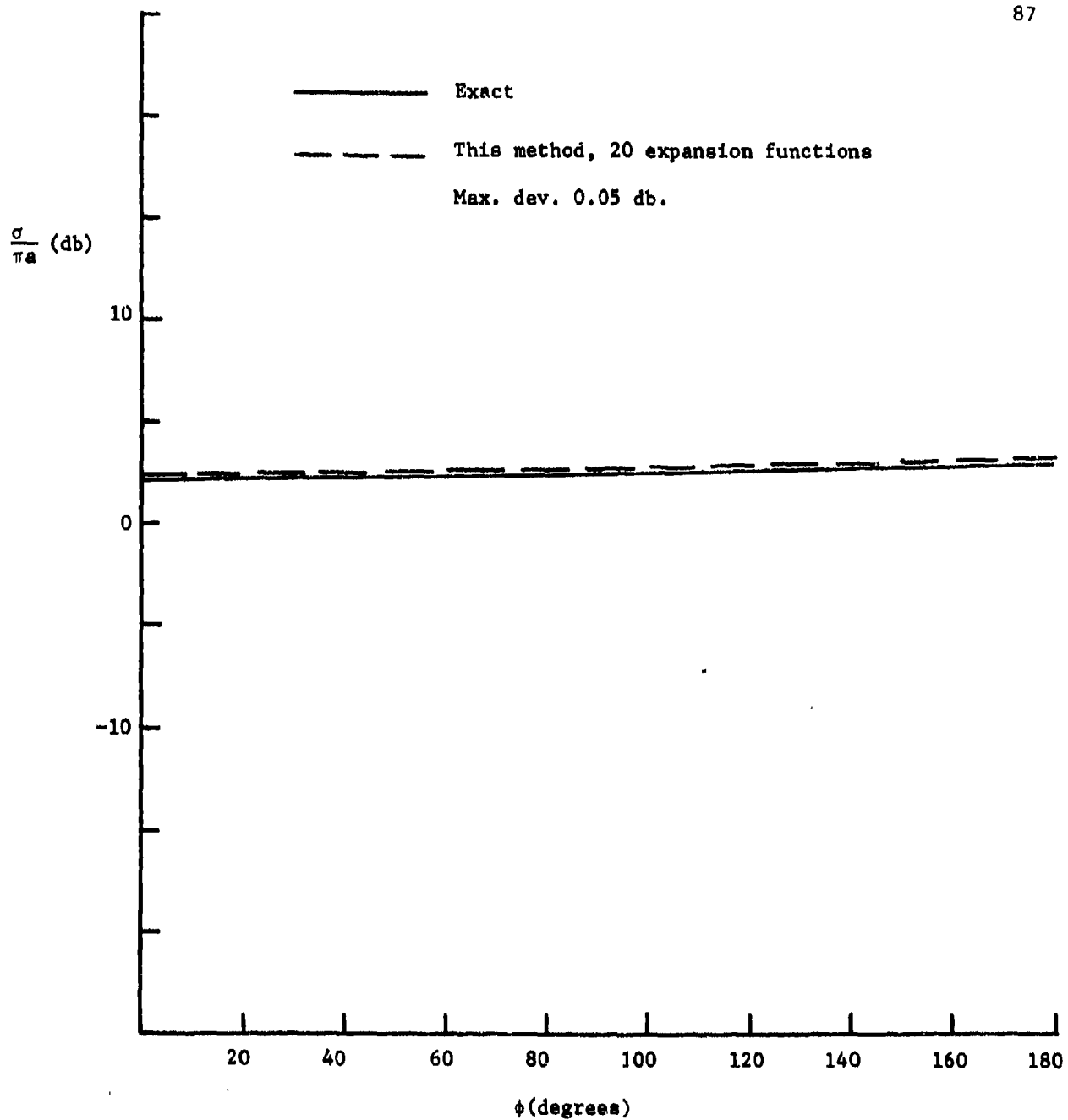


Fig. 4-20. Normalized scattering cross section of a circular cylinder with  $\epsilon_r = 50.0$ ,  $\mu_r = 1.0$ ,  $ka = 0.7$ , parallel polarization (TM).

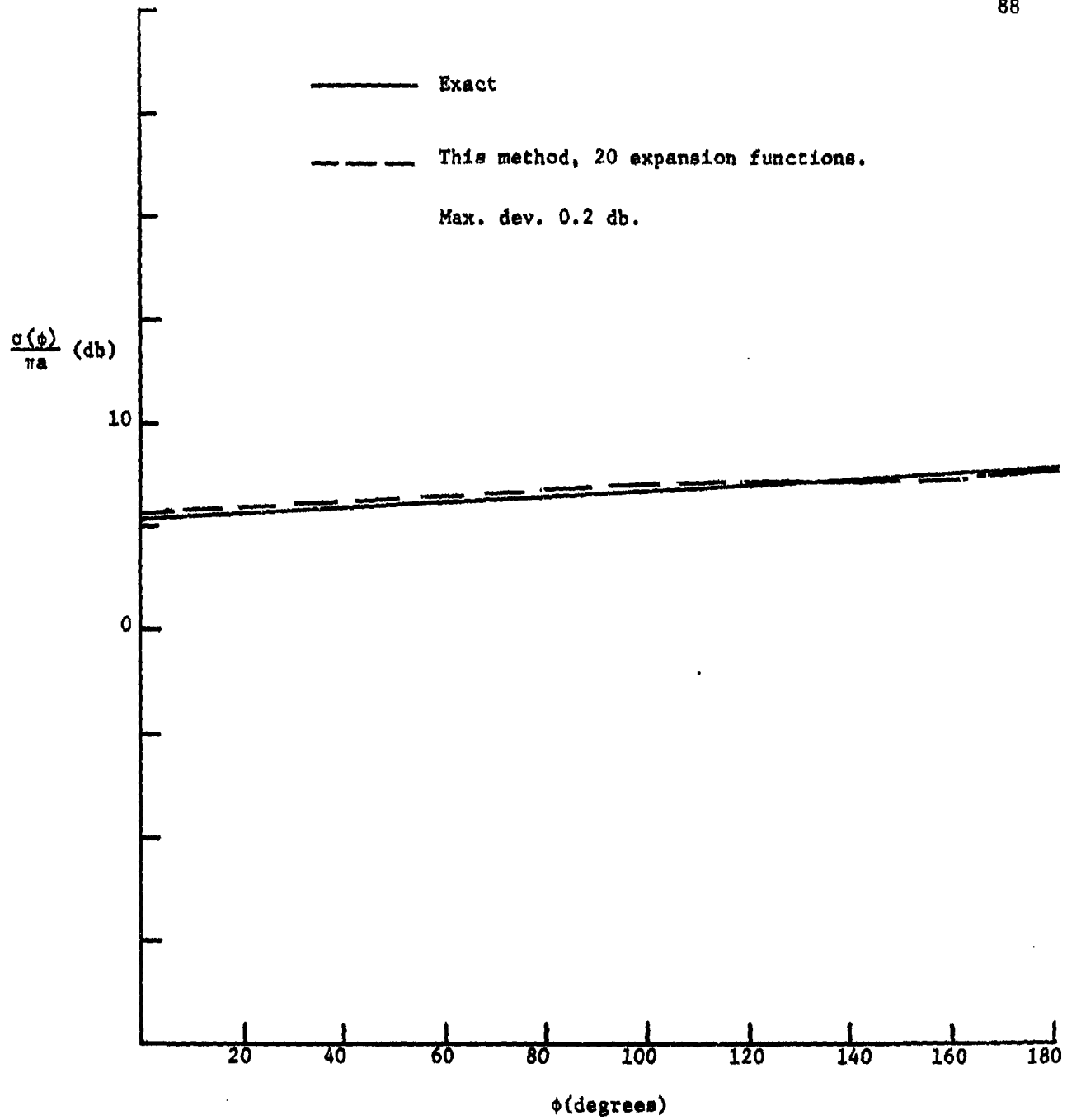


Fig. 4-21. Normalized scattering cross section of a circular material cylinder, with  $\epsilon_r = 4.0$ ,  $\mu_r = 1.0$ ,  $ka = 0.7$  parallel polarization (TM).

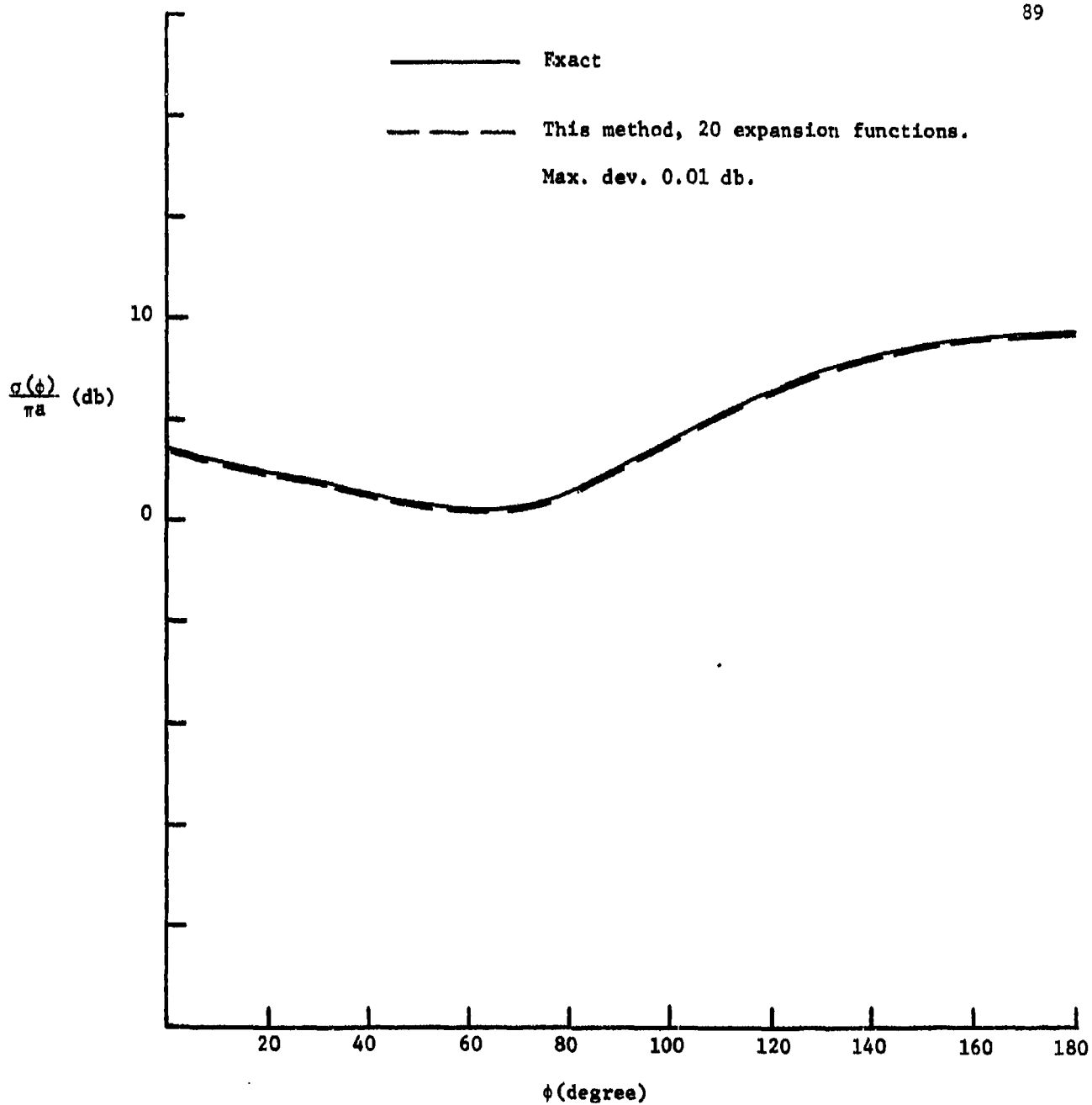


Fig. 22. Normalized scattering cross section of a circular cylinder with  $\epsilon_r = 9.5$ ,  $\mu_r = 1.0$ .

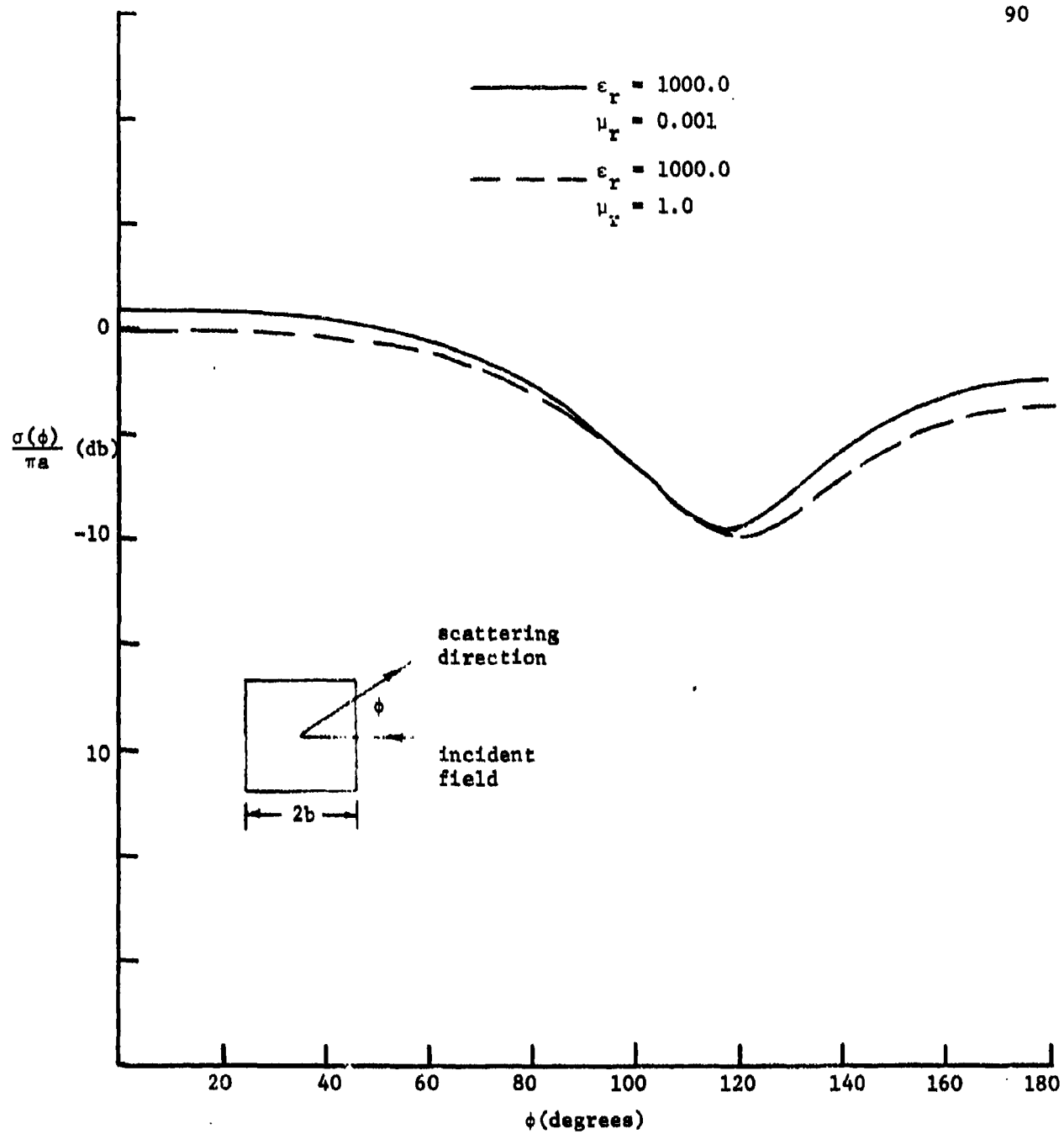


Fig. 4-23. Normalized scattering cross section of a square cylinder with  $kb = 1.4$ , perpendicular polarization (TE).

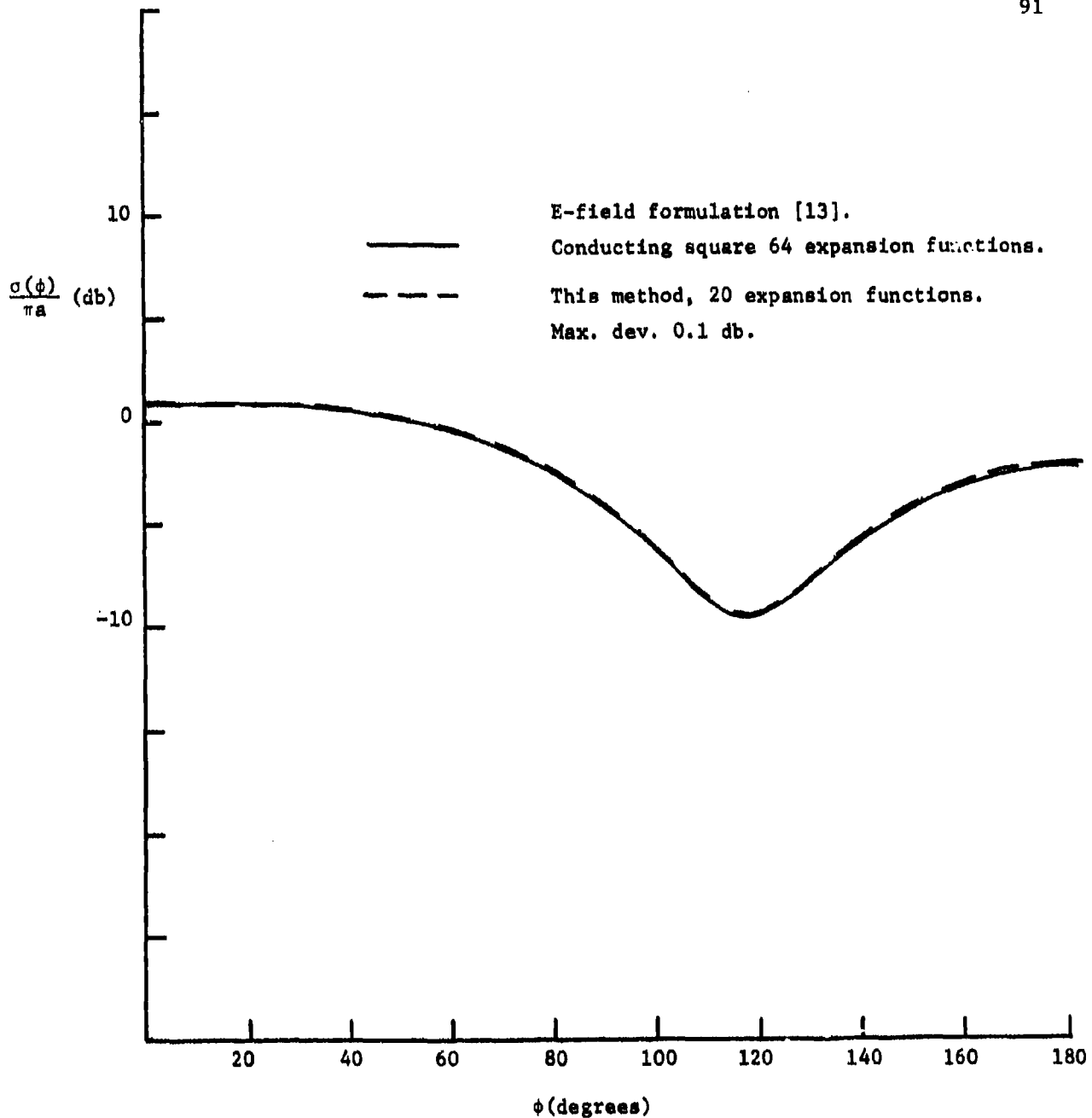


Fig. 4-24. Normalized scattering cross section of a square cylinder with  $\epsilon_r = 10000.0$ ,  $\mu_r = 0.0001$ ,  $kb = 1.4$ , perpendicular polarization (TE).



This method, 20 expansion functions.

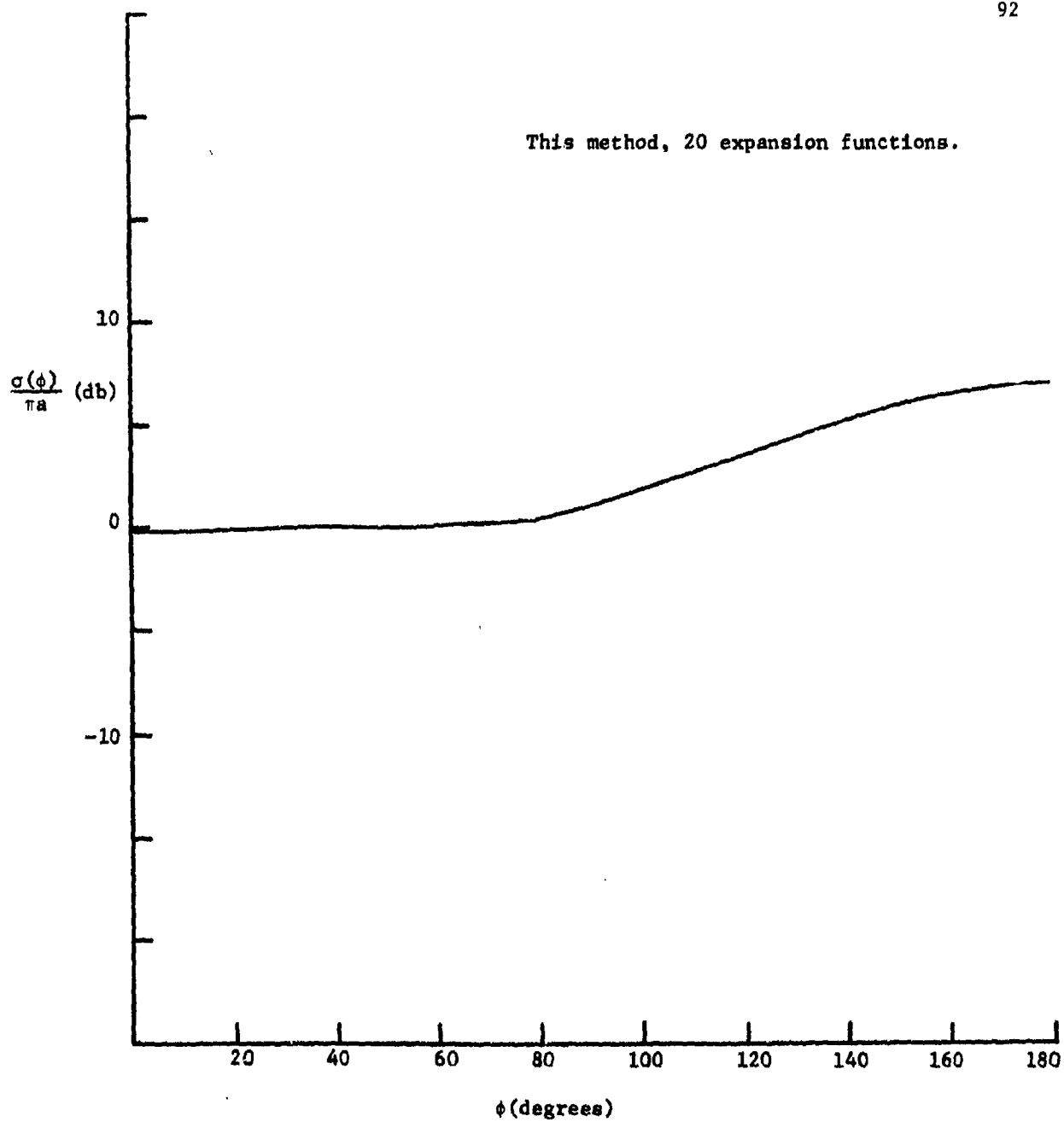


Fig. 4-25. Normalized scattering cross section of a square cylinder with  $\epsilon_r = 9.0$ ,  $\mu_r = 1.0$ ,  $kb = 1.4$ , perpendicular polarization (TE).

This method, 20 expansion functions.

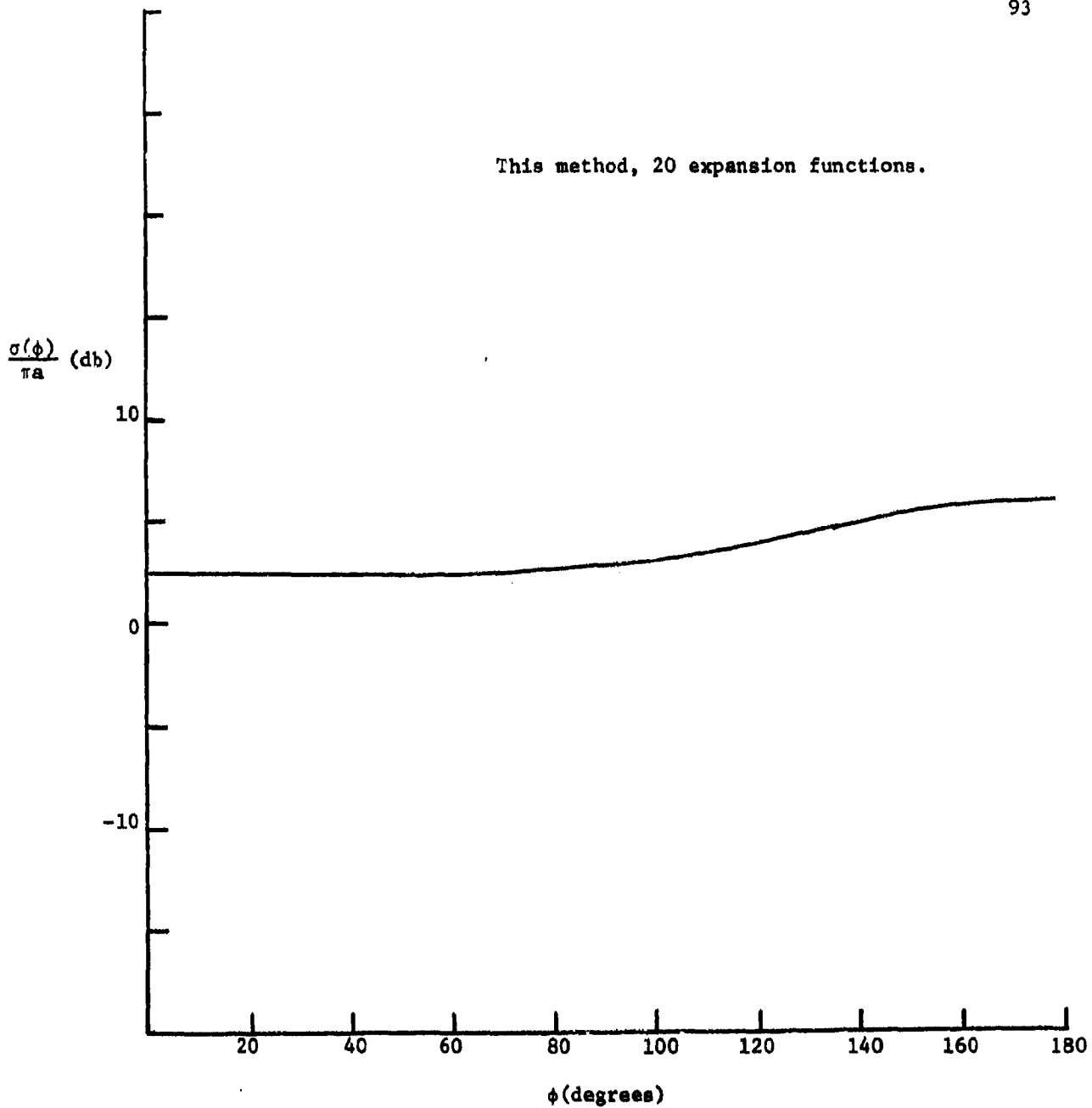


Fig. 4-26. Normalized scattering cross section of a square cylinder with  $\epsilon_r = 100.0$ ,  $\mu_r = 1.0$ ,  $kb = 1.4$ , parallel polarization (TM).

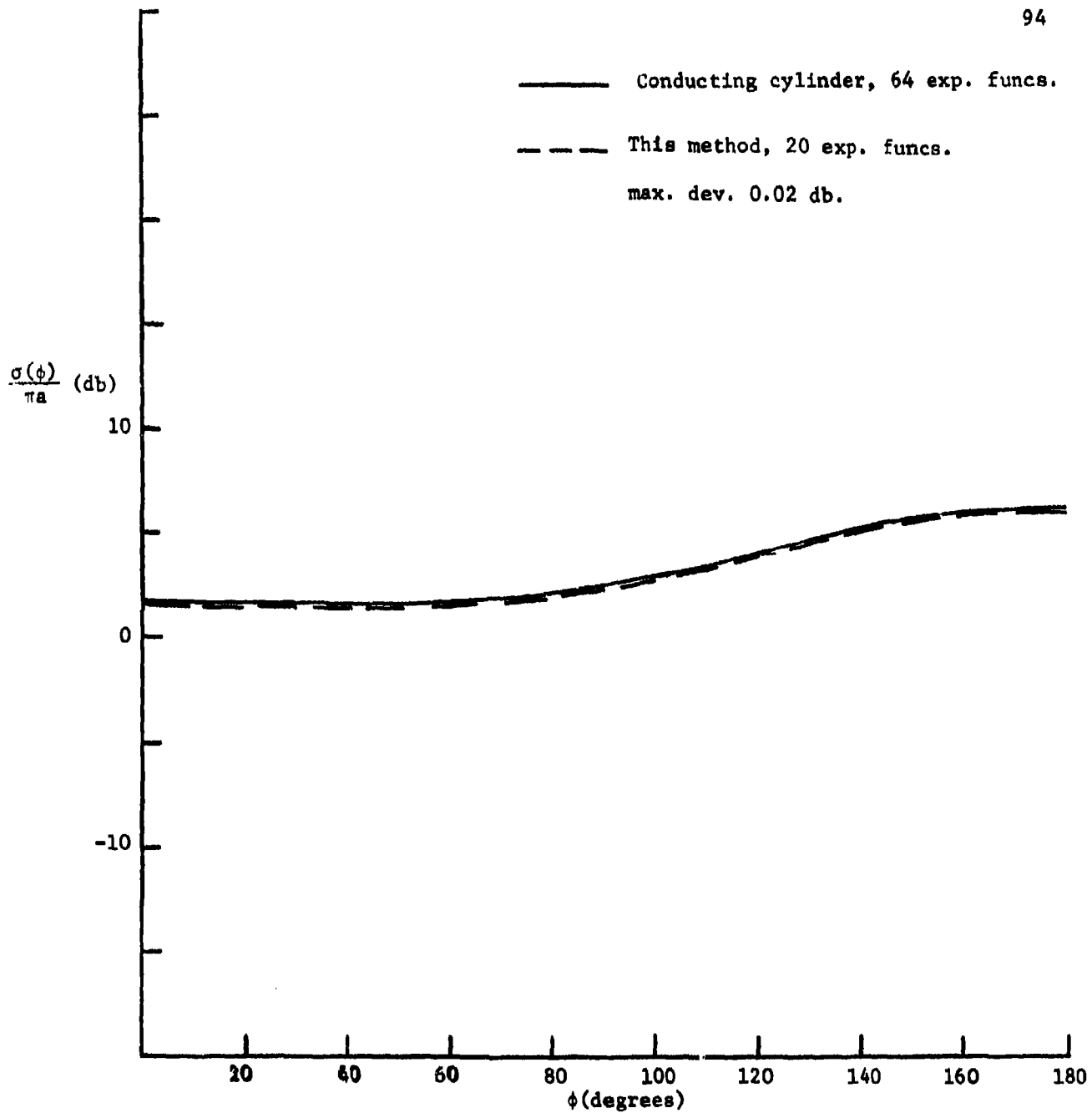


Fig. 4-27. Normalized scattering cross section of a square cylinder with  $\epsilon_r = 10000.0$ ,  $\mu_r = 0.0001$ ,  $kb = 1.4$ , parallel polarization (TM).

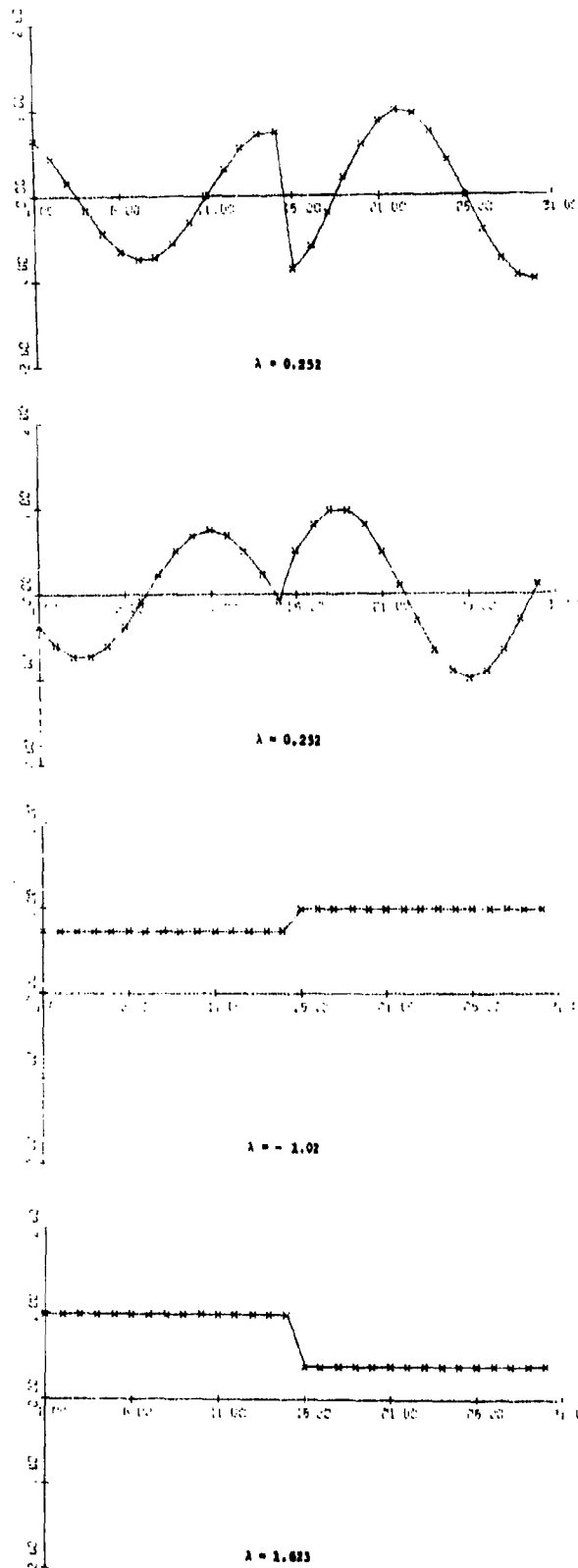


FIG. 4-20. Characteristic currents for a circular cylinder,  $\epsilon_p = 9.5$ ,  $k_0 = 0.7$ , perpendicular polarization.

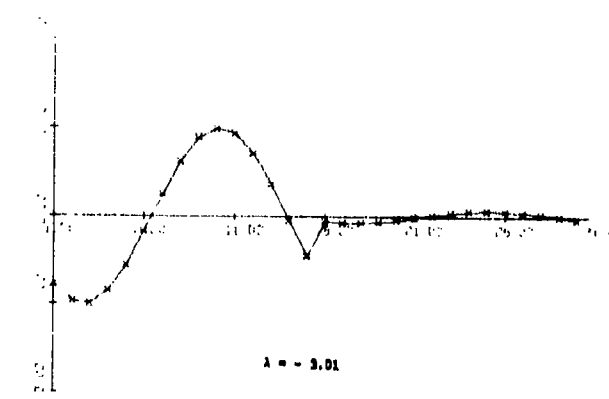
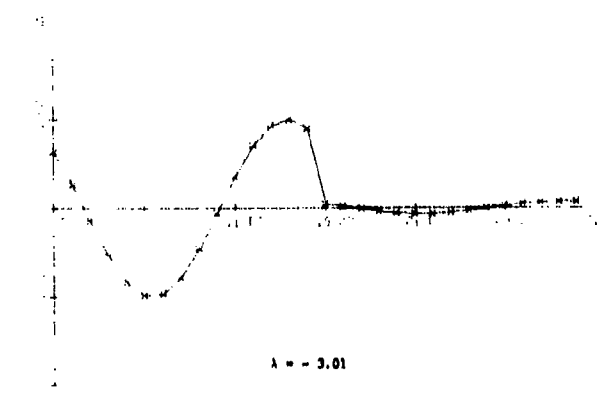
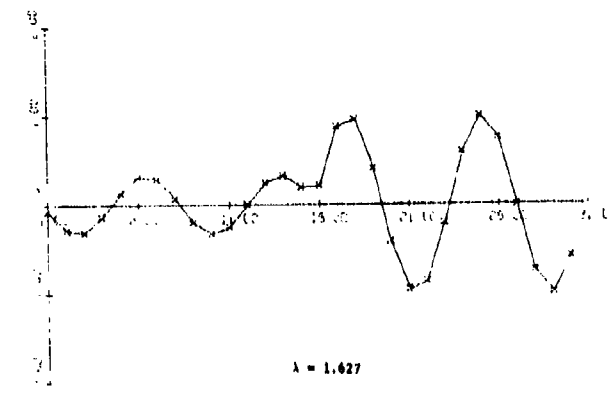
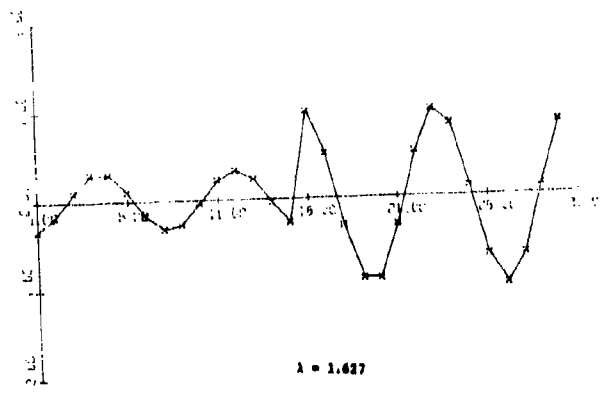
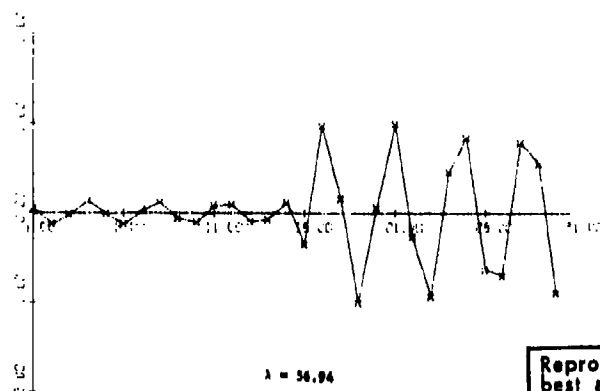
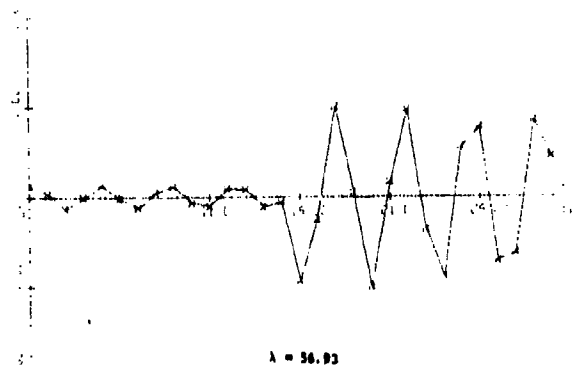
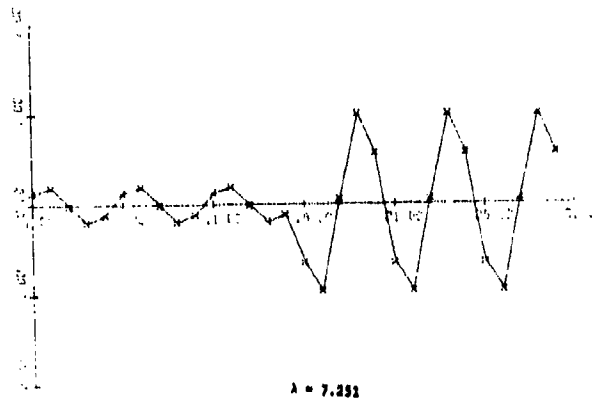
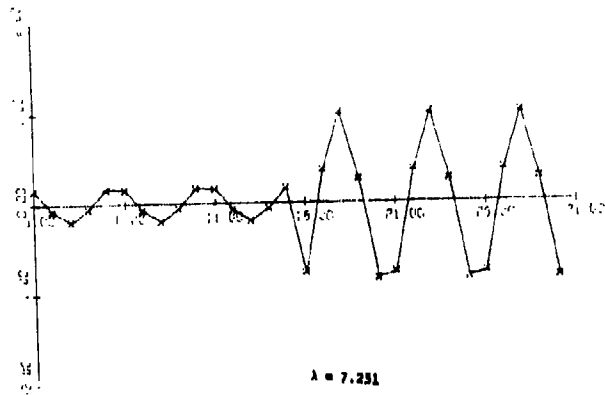


Fig. 4-28 continued



Reproduced from best available copy.

Fig. 4-28 continued

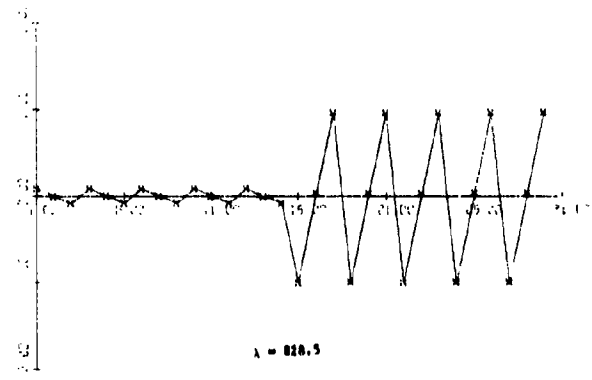
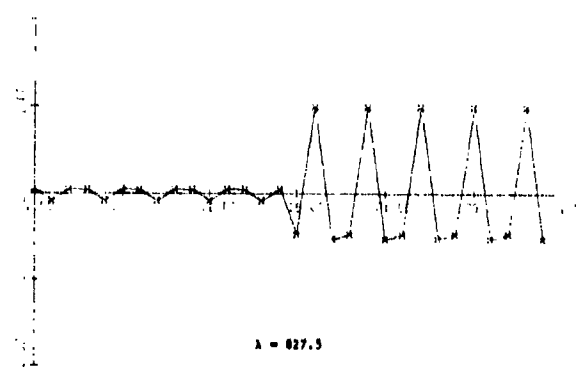
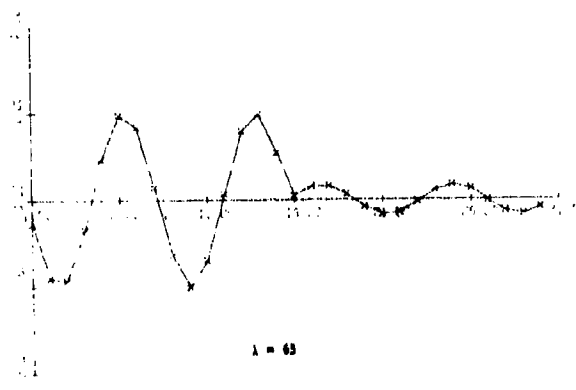
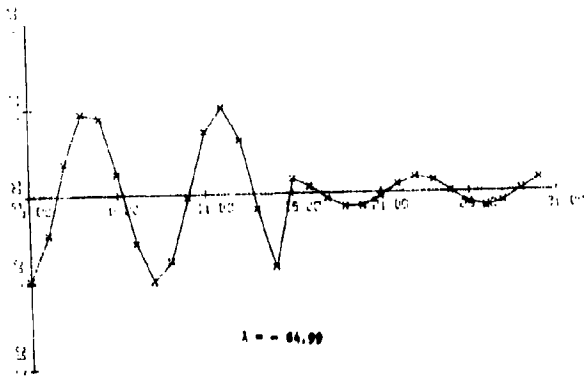
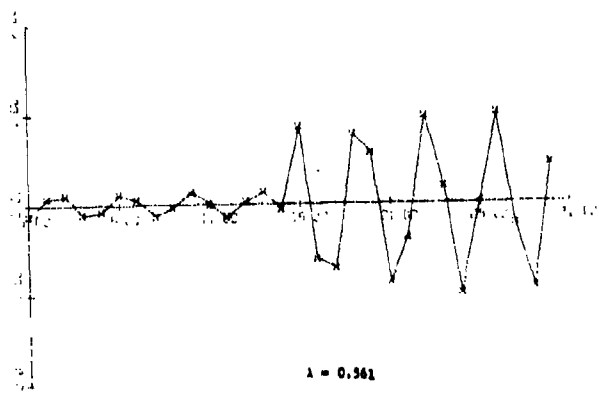
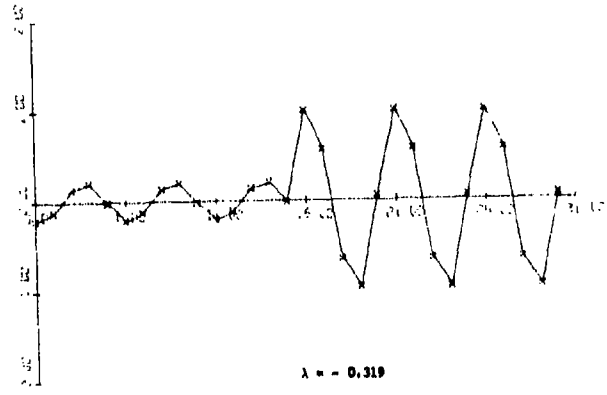
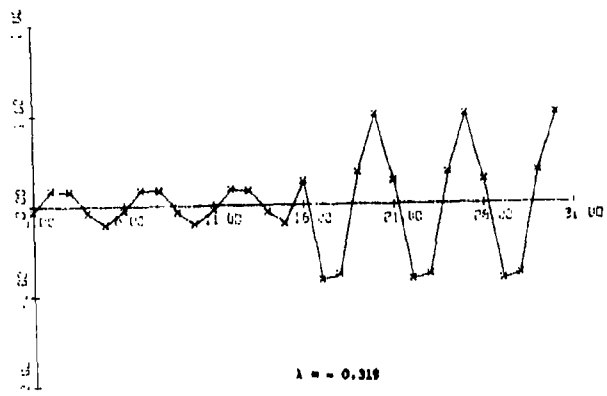


Fig. 4-20 continued.



Reproduced from  
best available copy.

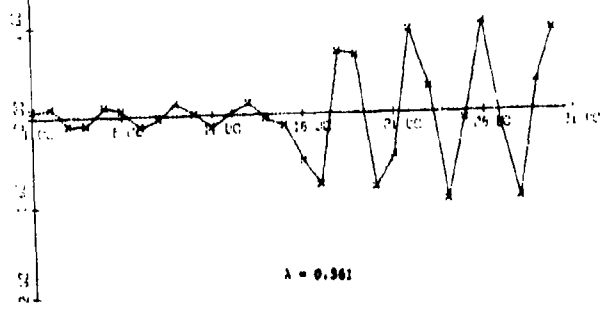


Fig. 4-29. Characteristic currents for a circular cylinder,  $\epsilon_p = 50.0$ ,  $ka = 0.7$ , perpendicular polarization.



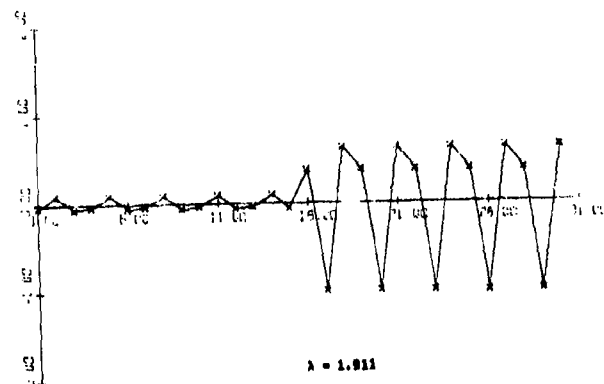
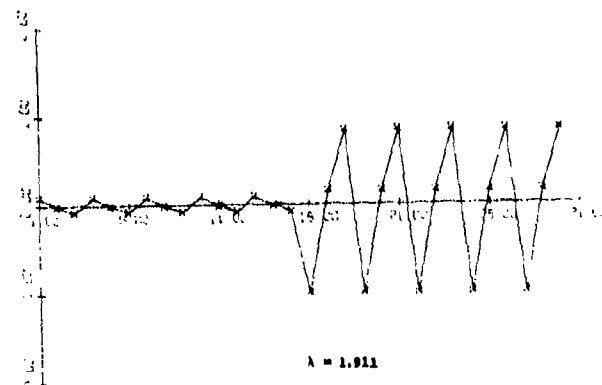
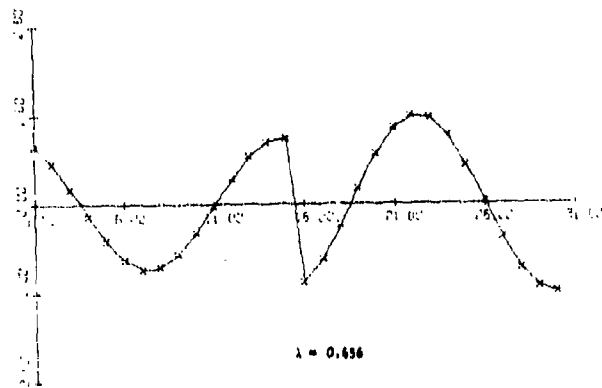
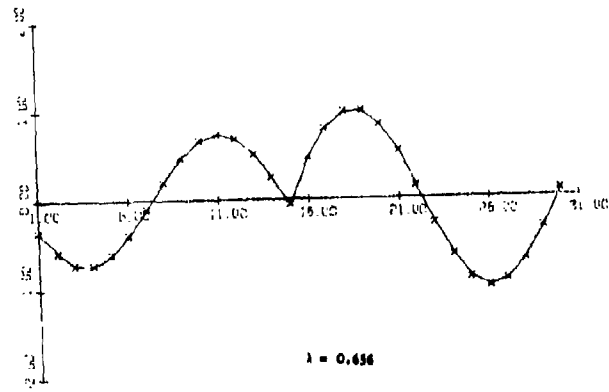


Fig. 4-22. continued.

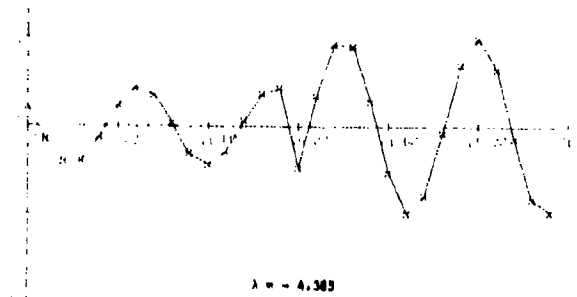
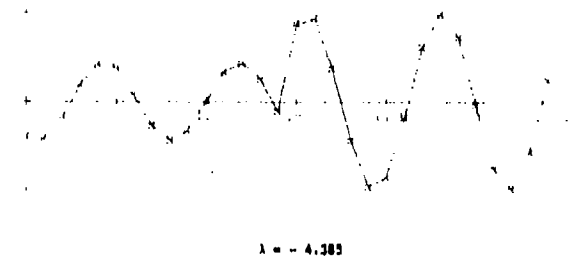
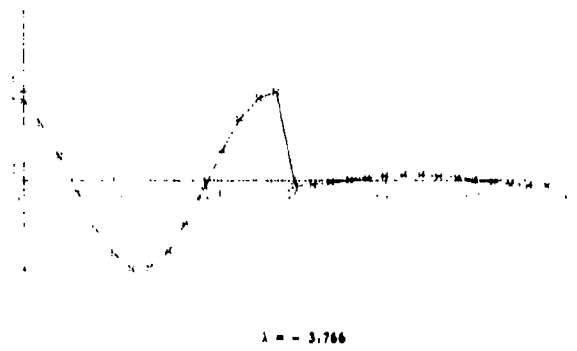
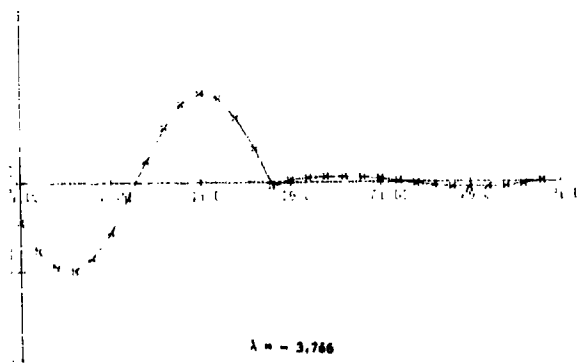


Fig. 4-29. continued.

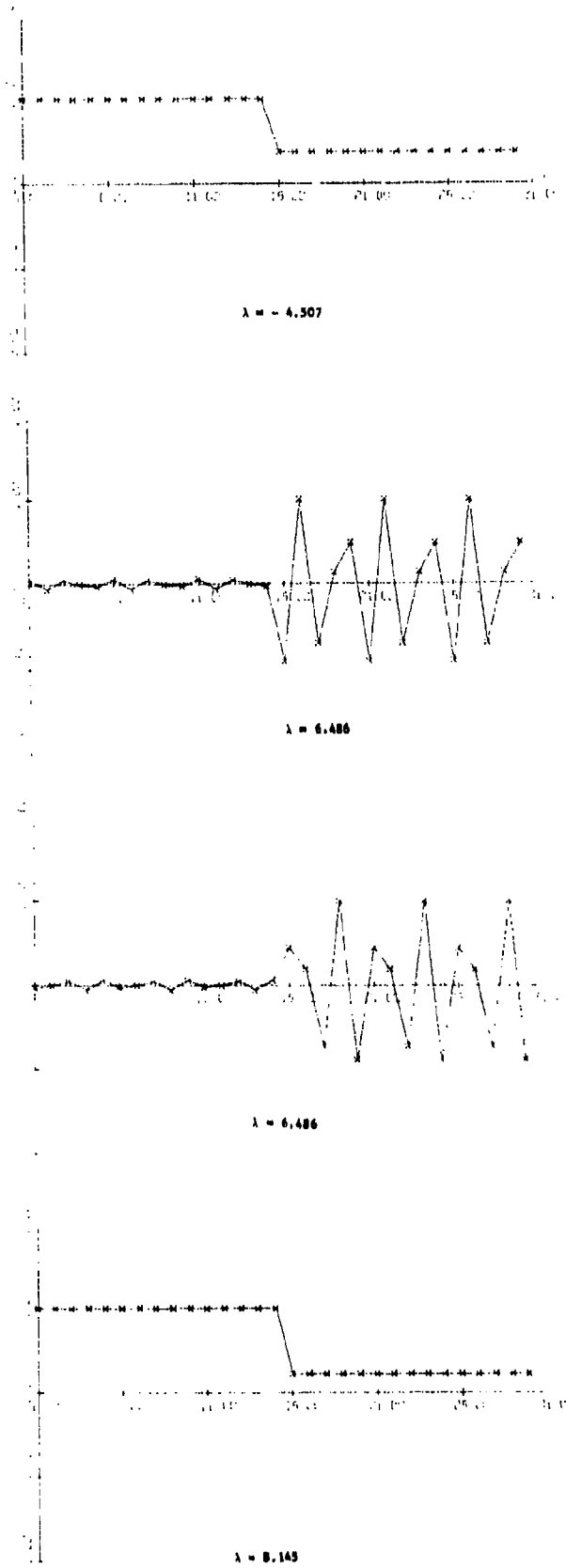


Fig. 4-29. Continued.

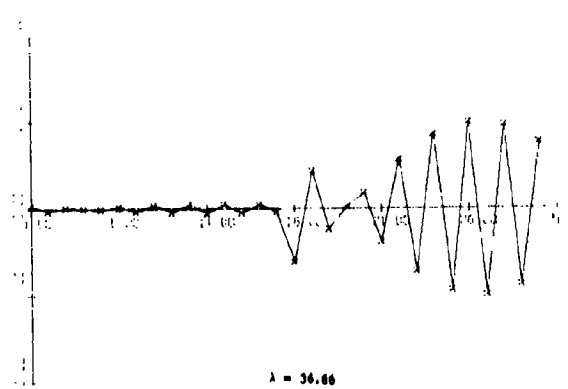
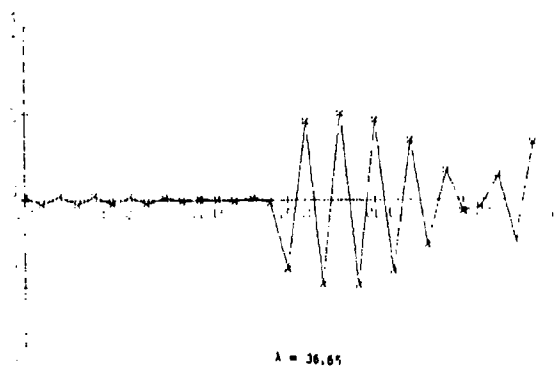
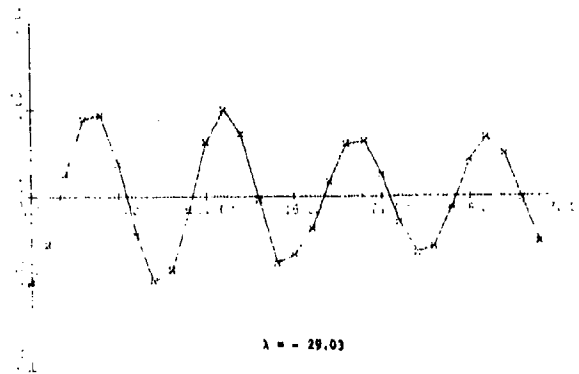
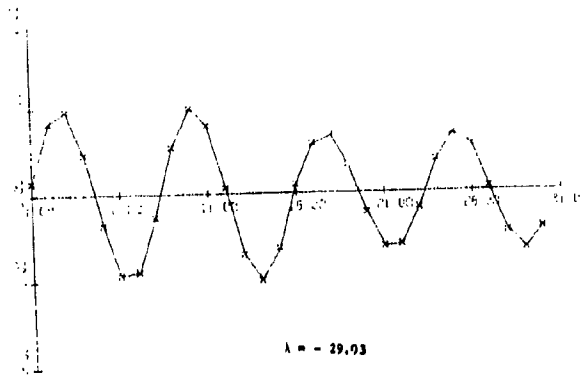


Fig. 4-29. continued.

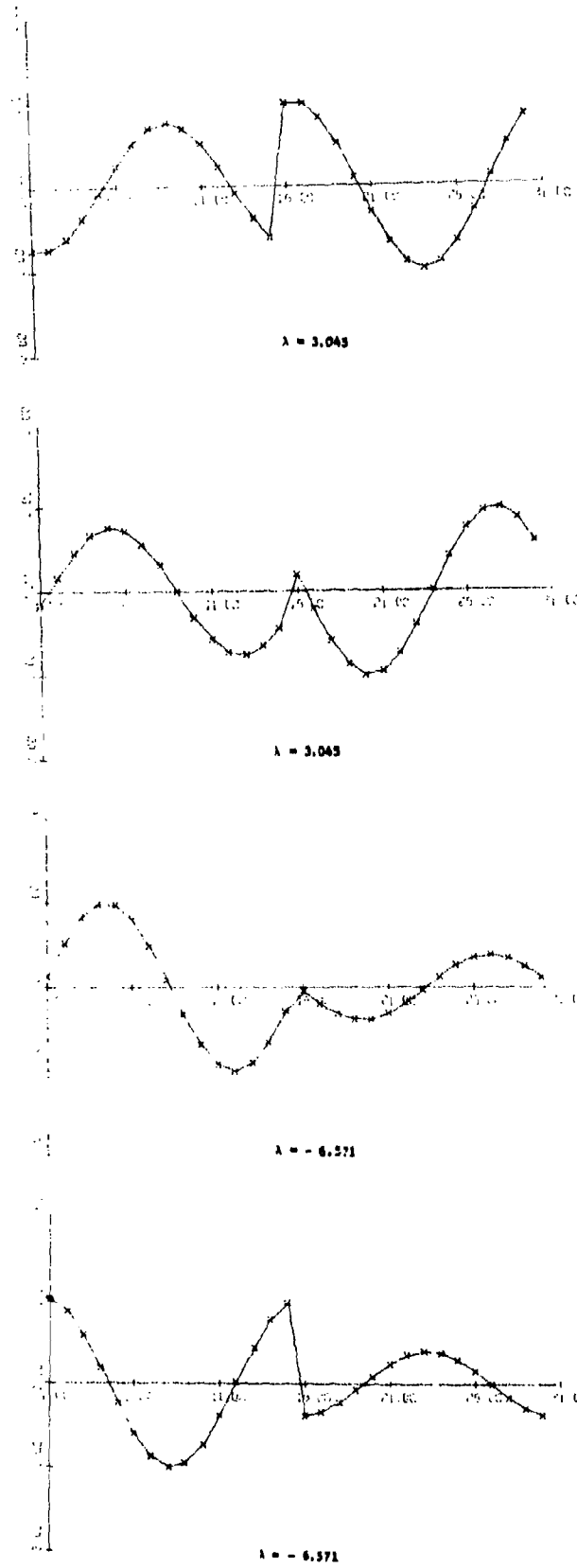


Fig. 4-30. Characteristic currents for a circular cylinder,  $\epsilon_r = 1.56$ ,  $h_0 = 0.7$ , perpendicular polarization.

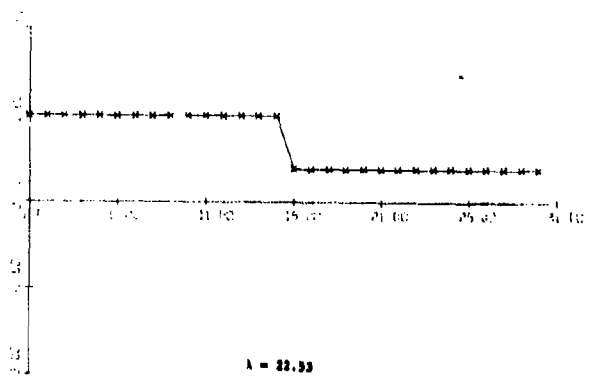
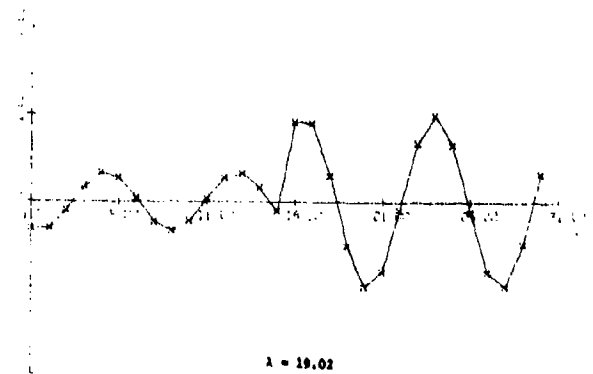
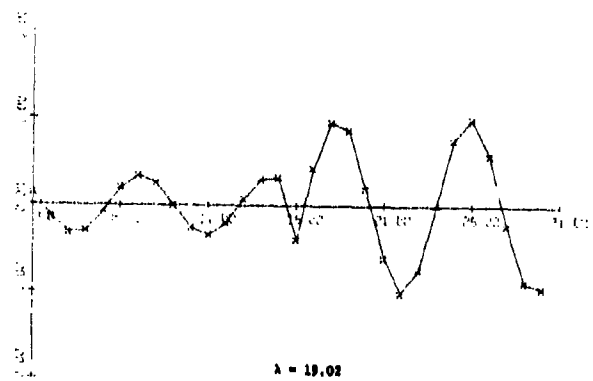
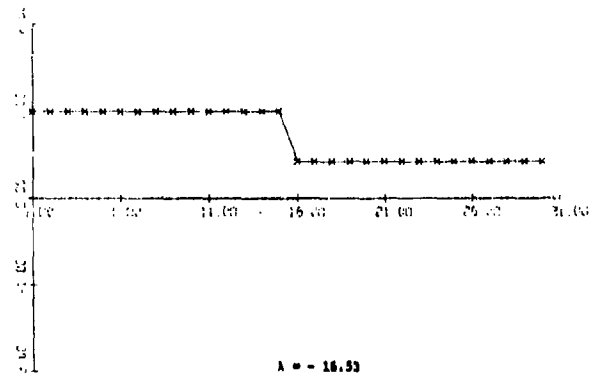


Fig. 4-30. continued.

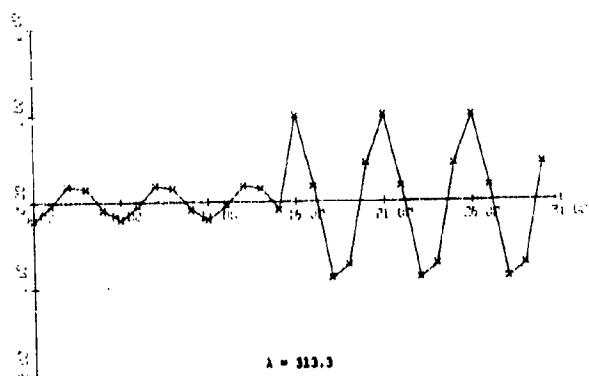
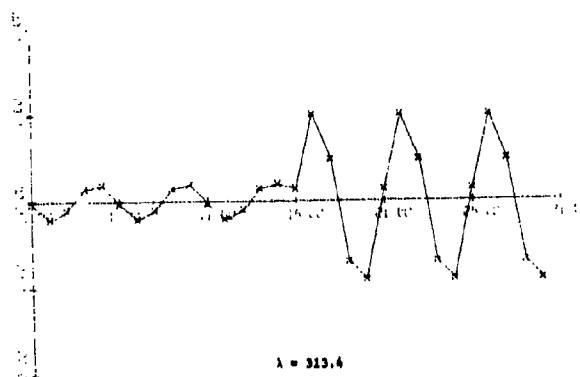
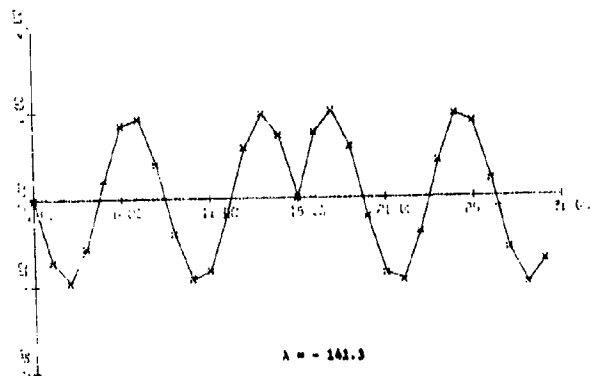
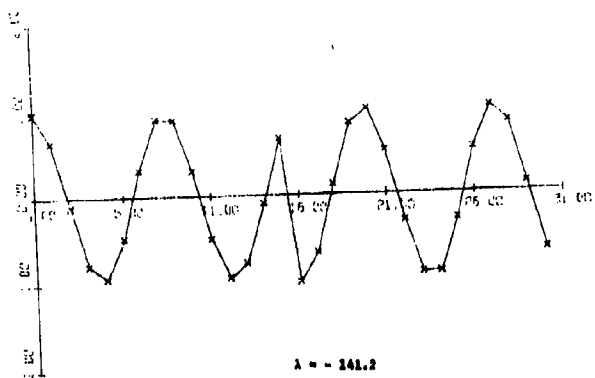


Fig. 4-30. continued.

## CHAPTER 5

## DISCUSSION

A surface formulation is developed for solving two-dimensional electromagnetic scattering problems. A basic theory for characteristic modes of dielectric and magnetic bodies based on the surface formulation is derived. The method of computing characteristic modes can be used for homogeneous material bodies of arbitrary shape provided the body is not electrically large. The characteristic modes of material bodies have most of the properties of those for perfectly conducting bodies, and should find similar uses. The theory presented here is in contrast to that for the volume formulation [4]. The basic difference is that the current in the material body has been treated as equivalent surface currents instead of a volume distribution. The characteristic currents are real and their corresponding eigenvalues are also real. The eigenvectors given by equation (3-73) are those corresponding to the lowest eigenvalues, and they are usually very efficient radiators. Characteristic currents associated with large eigenvalues generally indicate higher order modes which do not radiate very much.

Two ways for computing the scattered fields are given here. The simple material cylinders. The matrix inversion method is easier to use and gives very good results. The characteristic mode method may require slightly longer computing time, but it does provide more insight into the problem. As in the conducting body case, the characteristic mode method should prove to be of value, both theoretically and computationally for scattering and radiation problems. The versatility of characteristic modes has been



adequately demonstrated in analysis and synthesis problems dealing with conducting bodies. The two approaches are based on a surface formulation, and they require the material body to be homogeneous since the unknowns are surface currents. For inhomogeneous bodies the surface formulation is not appropriate, and a volume current distribution must be used which requires sample points inside the scattering body.

## APPENDIX A

## MATRIX ELEMENTS FOR PARALLEL POLARIZATION

For the incident field

$$\underline{E} = \underline{u}_z e^{-jkz} \quad (A-1)$$

the following formulas are obtained ( $\underline{u}_z$  is the axially directed unit vector). The procedures involved are identical to that given in Chapter 2, except that the directions of the surface currents are different.

A.1 Formulas for [Z] Matrix Elements

$$Z_{mn} = \frac{\omega\mu}{4} \sum_{q=1}^4 \sum_{p=1}^4 T_p T_q Z \quad (A-2)$$

where

$$Z = \Delta t_p \Delta t_q H_o^{(2)}(kR_{pq}) \quad (\text{non-coincident intervals})$$

$$= t_p \left[ 1 - j \frac{2}{\pi} \log \frac{\gamma k \Delta t_p}{4e} \right] \quad (\text{coincident intervals})$$

A.2 Formulas for [B] Matrix Elements

$$B_{mn} = -\frac{1}{4} \sum_{q=1}^4 \sum_{p=1}^4 \Delta t_q T_p T_q B \quad (A-3)$$

$$B = -\frac{k H_1^{(2)}(kR_{pq})}{R_{pq}} \left[ - (x_p - x_q) \Delta y_p + (y_p - y_q) \Delta x_p \right]$$

(non-coincident intervals)

$$= -j2 \quad (\text{coincident intervals})$$

### A.3 Formulas for [C] Matrix Elements

$$C_{mn} = -\frac{1}{4} \sum_{q=1}^4 \sum_{p=1}^4 \Delta t_p T_p T_q C \quad (A-4)$$

$$C = -\frac{kH_1^{(2)}(kR_{pq})}{R_{pq}} [ -(y_p - y_q)\Delta x_q + (x_p - x_q)\Delta y_q ]$$

(non-coincident intervals)

$$= -j2 \quad (\text{coincident intervals})$$

### A.4 Formulas for [Y] Matrix Elements

$$Y_{mn} = \frac{1}{4} \sum_{q=1}^4 \sum_{p=1}^4 \Delta t_p \Delta t_q [ \omega \epsilon T_p T_q (u_p \cdot u_q) - \frac{1}{\omega \mu} T_p' T_q' ] Y \quad (A-5)$$

where

$$Y = H_0^{(2)}(kR_{pq}) \quad (\text{non-coincident intervals})$$

$$= 1 - \frac{2}{\pi} \log \frac{\gamma k \Delta t_p}{4a} \quad (\text{coincident intervals})$$

### A.5 Excitation Matrix Elements

$$V_m^i = \sum_{p=1}^4 T_p \Delta t_p e^{jk(x_{mp} \cos \phi^i + y_{mp} \sin \phi^i)} \quad (A-6)$$

$$I_m^i = -\frac{1}{n} \sum_{p=1}^4 T_p [ -\Delta x \sin \phi^i + \Delta y \cos \phi^i ] e^{jk(x_{mp} \cos \phi^i + y_{mp} \sin \phi^i)} \quad (A-7)$$

APPENDIX B  
COMPUTER PROGRAMS

A.1 Listing of the program to compute scattering cross sections,  
perpendicular polarization(7E).

```

//YIKHANG,DIR (0.639,FF,2M995),CHANG,Y,REGION=250K,CLASS=8
//KUC,MAJLIV
//002585,IN 001 *
SUBM CHANG,IMP=3,MAGE=30
SUBROUTINE FPO(7,F0,P0)
  Y=3.0/7
  F0=0.7878A456+Y*(0.0000077+Y*(-0.005574+Y*(-0.0000512+Y*(0.001
  137237+Y*(0.00072805+Y*(0.000447411)))
  P0=0.7859A16+Y*(0.0416A397+Y*(0.0000394+Y*(-0.00267573+Y*(0.0005
  14238+Y*(0.00029333+Y*(0.000135311)))
  N=1000
  END
SUBROUTINE FP1(7,F1,P1)
  Y=3.0/7
  F1=0.7878A456+Y*(0.0000154+Y*(0.01650A67+Y*(0.00017105+Y*(-0.0024
  19411+Y*(0.00114631+Y*(0.000200331)))
  P1=0.7859A16+Y*(0.17490612+Y*(0.00005650+Y*(0.00637879+Y*(-0.00
  10238+Y*(-0.0007924+Y*(0.00021AA11)))
  N=1000
  END
FUNCTION NSJ(X)
  IF(X,0.0,DIRM17E3,10IX
  NSJ=1.0
  IF(X,0.0,DIRM17E3,10IX
  Z=ANST(X)
  IF(Z,0.1,0.0100 TO 1
  Y=2/7*Y
  NSJ=1.0*Y+1-2.2444097+Y*(1.269A20R+Y*(0.3163AA+Y*(0.0444479+Y*(
  1-0.003844+Y*(0.0002111)))
  RETURN
1 CALL FPO(7,F0,P0)
  NSJ=NSJ*NSJ(2-PI)/SURT(2)
  N=1000
10 FORMAT(1M,'WARNING - AN ARGUMENT OF F,15,4,3Z, HAS BEEN ENCOUNTER-
  ED IN CALCULATING A BESSEL FUNCTION OF ORDER 78ND/2)
  END
FUNCTION NSY(X)
  IF(X,0.0,DIRM17E3,10IX
  NSY=1.0*Y
  IF(X,0.0,DIRM17E3,10IX
  Z=ANST(X)
  IF(Z,0.1,0.0100 TO 1
  Y=2/7*Y
  NSY=0.0A36A1977A10G(0.507)R(5,017)+0.9A24AA9+Y*(0.405593AA+Y*(0
  1.76380A8+Y*(0.25300117+Y*(0.04261214+Y*(0.00427916+Y*(0.000288A)
  21))
  RETURN
1 CALL FPI(7,F1,P1)
  NSY=NSY*NSY(2-PI)/SURT(2)
  N=1000
10 FORMAT(1M,'WARNING - AN ARGUMENT OF F,15,4,3Z, HAS BEEN ENCOUNTER-
  ED IN CALCULATING A NEUMANN FUNCTION OF ORDER 78ND ANSX) USED/2)
  END
FUNCTION NSJ1(X)
  IF(X,0.0,DIRM17E3,10IX
  NSJ1=1.0
  IF(X,0.0,DIRM17E3,10IX
  Z=ANST(X)
  IF(Z,0.1,0.0100 TO 1
  Y=2/7*Y
  NSJ1=0.055+Y*(0.8A24445+Y*(0.2109573+Y*(0.0394629+Y*(0.0044
  1314+Y*(0.00041761+Y*(0.0006110N111)))
  RETURN
1 CALL FPI(7,F1,P1)
  NSJ1=NSJ1*NSJ1(2-PI)/SURT(2)
  N=1000
10 FORMAT(1M,'WARNING - AN ARGUMENT OF F,15,4,3Z, HAS BEEN ENCOUNTER-
  ED IN CALCULATING A NEUMANN FUNCTION OF ORDER 78ND ANSX) USED/2)
  END
FUNCTION NSY1(X)
  IF(X,0.0,DIRM17E3,10IX
  NSY1=1.0*Y
  IF(X,0.0,DIRM17E3,10IX
  Z=ANST(X)
  IF(Z,0.1,0.0100 TO 1
  Y=2/7*Y
  NSY1=0.0A36A1977A10G(0.507)R(5,017)+0.9A24AA9+Y*(0.41A427A4Y*(0.312
  1A81+Y*(0.04004A1977A10G(0.27120N1)+Y*(1.8A27094+Y*(-1.31A427A4Y*(0.312
  1A81)+Y*(0.04004A1977A10G(0.507)R(5,017)
  21))
  RETURN
1 CALL FP1(7,F1,P1)
  NSY1=NSY1*NSY1(2-PI)/SURT(2)
  N=1000
10 FORMAT(1M,'WARNING - AN ARGUMENT OF F,15,4,3Z, HAS BEEN ENCOUNTER-
  ED IN CALCULATING A NEUMANN FUNCTION OF ORDER 78ND ANSX) USED/2)
  END
SUBROUTINE L(IMP,ST0,ST1,ST2)
  DIMENSION L(1:60)
  DO 20 J=1,60
  L(J)=1
  20 CONTINUE
  N=60
  DO 10 M=1,60
  K=M
  N2=M+K
  N1=ABS(IMP*(K+1)+ANST(1A6G(C(K2)))
  DO 2 J=1,M+1
  N1=N1+J
  N2=N2+J
  N3=ABS(IMP*(K+1)+ANST(1A6G(C(K3)))
  IF(N2>N1) 2,2,K
  K=1
  N1=N2
  2 CONTINUE
  N=L(N)
  L=N
  N2=N+K
  L=L+2
  40 CONTINUE
  L=L+2
  50 CONTINUE

```

```

J1=0
DO 7 J=1,60
  K1=J+K
  K2=J+K
  ST0=C(K1)
  C(K2)=C(K1)/ST0
  J1=J+LL
7 CONTINUE
  K1=M+K
  C(K1)=1./ST0
  DO 11 J=1,11
  IF(C(M+J2+1,1)2
  12 K1=M+1
  ST0=C(K1)
  C(K1)=0.
  J1=0
  DO 10 J=1,LL
  K1=J+1
  K2=J+M
  C(K1)=C(K1)-C(K2)*Y
  J1=J+LL
10 CONTINUE
11 CONTINUE
  M1=M+LL
18 CONTINUE
  J1=0
  DO 9 J=1,LL
  IF(J=1) 14,M,14
  14 L(J)=L(J)
  J2=L(J)+1
  K2=J2+1
  K1=J1+1
  S=C(K2)
  C(K2)=C(K1)
  C(K1)=S
  13 CONTINUE
  L(J)=L(J)+1
  L(L(J))=L(J)
  4 J1=J+LL
  9 CONTINUE
  END
SUBROUTINE HANR(G)
  DIMENSION C(1:M,MP,4,2),Y,FV
  COMMON D(1:62),D(1:62),D(1:62),D(1:62),D(1:62)
  COMMON I(1:20),I(1:20),I(1:20),I(1:20),I(1:20)
  COMMON M(1:62),M(1:62),M(1:62),M(1:62),M(1:62)
  COMMON X(1:62),Y(1:62),Z
  M1=3.141593
  M2=0.3141593
  N1=N2+1
  F=4.0,2.71828
  EL=1.781072
  I1=0
  DO 30 J=1,N1
  DO 40 J1=1,J
  I1=I1+1
  IF I1 40, 3160 TO 24
  IF I1 40, 1 4AND, 1 40, N210 TO 25
  IF I1 40, 2 4AND, 1 40, N110 TO 24
  N1=N2+1+I1
  M1(1)=NSJ1(I1R1)+C(J0NSY1(I1K)
  M1(1)=NSJ1(I1R1)-C(J0NSY1(I1K)
  GO TO 40
  25 CONTINUE
  A=C(L0R0K0L(1))/FF
  M1(1)=1.0-C(J0NSY1(I1A)
  40 CONTINUE
  50 CONTINUE
  END
SUBROUTINE CALZ(Y,M,IMP)
  DIMENSION C(1:M,MP,4,2),Y,FV
  COMMON D(1:62),D(1:62),D(1:62),D(1:62),D(1:62)
  COMMON I(1:20),I(1:20),I(1:20),I(1:20),I(1:20)
  COMMON M(1:62),M(1:62),M(1:62),M(1:62),M(1:62)
  COMMON X(1:62),Y(1:62),Z
  M1=3.141593
  I1=0
  DO 30 J=1,N2+2
  I1=I1+2
  I2=I1+1
  I4=I1+1
  J4=J+1
  K=0
  DO 40 J1=1,N2+2
  I1=I1+1
  I2=I1+2
  I3=I1+1
  I4=I1+1
  Z(I1)=0.0
  Y(I1)=0.0
  DO 70 M=1,J4
  LL=M+L
  DO 80 N=1,14
  N1=N+M
  IF(N=1) 100,120,120+M
  100 J1=IMP*(N-1)/2+M
  DO 110 J=1,130
  120 J1=IMP*(N-1)/2+M
  130 CONTINUE
  (C(I1R1)+D(I1)+Y(I1M)+Y(I1N))/D(I1M)+D(I1N)
  Z(I1)=D(I1R1)+D(I1L)+D(I1M)
  Z(I1)=D(I1R1)+D(I1L)+D(I1M)
  Z(I1)=Z(I1)+Z(I1)
  Z(I1)=Z(I1)
  Z(I1)=0.250D1(N1)+D(I1+Z(I1)+Z(I1)
  Y(I1)=0.250M(I1R1)+D(I1L)+D(I1M)+Z(I1)
  80 CONTINUE
  70 CONTINUE
  Y(I1)=Y(I1)
  Z(I1)=Z(I1)/177.09377,0)
  K=M+2
  40 CONTINUE
  L=L+2
  50 CONTINUE

```

```

RETURN
END
SUBROUTINE CALC(CM)
COMPLEX C,CM,MP(A,Z,Y,XY)
COMMON DE(A2),DY(A2),DL(A2),X(A2),Y(A2)
COMMON T(120),T0(120),FV(A0),RR(195)
COMMON H(195),H0(195),A(1300),Z(100),Y(100),CJ
N1=N2+1
L=0
DO 50 J=3,N2,2
  J1=J-2
  J2=J-1
  J3=J+1
  K=0
  DO 40 I=3,N2,2
    I1=I+1
    I2=I-2
    I3=I+1
    Z(I1)=0,0
    DO 30 M=3,14
      U=0
      DO 20 N=1,14
        K=K+N
        I=(N-1)*100+150,170
        J=(N-1)*112+20
        I1=N, I2=1, I3=2, N1=1, N2=150
        J1=N, J2=2, I3=2, N1=1, N2=150
        GO TO 130
      I1=N, I2=1, I3=2, N1=1, N2=150
      J1=N, J2=2, I3=2, N1=1, N2=150
      GO TO 140
    CONTINUE
    HRR=H(I1,J1)/R(I1,J1)
    D1=(DL(I1)*T(I1)+T(I1)*X(I1)
    C1=(FV(I1)-X(I1))*Y(I1)+(Y(I1)-Y(I1))*X(I1)
    Z(I1)=0,0,C1/2*(HRR+HRR)*Z(I1)
    GO TO 140
  CONTINUE
  H0=H(I1,J1)/R(I1,J1)
  D1=(DL(I1)*T0(I1)+T0(I1)*X(I1)
  C1=(FV(I1)-X0(I1))*Y0(I1)+(Y0(I1)-Y0(I1))*X0(I1)
  Z(I1)=0,0,C1/2*(H0+H0)*Z(I1)
  GO TO 140
CONTINUE
HRR=H(I1,J1)/R(I1,J1)
D1=(DL(I1)*T(I1)+T(I1)*X(I1)
C1=(FV(I1)-X(I1))*Y(I1)+(Y(I1)-Y(I1))*X(I1)
Z(I1)=0,0,C1/2*(HRR+HRR)*Z(I1)
GO TO 140
CONTINUE
H0=H(I1,J1)/R(I1,J1)
D1=(DL(I1)*T0(I1)+T0(I1)*X0(I1)
C1=(FV(I1)-X0(I1))*Y0(I1)+(Y0(I1)-Y0(I1))*X0(I1)
Z(I1)=0,0,C1/2*(H0+H0)*Z(I1)
GO TO 140
CONTINUE
RETURN
END
SUBROUTINE FEMX(PH,I,OP)
COMPLEX C,CM,MP(A,Z,Y,XY)
COMMON DE(A2),DY(A2),DL(A2),X(A2),Y(A2)
COMMON T(120),T0(120),FV(A0),RR(195)
COMMON H(195),H0(195),A(1300),Z(100),Y(100),CJ
COMMON X(A3),Y(A3),N2
I1=170,170)

```

```

N1=N2-112
M=COS(PH)
N=SIN(PH)
I1=0
L=0
DO 200 J=3,N2,2
  J1=J+1
  J2=J-2
  J3=J-1
  J4=J+1
  K=0
  DO 190 I=3,N2,2
    I1=I+1
    I2=I-2
    I3=I+1
    U=0
    DO 180 M=3,14
      U=0
      DO 170 N=1,14
        K=K+N
        I=(N-1)*100+150,170
        J=(N-1)*112+20
        I1=N, I2=1, I3=2, N1=1, N2=150
        J1=N, J2=2, I3=2, N1=1, N2=150
        GO TO 130
      I1=N, I2=1, I3=2, N1=1, N2=150
      J1=N, J2=2, I3=2, N1=1, N2=150
      GO TO 140
    CONTINUE
    HRR=H(I1,J1)/R(I1,J1)
    D1=(DL(I1)*T(I1)+T(I1)*X(I1)
    C1=(FV(I1)-X(I1))*Y(I1)+(Y(I1)-Y(I1))*X(I1)
    Z(I1)=0,0,C1/2*(HRR+HRR)*Z(I1)
    GO TO 140
  CONTINUE
  H0=H(I1,J1)/R(I1,J1)
  D1=(DL(I1)*T0(I1)+T0(I1)*X0(I1)
  C1=(FV(I1)-X0(I1))*Y0(I1)+(Y0(I1)-Y0(I1))*X0(I1)
  Z(I1)=0,0,C1/2*(H0+H0)*Z(I1)
  GO TO 140
CONTINUE
RETURN
END
COMPLEX C,CM,MP(A,Z,Y,XY)
COMMON DE(A2),DY(A2),DL(A2),X(A2),Y(A2)
COMMON T(120),T0(120),FV(A0),RR(195)
COMMON H(195),H0(195),A(1300),Z(100),Y(100),CJ
COMMON X(A3),Y(A3),N2
I1=170,170)

```

```

C=10,0,1,1
PH=0,0
OP=0,0
I1=170,170)
DO 5 J=3,N2,2
  J1=J+1
  J2=J-2
  J3=J-1
  J4=J+1
  K=0
  DO 4 CONTINUE
    HRR=H(I1,J1)/R(I1,J1)
    D1=(DL(I1)*T(I1)+T(I1)*X(I1)
    C1=(FV(I1)-X(I1))*Y(I1)+(Y(I1)-Y(I1))*X(I1)
    Z(I1)=0,0,C1/2*(HRR+HRR)*Z(I1)
    GO TO 4 CONTINUE
  CONTINUE
  H0=H(I1,J1)/R(I1,J1)
  D1=(DL(I1)*T0(I1)+T0(I1)*X0(I1)
  C1=(FV(I1)-X0(I1))*Y0(I1)+(Y0(I1)-Y0(I1))*X0(I1)
  Z(I1)=0,0,C1/2*(H0+H0)*Z(I1)
  GO TO 4 CONTINUE
CONTINUE
RETURN
END
COMPLEX C,CM,MP(A,Z,Y,XY)
COMMON DE(A2),DY(A2),DL(A2),X(A2),Y(A2)
COMMON T(120),T0(120),FV(A0),RR(195)
COMMON H(195),H0(195),A(1300),Z(100),Y(100),CJ
COMMON X(A3),Y(A3),N2
I1=170,170)

```

```

DO 500 I=1,N
KK=JAK
LCL=J
J1=LANJ
A(I1)=A(IKK)
K=K+KK
480 CONTINUE
LCL=N
490 CONTINUE
4 FORMAT(//Z,1H * |DE-11,4I
CALL LTIME(IBM)
CALL FWRITE(AN,IX)
WRITE(I,5,95)
WRITE(I,6,96) (EV(I),I=1,NM)
WRITE(I,3,94)
504 FORMAT(1H *, 'CURRENT I/Z' 11, 'A', 'REFL', 'TQ', 'IMAG', 'TQ', 'MAGNITUDE', 'TQ
I, 'PHASE')
DO 50 I=1,N
EV(I)=V(I)/377.0
50 CONTINUE
DO 270 J=1,NM
AF(I)=-0.0
DO 400 I=1,NM
J=1-1/2*NM*I
AF(I1)=AF(I1)+EV(I)*AF(I)
400 CONTINUE
270 CONTINUE
DO 70 I=1,N
AF(I)=AF(I)/377.0
70 CONTINUE
DO 80 I=1,NM
C=C+CAF*I*AF(I)
C=CMRAT*2*1MAG*AF(I1),H*AF(I111)*0.5,2*AS
WRITE(I,7,95) I,AF(I1),C,C*CPH
80 CONTINUE
WRITE(I,7,96) (X,13,97)A,AF(I),3)
276 FORMAT(///I SCATTERING ANGLE = PHI',10X,' ECHI LENGTH/WAVELENGTH')
AND,N
N1=1/2*NM
DO 320 I=1,36
CALL FWRITE(AN,IX)
H=H+0.0
DO 330 J=1,NM
WRITE(I,J,98)B(I),H*H
330 CONTINUE
L=CMRAT*AN(H)
C=CMRAT*AN*H*0.2,0
FLL=ELCH/(H*H*2)
FMT=FL/PA
KLL=10.0*H*(H+1/2*NM)
WRITE(I,9,99)AN,FLL
999 FORMAT(1H * |D,2F,2,20X,F14,7)
AN=N+3
320 CONTINUE
STOP
END

```

R.7 listing of the program to compute characteristic currents.

```

//ZM MARG,DIR,1968N,IF,2,2,000),IC,MANYI,REGIONS,100K,CLASS+
//SYN,SYN,N,DL,4
//
C
C *****EIGENVALUE 40 - INPUT COMPLEX TORG
C
COMPLEX Z(1000),U(1,1,30)
COMPLEX L(1,1,110)
DIMENSION U(1000),W(1000),I(1000),A(22000),R(1000),K(1000),A(1000)
DIMENSION U(1000),V(1000),I(1000),P(1000),Q(1000),D(1000),AM(1000),LM(1000)
DIMENSION W(1000),R(1000),A(22000)
DIMENSION K(1000)
DIMENSION O(1000),W(1000)
DIMENSION D(1000)
DIMENSION K(1000)
DIMENSION A(1000)
DIMENSION V(1000)
FOURVALUES = (R(1),I(1),A(2211),W(1),V(1),A(1),V(1))
FOURVALUES = (I(1),I(1),I(1),I(1),AM(1))
C(1,1,1,1,1)
WRITE(I,26)A
26 FORMAT(I,2,6)
WRITE(I,27)A
27 FORMAT(I,2,6)
N1=N*2
N2=N*N
N3=N*N*2
N4=2*(1,2001/(1,1,1),N25)
280 FORMAT(I,2,7)
DO 300 I=1,NM
DO 400 J=1,NM
P(I,J)=A(I,J)
R(I,J)=W(I,J)
Q(I,J)=V(I,J)
400 CONTINUE
300 CONTINUE
DO 50 I=1,N
DO 60 J=1,N
V(I,J)=P(I,J)+I*Q(I,J)
60 CONTINUE
50 CONTINUE
40 CONTINUE

```

```

KK=0
NM=N-1
DO 45 K=1,1000
L=K+1
DO 35 I=1,N
E=EV(I)
I1=1-1/2*NM*I
WRITE(I,10,11)
A(I)=A(I)
35 CONTINUE
KK=KK+K
45 CONTINUE
DO 46 I=1,67
K(I)=K(I)
46 CONTINUE
WRITE(I,20) N
201 FORMAT(1H *, 'R MATRIX (STORED IN SYM. MODE) OF ORDER, I')
WRITE(I,2,202) (R(I),I=1,N25)
202 FORMAT(1H *, 'P')
WRITE(I,2,203) N
203 FORMAT(1H *, 'K MATRIX (STORED COLUMNWISE) OF ORDER, I')
WRITE(I,2,204) (K(I),I=1,N2)
130 CALL EIGENR(0,N,0)
J=0
DO 104 J=1,N
J1=J+1
P(J)=R(J)
R(J)=1/FWRITE(AN,IX)
104 CONTINUE
WRITE(I,14)I(R(J),J)
141 FORMAT(10F10.0)VALUES OF THE MATRIX P(I),R(J),A(I)
DO 75 J=1,N
J1=J+1
DO 76 K=1,N
J2=J+1
J3=J+1
DO 77 K=1,N
R(K)=I
K2=K+1
J2(J)=I2(J2)+K(I)*R(K2)
77 CONTINUE
76 CONTINUE
75 CONTINUE
DO 78 J=1,N
J1=J+1
DO 79 I=1,3
J2=J+1
A(J2)=0
J3=J+1
DO 80 K=1,N
K3=K+1
K2=K+1
A(J2)+A(J2)+R(I)*K(I)*J2(K2)
80 CONTINUE
J4=J+1
A(J4)=A(J2)
79 CONTINUE
78 CONTINUE

```

```

X2=X(1)+I*Y2
DO 70 J=1,N
IF(P(I)=X2) J2,144,144
144 J=J
70 CONTINUE
72 J=N-J
J(1,0)=J
J(1,N)=144,144,144

```

C IF NO EIGENVALUES OF H ARE SKI TO 1000, I=0-0, I=0-1, I=0-1, I=0-1  
C RETURN 144 AND 141 ARE CARRIED OUT.

```

144 J=0
DO 148 J=1,N
J1=J+1
DO 149 I=1,3
J2=J+1
J3=J+1
DO 152 I=1,3
DO 150 K=1,N
A(K)=I
K2=K+1
J2(J)=I2(J2)+K(I)*A(K2)
150 CONTINUE
WRITE(I,5,99)A(1),I(1),I(1),I(1)
DO 151 J=1,N
J1=J+1
DO 152 I=1,3
J2=J+1
J3=J+1
152 CONTINUE
151 CONTINUE
GO TO 147

```

L IF SOME EIGENVALUES OF H ARE NOT SKI TO 1000, I=0-0, I=0-1, I=0-1, I=0-1  
C THEN INSTRUCTIONS BETWEEN 145 AND 147 ARE CARRIED OUT.

```

145 J=0
DO 75 J=1,N
J2=J+1
DO 76 K=1,N
J3=J+1
J4=J+1
A(221,1)=A(221)
A(221,1)=A(221)
74 CONTINUE
73 CONTINUE
DO 75 J=1,N
WRITE(I,9,100) (A(221),I=1,NM)
999 *****
ADD FWRITE(1022 MATRIX I/I(1),I=1,NM)
128 CALL INTRJN,A(221,1)
WRITE(I,6,101) (A(221),I=1,NM)
A(1) FWRITE(1022 INVERSE I/I(1),I=1,NM)
J=0
DO 700 I=1,N
K1=1-1/2*NM*I
DO 710 J=1,N

```

```

110 J1=1
120 J2=0
130 K=1
140 K=K+1
150 J1=K-1
160 J2=J2+1
170 CONTINUE
180 CONTINUE
190 CONTINUE
200 CONTINUE
210 FORMAT('A22 INVERSE')/1(D1X,F14.7)
220
230 J1=0
240 J2=1
250 K=1
260 K=K+1
270 J1=J1+1
280 J2=J2+1
290 K=K+1
300 J1=J1+1
310 J2=J2+1
320 K=K+1
330 J1=J1+1
340 J2=J2+1
350 K=K+1
360 J1=J1+1
370 J2=J2+1
380 K=K+1
390 J1=J1+1
400 J2=J2+1
410 K=K+1
420 J1=J1+1
430 J2=J2+1
440 K=K+1
450 J1=J1+1
460 J2=J2+1
470 K=K+1
480 J1=J1+1
490 J2=J2+1
500 K=K+1
510 J1=J1+1
520 J2=J2+1
530 K=K+1
540 J1=J1+1
550 J2=J2+1
560 K=K+1
570 J1=J1+1
580 J2=J2+1
590 K=K+1
600 J1=J1+1
610 J2=J2+1
620 K=K+1
630 J1=J1+1
640 J2=J2+1
650 K=K+1
660 J1=J1+1
670 J2=J2+1
680 K=K+1
690 J1=J1+1
700 J2=J2+1
710 K=K+1
720 J1=J1+1
730 J2=J2+1
740 K=K+1
750 J1=J1+1
760 J2=J2+1
770 K=K+1
780 J1=J1+1
790 J2=J2+1
800 K=K+1
810 J1=J1+1
820 J2=J2+1
830 K=K+1
840 J1=J1+1
850 J2=J2+1
860 K=K+1
870 J1=J1+1
880 J2=J2+1
890 K=K+1
900 J1=J1+1
910 J2=J2+1
920 K=K+1
930 J1=J1+1
940 J2=J2+1
950 K=K+1
960 J1=J1+1
970 J2=J2+1
980 K=K+1
990 J1=J1+1
1000 J2=J2+1
1010 K=K+1
1020 J1=J1+1
1030 J2=J2+1
1040 K=K+1
1050 J1=J1+1
1060 J2=J2+1
1070 K=K+1
1080 J1=J1+1
1090 J2=J2+1
1100 K=K+1
1110 J1=J1+1
1120 J2=J2+1
1130 K=K+1
1140 J1=J1+1
1150 J2=J2+1
1160 K=K+1
1170 J1=J1+1
1180 J2=J2+1
1190 K=K+1
1200 J1=J1+1
1210 J2=J2+1
1220 K=K+1
1230 J1=J1+1
1240 J2=J2+1
1250 K=K+1
1260 J1=J1+1
1270 J2=J2+1
1280 K=K+1
1290 J1=J1+1
1300 J2=J2+1
1310 K=K+1
1320 J1=J1+1
1330 J2=J2+1
1340 K=K+1
1350 J1=J1+1
1360 J2=J2+1
1370 K=K+1
1380 J1=J1+1
1390 J2=J2+1
1400 K=K+1
1410 J1=J1+1
1420 J2=J2+1
1430 K=K+1
1440 J1=J1+1
1450 J2=J2+1
1460 K=K+1
1470 J1=J1+1
1480 J2=J2+1
1490 K=K+1
1500 J1=J1+1
1510 J2=J2+1
1520 K=K+1
1530 J1=J1+1
1540 J2=J2+1
1550 K=K+1
1560 J1=J1+1
1570 J2=J2+1
1580 K=K+1
1590 J1=J1+1
1600 J2=J2+1
1610 K=K+1
1620 J1=J1+1
1630 J2=J2+1
1640 K=K+1
1650 J1=J1+1
1660 J2=J2+1
1670 K=K+1
1680 J1=J1+1
1690 J2=J2+1
1700 K=K+1
1710 J1=J1+1
1720 J2=J2+1
1730 K=K+1
1740 J1=J1+1
1750 J2=J2+1
1760 K=K+1
1770 J1=J1+1
1780 J2=J2+1
1790 K=K+1
1800 J1=J1+1
1810 J2=J2+1
1820 K=K+1
1830 J1=J1+1
1840 J2=J2+1
1850 K=K+1
1860 J1=J1+1
1870 J2=J2+1
1880 K=K+1
1890 J1=J1+1
1900 J2=J2+1
1910 K=K+1
1920 J1=J1+1
1930 J2=J2+1
1940 K=K+1
1950 J1=J1+1
1960 J2=J2+1
1970 K=K+1
1980 J1=J1+1
1990 J2=J2+1
2000 K=K+1

```

```

90 CONTINUE
91 J1=1
92 J2=0
93 K=1
94 K=K+1
95 J1=K-1
96 J2=J2+1
97 CONTINUE
98 CONTINUE
99 CONTINUE
100 CONTINUE
101 FORMAT('A22 INVERSE')/1(D1X,F14.7)
102
103 J1=0
104 J2=1
105 K=1
106 K=K+1
107 J1=J1+1
108 J2=J2+1
109 K=K+1
110 J1=J1+1
111 J2=J2+1
112 K=K+1
113 J1=J1+1
114 J2=J2+1
115 K=K+1
116 J1=J1+1
117 J2=J2+1
118 K=K+1
119 J1=J1+1
120 J2=J2+1
121 K=K+1
122 J1=J1+1
123 J2=J2+1
124 K=K+1
125 J1=J1+1
126 J2=J2+1
127 K=K+1
128 J1=J1+1
129 J2=J2+1
130 K=K+1
131 J1=J1+1
132 J2=J2+1
133 K=K+1
134 J1=J1+1
135 J2=J2+1
136 K=K+1
137 J1=J1+1
138 J2=J2+1
139 K=K+1
140 J1=J1+1
141 J2=J2+1
142 K=K+1
143 J1=J1+1
144 J2=J2+1
145 K=K+1
146 J1=J1+1
147 J2=J2+1
148 K=K+1
149 J1=J1+1
150 J2=J2+1
151 K=K+1
152 J1=J1+1
153 J2=J2+1
154 K=K+1
155 J1=J1+1
156 J2=J2+1
157 K=K+1
158 J1=J1+1
159 J2=J2+1
160 K=K+1
161 J1=J1+1
162 J2=J2+1
163 K=K+1
164 J1=J1+1
165 J2=J2+1
166 K=K+1
167 J1=J1+1
168 J2=J2+1
169 K=K+1
170 J1=J1+1
171 J2=J2+1
172 K=K+1
173 J1=J1+1
174 J2=J2+1
175 K=K+1
176 J1=J1+1
177 J2=J2+1
178 K=K+1
179 J1=J1+1
180 J2=J2+1
181 K=K+1
182 J1=J1+1
183 J2=J2+1
184 K=K+1
185 J1=J1+1
186 J2=J2+1
187 K=K+1
188 J1=J1+1
189 J2=J2+1
190 K=K+1
191 J1=J1+1
192 J2=J2+1
193 K=K+1
194 J1=J1+1
195 J2=J2+1
196 K=K+1
197 J1=J1+1
198 J2=J2+1
199 K=K+1
200 J1=J1+1
201 J2=J2+1
202 K=K+1
203 J1=J1+1
204 J2=J2+1
205 K=K+1
206 J1=J1+1
207 J2=J2+1
208 K=K+1
209 J1=J1+1
210 J2=J2+1
211 K=K+1
212 J1=J1+1
213 J2=J2+1
214 K=K+1
215 J1=J1+1
216 J2=J2+1
217 K=K+1
218 J1=J1+1
219 J2=J2+1
220 K=K+1
221 J1=J1+1
222 J2=J2+1
223 K=K+1
224 J1=J1+1
225 J2=J2+1
226 K=K+1
227 J1=J1+1
228 J2=J2+1
229 K=K+1
230 J1=J1+1
231 J2=J2+1
232 K=K+1
233 J1=J1+1
234 J2=J2+1
235 K=K+1
236 J1=J1+1
237 J2=J2+1
238 K=K+1
239 J1=J1+1
240 J2=J2+1
241 K=K+1
242 J1=J1+1
243 J2=J2+1
244 K=K+1
245 J1=J1+1
246 J2=J2+1
247 K=K+1
248 J1=J1+1
249 J2=J2+1
250 K=K+1
251 J1=J1+1
252 J2=J2+1
253 K=K+1
254 J1=J1+1
255 J2=J2+1
256 K=K+1
257 J1=J1+1
258 J2=J2+1
259 K=K+1
260 J1=J1+1
261 J2=J2+1
262 K=K+1
263 J1=J1+1
264 J2=J2+1
265 K=K+1
266 J1=J1+1
267 J2=J2+1
268 K=K+1
269 J1=J1+1
270 J2=J2+1
271 K=K+1
272 J1=J1+1
273 J2=J2+1
274 K=K+1
275 J1=J1+1
276 J2=J2+1
277 K=K+1
278 J1=J1+1
279 J2=J2+1
280 K=K+1
281 J1=J1+1
282 J2=J2+1
283 K=K+1
284 J1=J1+1
285 J2=J2+1
286 K=K+1
287 J1=J1+1
288 J2=J2+1
289 K=K+1
290 J1=J1+1
291 J2=J2+1
292 K=K+1
293 J1=J1+1
294 J2=J2+1
295 K=K+1
296 J1=J1+1
297 J2=J2+1
298 K=K+1
299 J1=J1+1
300 J2=J2+1
301 K=K+1
302 J1=J1+1
303 J2=J2+1
304 K=K+1
305 J1=J1+1
306 J2=J2+1
307 K=K+1
308 J1=J1+1
309 J2=J2+1
309 K=K+1
310 J1=J1+1
311 J2=J2+1
312 K=K+1
313 J1=J1+1
314 J2=J2+1
315 K=K+1
316 J1=J1+1
317 J2=J2+1
318 K=K+1
319 J1=J1+1
320 J2=J2+1
321 K=K+1
322 J1=J1+1
323 J2=J2+1
324 K=K+1
325 J1=J1+1
326 J2=J2+1
327 K=K+1
328 J1=J1+1
329 J2=J2+1
329 K=K+1
330 J1=J1+1
331 J2=J2+1
332 K=K+1
333 J1=J1+1
334 J2=J2+1
335 K=K+1
336 J1=J1+1
337 J2=J2+1
338 K=K+1
339 J1=J1+1
340 J2=J2+1
341 K=K+1
342 J1=J1+1
343 J2=J2+1
344 K=K+1
343 CONTINUE
344 J1=1
345 J2=0
346 K=1
347 K=K+1
348 J1=K-1
349 J2=J2+1
350 CONTINUE
351 CONTINUE
352 CONTINUE
353 CONTINUE
354 CONTINUE
355 CONTINUE
356 CONTINUE
357 CONTINUE
358 CONTINUE
359 CONTINUE
360 CONTINUE
361 CONTINUE
362 CONTINUE
363 CONTINUE
364 CONTINUE
365 CONTINUE
366 CONTINUE
367 CONTINUE
368 CONTINUE
369 CONTINUE
370 CONTINUE
371 CONTINUE
372 CONTINUE
373 CONTINUE
374 CONTINUE
375 CONTINUE
376 CONTINUE
377 CONTINUE
378 CONTINUE
379 CONTINUE
380 CONTINUE
381 CONTINUE
382 CONTINUE
383 CONTINUE
384 CONTINUE
385 CONTINUE
386 CONTINUE
387 CONTINUE
388 CONTINUE
389 CONTINUE
390 CONTINUE
391 CONTINUE
392 CONTINUE
393 CONTINUE
394 CONTINUE
395 CONTINUE
396 CONTINUE
397 CONTINUE
398 CONTINUE
399 CONTINUE
400 CONTINUE
401 CONTINUE
402 CONTINUE
403 CONTINUE
404 CONTINUE
405 CONTINUE
406 CONTINUE
407 CONTINUE
408 CONTINUE
409 CONTINUE
410 CONTINUE
411 CONTINUE
412 CONTINUE
413 CONTINUE
414 CONTINUE
415 CONTINUE
416 CONTINUE
417 CONTINUE
418 CONTINUE
419 CONTINUE
420 CONTINUE
421 CONTINUE
422 CONTINUE
423 CONTINUE
424 CONTINUE
425 CONTINUE
426 CONTINUE
427 CONTINUE
428 CONTINUE
429 CONTINUE
430 CONTINUE
431 CONTINUE
432 CONTINUE
433 CONTINUE
434 CONTINUE
435 CONTINUE
436 CONTINUE
437 CONTINUE
438 CONTINUE
439 CONTINUE
440 CONTINUE
441 CONTINUE
442 CONTINUE
443 CONTINUE
444 CONTINUE
445 CONTINUE
446 CONTINUE
447 CONTINUE
448 CONTINUE
449 CONTINUE
450 CONTINUE
451 CONTINUE
452 CONTINUE
453 CONTINUE
454 CONTINUE
455 CONTINUE
456 CONTINUE
457 CONTINUE
458 CONTINUE
459 CONTINUE
460 CONTINUE
461 CONTINUE
462 CONTINUE
463 CONTINUE
464 CONTINUE
465 CONTINUE
466 CONTINUE
467 CONTINUE
468 CONTINUE
469 CONTINUE
470 CONTINUE
471 CONTINUE
472 CONTINUE
473 CONTINUE
474 CONTINUE
475 CONTINUE
476 CONTINUE
477 CONTINUE
478 CONTINUE
479 CONTINUE
480 CONTINUE
481 CONTINUE
482 CONTINUE
483 CONTINUE
484 CONTINUE
485 CONTINUE
486 CONTINUE
487 CONTINUE
488 CONTINUE
489 CONTINUE
490 CONTINUE
491 CONTINUE
492 CONTINUE
493 CONTINUE
494 CONTINUE
495 CONTINUE
496 CONTINUE
497 CONTINUE
498 CONTINUE
499 CONTINUE
500 CONTINUE
501 CONTINUE
502 CONTINUE
503 CONTINUE
504 CONTINUE
505 CONTINUE
506 CONTINUE
507 CONTINUE
508 CONTINUE
509 CONTINUE
510 CONTINUE
511 CONTINUE
512 CONTINUE
513 CONTINUE
514 CONTINUE
515 CONTINUE
516 CONTINUE
517 CONTINUE
518 CONTINUE
519 CONTINUE
520 CONTINUE
521 CONTINUE
522 CONTINUE
523 CONTINUE
524 CONTINUE
525 CONTINUE
526 CONTINUE
527 CONTINUE
528 CONTINUE
529 CONTINUE
530 CONTINUE
531 CONTINUE
532 CONTINUE
533 CONTINUE
534 CONTINUE
535 CONTINUE
536 CONTINUE
537 CONTINUE
538 CONTINUE
539 CONTINUE
540 CONTINUE
541 CONTINUE
542 CONTINUE
543 CONTINUE
544 CONTINUE
545 CONTINUE
546 CONTINUE
547 CONTINUE
548 CONTINUE
549 CONTINUE
550 CONTINUE
551 CONTINUE
552 CONTINUE
553 CONTINUE
554 CONTINUE
555 CONTINUE
556 CONTINUE
557 CONTINUE
558 CONTINUE
559 CONTINUE
560 CONTINUE
561 CONTINUE
562 CONTINUE
563 CONTINUE
564 CONTINUE
565 CONTINUE
566 CONTINUE
567 CONTINUE
568 CONTINUE
569 CONTINUE
570 CONTINUE
571 CONTINUE
572 CONTINUE
573 CONTINUE
574 CONTINUE
575 CONTINUE
576 CONTINUE
577 CONTINUE
578 CONTINUE
579 CONTINUE
580 CONTINUE
581 CONTINUE
582 CONTINUE
583 CONTINUE
584 CONTINUE
585 CONTINUE
586 CONTINUE
587 CONTINUE
588 CONTINUE
589 CONTINUE
590 CONTINUE
591 CONTINUE
592 CONTINUE
593 CONTINUE
594 CONTINUE
595 CONTINUE
596 CONTINUE
597 CONTINUE
598 CONTINUE
599 CONTINUE
600 CONTINUE

```

```
150 IF (IND-1) 160,155,160
155 IND=0
GO TO 50
160 (FTHB-AMRM) 165,165,155
165 DO 15X I=1,N
  10=I0+N
  LL=I*(I-1)/2
  J0=N*(I-2)
  DO 15X J=1,N
    30=J0+N
    MM=J*(I-1)/2
    J=(ALL)-AMMM1 170,165,165
170 X=(ALL)
    ALL=(AMM)
    AMM=I+J
    I=(MM-1) 175,165,175
    DO 15X K=1,N
      ILR=I0K
      IMR=J0K
      XR=(ILR)
      R(ILR)=R(IMR)
180 R(I0M)=X
185 CONTINUE
RETURN
END
SUBROUTINE LINERILL(C,LR1)
  DIMENSION LR(30),C(400)
  DO 20 I=1,LL
    CR(I)=I
  20 CONTINUE
  M=0
  DO 14 M=1,LL
    K=M
    DO 2 J=M+1,LL
      K1=M+J
      K2=M+K
      I=(ASC(C(K1))-ASC(C(K2))) 2/2,6
  4 K=I
  2 CONTINUE
  LS=LR(M)
  LR(M)=LR(K)
  LR(K)=LS
  K2=M+K
  I=ASC(C(K2))
  I1=J+LL
  J=CONTINUE
  K1=M+M
  I(K1)=I/250P
  DO 11 I=1,LL
    I1(I)=I2+11,12
  12 K1=M+I
    S=C(K1)
  14 CR(I)=0
  15X DO 10 I=1,LL
    K1=I+1
    K2=I+M
    CR(I)=CR(I1)+CR(K2)+S
  10 CONTINUE
  11 CONTINUE
  M=M+LL
  18 CONTINUE
  GO TO 4
  16 CR(M)=0
  17 CR(M)=11*LL
  21 DO 13 I=1,LL
    K2=J+I
    K1=I+I
    S=C(K2)
    CR(I)=CR(I1)
  13 CONTINUE
  CR(I)=S
  CR(I)=S+R(I,K)
  CR(I)=S+R(I,K)
  14 CR(I)=11*LL
  15 CONTINUE
  M=11*LL
  16 CONTINUE
  RETURN
END
```

```
//G0,VS14 DO *
G1,0000-05
DO
2*
//
```

B.3 listing of the program to compute generalised impedance elements

```
perpendicular polarizer(ON(T)).
//YULHANG JOB TOA49,1E,2,2,0001,7,CHANG,1,1,05,10N,250P,11,1,1,1
// FAPL,041FV
//001,10,0001 GO SYSDIRK
//G0,VS14 DO *
$JOB CHANG
SUBROUTINE FPIZ(FI,PI)
  Y=3.0/2
  F=0.78788454*(1-0.0000077+Y*(1-0.0055274+Y*(1-0.0000512+Y*(10,10)
  137237+Y*(1-0.0072805+Y*(0.0074676)))
  P=0.78588165*(1-0.1248812+Y*(1-0.0005450+Y*(10,0043749+Y*(1-0,00
  1472944+Y*(1,00029334-Y(0,000455)))
  R=I*Y
  END
SUBROUTINE FPIZ(FI,PI)
  Y=3.0/2
  F=0.78788454*(1+0.0000154+Y*(0.01659667+Y*(0.0001705+Y*(1-0.0024
  193114+Y*(0,0011365+Y*(0,0002003)))
  P=0.78588165*(1-0.1248812+Y*(1-0.0005450+Y*(10,0043749+Y*(1-0,00
  1072944+Y*(1-0.00029334+Y*(0.0002911+1)))
  RETURN
END
FUNCTION H5(J0K)
  I=(X,LL,0,0)H5(I1,101X
  H5=0,0
  I=(X,0,0,0)H5(I0M)
  Z=ASC(I)
  I=(Z,0,1,0)GO TO 1
  Y=2/2/0
  H5(I)=H5(I+Y*(1-2,2449987+Y*(1,2656208+Y*(1-0,1143644+Y*(10,0444479+Y
  1-0,0039444+Y*(0,000211)))
  RETURN
1 CALL FPIZ(FI,PI)
  H5=H5*(C(I)-PI)/SQRT(Z)
  RETURN
10 FORMAL(1) *WARNING - AN ARGUMENT OF 1,15,4,37,0045 BEEN DETECTED -
  LED IN CALCULATING A NEUMANN FUNCTION OF ORDER 7800 (X=1)
  END
FUNCTION H5(J0K)
  I=(X,LL,0,0)H5(I1,101X
  H5=0,0
  I=(X,0,0,0)H5(I0M)
  Z=ASC(I)
  I=(Z,0,1,0)GO TO 1
  Y=2/2/0
  H5(I)=H5(I+Y*(1-2,2449987+Y*(1,2656208+Y*(1-0,1143644+Y*(10,0444479+Y
  1,2656208+Y*(1,25300117+Y*(1-0,04261214+Y*(1,00029334+Y*(1,00029334
  2)))
  RETURN
1 CALL FPIZ(FI,PI)
  H5=H5*(I1-Z)/SQRT(Z)
  RETURN
10 FORMAL(1) *WARNING - AN ARGUMENT OF 1,15,4,37,0045 BEEN DETECTED -
  LED IN CALCULATING A NEUMANN FUNCTION OF ORDER 7800 (X=1)
  END
FUNCTION H5(J0K)
  I=(X,LL,0,0)H5(I1,101X
  H5=0,0
  I=(X,0,0,0)H5(I0M)
  Z=ASC(I)
  I=(Z,0,1,0)GO TO 1
  Y=2/2/0
  H5(I)=H5(I+Y*(1-2,2449987+Y*(1,2656208+Y*(1-0,1143644+Y*(10,0444479+Y
  1,2656208+Y*(1,25300117+Y*(1-0,04261214+Y*(1,00029334+Y*(1,00029334
  2)))
  RETURN
1 CALL FPIZ(FI,PI)
  H5=H5*(I1-Z)/SQRT(Z)
  RETURN
10 FORMAL(1) *WARNING - AN ARGUMENT OF 1,15,4,37,0045 BEEN DETECTED -
  LED IN CALCULATING A NEUMANN FUNCTION OF ORDER 7800 (X=1)
  END
SUBROUTINE HANK(IG)
  COMMON /J0M,0,4,2,5,6V
  COMMON /H5051,0,110631,1,13601,2,1001,1,1001,1,1001,1
  COMMON /I1201,111120,1,0,11944
  COMMON /I1621,11621,1,0,1621,1,1621,1,1621,1
  COMMON /I1651,1,1651,1,162
  P=3.141593
  P=2.071,141593
  N1=N2=1
  P=4.02,71828
  R=1.781072
  I=0
  DO 30 I=1,N1
  DO 40 J=1,N2
    I1=I+J
    I1=(I,0,1)GO TO 24
    I1=(I,0,1)AND, J,0, N2IG TO 24
    I1=(I,0,2)AND, J,0, N1IG TO 24
    H5(I1)=H5(I1)+I1
    H5(I1)=H5(I1)+I1
    H5(I1)=H5(I1)+I1
  GO TO 40
```







```

J1=0
DO 7 J=1,LL
K1=J+K
K2=J+M
S10=C(K1)
C(K1)=C(K2)
C(K2)=S10/S10R
J1=J+1
7 CONTINUE
K1=M+K
C(K1)=1./S10R
IF (J-1) 12,11,12
12 K1=M+1
S1=C(K1)
C(K1)=0.
J1=0
DO 10 J=1,LL
K1=J+1
K2=J+M
C(K1)=C(K1)-C(K2)*ST
J1=J+1
10 CONTINUE
11 CONTINUE
M1=M+LL
1A CONTINUE
J1=0
DO 9 J=1,LL
S1=C(J)
14 L=J+1
J1=J+1
21 DO 13 J=1,LL
K2=J+1
K1=J+1
S=C(K2)
C(K2)=C(K1)
C(K1)=S
13 CONTINUE
LW=C(J)*R(L*J)
LW1=C(L*J)
IF (J-1) 14,M,14
M J1=J+1
9 CONTINUE
RETURN
END
SUBROUTINE HANKIGK
COMPLEX C,J,M,MP,A,Z,Y,EV
COMMON DX(A2),DY(A2),DL(A2),XMA(A2),YMA(A2)
COMMON T1(Z0),T01(Z0),FV(A0),RR(1953)
COMMON H(1953),HF(1953),A(3A00),Z(1900),Y(1900),C,J
COMMON XP(A3),YP(A3),N2
P1=3.141593
P2=0.73141593
N1=N2+1
F1=A*P2*71A2A
FL=1.7A1072
I1=0
DO 30 J=1,M1
DO 40 I=1,J
I1=I+1

```

```

IF (I .EQ. 1) GO TO 25
IF (I .EQ. 1 .AND. J .EQ. N2) GO TO 25
IF (I .EQ. 2 .AND. J .EQ. N1) GO TO 25
KK=RR(111)*K
H(11)=RSJ(KK)-CJARSY(KK)
HF(11)=RHSJ(KK)-CJARSY(KK)
DO 31 0
25 CONTINUE
AA(1)=RHS*DL(11)/FF
H(11)=1./CJARSY(KK)
40 CONTINUE
30 CONTINUE
RETURN
END
SUBROUTINE CALZY(M,M1)
COMPLEX C,J,M,MP,A,Z,Y,EV
COMMON DX(A2),DY(A2),DL(A2),XMA(A2),YMA(A2)
COMMON T1(Z0),T01(Z0),FV(A0),RR(1953)
COMMON H(1953),HF(1953),A(3A00),Z(1900),Y(1900),C,J
COMMON XP(A3),YP(A3),N2
P1=3.141593
I1=0
L=0
DO 50 J=1,N2,2
J1=J-2
J2=J-1
J4=J+1
K=0
DO 60 I=1,N2,2
I1=I+1
I2=I-2
I4=I+1
Z1(1)=0.0
Y1(1)=0.0
DO 70 M=1,14
L1=M+L
DO 80 N=1,14
KK=N+K
I1=(M-N)100,120,120
100 J1=(N+(M-1))/2+M
GO TO 130
120 J1=(M+(M-1))/2+M
DO I=I0,1 .AND. N .EQ. N2) GO TO 150
IF (N .EQ. 2 .AND. M .EQ. N1) GO TO 150
GO TO 140
130 CONTINUE
HRR=H(I1,11)/RR(J1)
D1=DL(M)1(11)*T(KK)
C1=(X(M)-X(M1))/DY(N)+(Y(N)-Y(M))10X(N)
Z1(1)=0.25*C1*DDIT*HRR*GG*(Z+Z1(1))
GO TO 50
140 CONTINUE
80 CONTINUE
70 CONTINUE
Z1(1)=CJARSY(KK)
KK=K+2
60 CONTINUE
L=L+2
50 CONTINUE
RETURN

```

```

END
SUBROUTINE CALCIGK
COMPLEX C,J,M,MP,A,Z,Y,EV
COMMON DX(A2),DY(A2),DL(A2),XMA(A2),YMA(A2)
COMMON T1(Z0),T01(Z0),FV(A0),RR(1953)
COMMON H(1953),HF(1953),A(3A00),Z(1900),Y(1900),C,J
COMMON XP(A3),YP(A3),N2
N1=N2+1
I1=0
L=0
DO 50 J=1,N2,2
J1=J-2
J2=J-1
J4=J+1
K=0
DO 60 I=1,N2,2
I1=I+1
I2=I-2
I4=I+1
Z1(1)=0.0
DO 70 M=1,14
L1=M+L
DO 80 N=1,14
KK=N+K
I1=(M-N)100,150,120
100 J1=(N+(M-1))/2+M
IF (N .EQ. 1 .AND. N .EQ. N2) GO TO 150
IF (N .EQ. 2 .AND. M .EQ. N1) GO TO 150
GO TO 140
120 J1=(M+(M-1))/2+M
IF (N .EQ. 1 .AND. M .EQ. N2) GO TO 150
IF (N .EQ. 2 .AND. M .EQ. N1) GO TO 150
130 CONTINUE
HRR=H(I1,11)/RR(J1)
D1=DL(M)1(11)*T(KK)
C1=(X(M)-X(M1))/DY(N)+(Y(N)-Y(M))10X(N)
Z1(1)=0.25*C1*DDIT*HRR*GG*(Z+Z1(1))
GO TO 50
140 CONTINUE
80 CONTINUE
70 CONTINUE
Z1(1)=CJARSY(KK)
KK=K+2
60 CONTINUE
L=L+2
50 CONTINUE
RETURN
END
SUBROUTINE EXM1(PH1,GK1)
COMPLEX C,J,M,MP,A,Z,Y,EV
COMMON DX(A2),DY(A2),DL(A2),XMA(A2),YMA(A2)
COMMON T1(Z0),T01(Z0),FV(A0),RR(1953)
COMMON H(1953),HF(1953),A(3A00),Z(1900),Y(1900),C,J
COMMON XP(A3),YP(A3),N2
F1=A*376.730
N1=N2-1/2
CP=COS(PH1)

```

```

SP=SIN(PH1)
I1=0
L=0
DO 200 J=1,N2,2
I1=I+1
J1=J+M
I2=I-2
I4=I+1
FV(1)=0.0
FV1(J)=0.0
DO 210 M=1,14
L1=M+L
F1=(X(M)-X(M1))/DY(M)*SP*GK
H1=(X(M)-X(M1))/DY(M)*CP
CP=COS(PH)
SP=SIN(PH)
H1=(CP+CJARSY(KK))*I1(1)
FV(1)=H1*RR(1953)+FV(1)
FV(1)=H1*RR(1953)+FV(1)
210 CONTINUE
FV1(J)=CJARSY(KK)*F1
L=L+2
200 CONTINUE
RETURN
END
COMPLEX HED
COMPLEX A(1A0)
COMPLEX C,J,M,MP,A,Z,Y,EV
COMMON DX(A2),DY(A2),DL(A2),XMA(A2),YMA(A2)
COMMON T1(Z0),T01(Z0),FV(A0),RR(1953)
COMMON H(1953),HF(1953),A(3A00),Z(1900),Y(1900),C,J
COMMON XP(A3),YP(A3),N2
A1=0.0
A10=10.0
P1=3.141593
P2=1.0073141593
N1=N2-1
N2=N2-2
N=(N1-2)/2
N1=N
H1=1.0
F1=A*376.730
P1=3.141593/100.0
A1=0.0
GK=CJARSY(KK)*F1
H1=H1*F1
A1=0.7
H1=H1*GK
H1=H1*F1
N1=N2+M
H1=1.0
I1=100.0
GK=H1*GK*H1*GK
H1=H1*GK*H1
H1=H1*GK*H1
C1=CJARSY(KK)
H1=H1*GK*H1
P2=A*P1

```

```

AS-RO/9.0
SD=AS
DO B11 1=1.4
SG=SG+AS
XP(1)=SD
VP(1)=SG
#11 CONTINUE
SG=RD
DO A22 1=7.11
SG=SG-AS
XP(1)=SG
VP(1)=RD
A22 CONTINUE
J=11
DO A33 1=17.16
J=J+1
XP(1)=XP(J)
VP(1)=VP(J)
A33 CONTINUE
J=A
DO A44 1=17.21
J=J+1
XP(1)=XP(J)
VP(1)=VP(J)
A44 CONTINUE
J=21
DO A55 1=27.26
J=J+1
XP(1)=XP(J)
VP(1)=VP(J)
A55 CONTINUE
J=36
DO A66 1=27.36
J=J+1
XP(1)=XP(J)
VP(1)=VP(J)
A66 CONTINUE
J=24
DO A77 1=37.44
J=J+1
XP(1)=XP(J)
VP(1)=VP(J)
A77 CONTINUE
WRITE(3,4) (XP(J),VP(J)),J=1,NP)
DO 10 J=1,NP
  J=J+1
  DY(J)=XP(J)-XP(J-1)
  DV(J)=VP(J)-VP(J-1)
  DL(J)=SORT(DX(J),DY(J))
  XM(J)=0.5*(XP(J)+XP(J-1))
  VM(J)=0.5*(VP(J)+VP(J-1))
10 CONTINUE
WRITE(3,45)
45 FORMAT(1777777)
WRITE(3,4) (D(I),I=1,NP)
WRITE(3,45)
WRITE(3,4) (DY(I),I=1,NP)
WRITE(3,45)
WRITE(3,4) (DV(I),I=1,NP)
11=0

```

```

DO 30 J=1,NP
DO 40 I=1,J
I=I+1
IF(I.EQ.1)GOTO 25
IF(I.EQ.1)AND(J.EQ.NP)GOTO 25
IF(I.EQ.2)AND(J.EQ.NP)GOTO 25
XPO=XP(I)-XP(J)
YPO=VP(I)-VP(J)
RR(I)=SORT(XPO,XPO+YPO+YPO)
25 CONTINUE
40 CONTINUE
30 CONTINUE
L=0
DO 20 M=1,N2*2
M1=M-1
M2=M+1
M3=M-1
L1=M1+L
L2=M1+1
L3=L2+1
L4=L3+1
TL1=(XPO+DM1*(M1)/(DM1+DL(M2)))
TL2=(XPO+DM2*(M1)+XPO*(M2)/(DM2+DL(M1)+DL(M2)))
TL3=(XPO+DM3*(M1)+DL(M2))/(DM3+DL(M1)+DL(M4))
TL4=(XPO+DM4*(M2))/(DM4+DL(M3)+DL(M4))
TL5=(XPO+DL(M1)+DL(M2))
TL6=(L1)+TL(L1)
TL7=(L2)+TL(L2)
TL8=(L3)+1.0*(L1*(M3)+DL(M4))
TL9=(L4)+TL(L3)
L=L+2
20 CONTINUE
WRITE(3,45)
WRITE(3,4) (TL(I),I=1,NP)
M=M*2
CALL MANK(OR)
CALL CALCTIME(WIM)
K=0
L=0
M=24*NS*N
DO 500 J=1,N
DO 510 I=1,J
L=L+1
KK=K+1
I1=N1+L
AL1=I1*KK
AL2=I1*VM1
510 CONTINUE
L=L+N
KK=K+N
500 CONTINUE
CALL CALC(OR)
K=K+N
I1=N
DO 540 J=1,N
DO 550 I=1,N
KK=K+I
I1=I+K
AL1(1)=7*(KK)+AL1(1)
AL2(1)=Y(KK)+AL2(1)
550 CONTINUE
K=K+N

```

```

I1=I+K
540 CONTINUE
CALL MANK(OR)
CALL CALCTIME(WIM)
K=K+N
I1=N
DO 520 J=1,N
DO 530 I=1,N
KK=K+I
I1=I+K
AL1(1)=7*(KK)+AL1(1)
AL2(1)=Y(KK)+AL2(1)
530 CONTINUE
K=K+N
I1=N
520 CONTINUE
CALL CALC(OR)
K=K+N
I1=N
DO 540 J=1,N
DO 570 I=1,N
KK=K+I
I1=I+K
AL1(1)=7*(KK)+AL1(1)
570 CONTINUE
K=K+N
I1=N
540 CONTINUE
M=2*NS
L=0
DO 580 J=1,N
K=K+N
DO 590 I=1,N
KK=K+K
L=L+1
I1=L+K
AL1(1)=4*(KK)
KK=K+N
590 CONTINUE
L=L+N
600 CONTINUE
4 FORMAT(777.777.777.777.777.777.777.777.777)
CALL LIND(INH,A)
CALL EXMTAN(OR)
WRITE(3,45) (FV(J),J=1,NP)
WRITE(3,300)
300 FORMAT(1H *CURRENT TIME: (F10.6),X(10),F10.6),X(10),F10.6)
300 CONTINUE
270 CONTINUE
DO 30 J=1,NH
30 CONTINUE
DO 300 I=1,NH
300 CONTINUE
DO 300 J=1,NH
300 CONTINUE
CA=CARS(AL(1))

```

```

CPRNATAN2(I,MAG(AF(1)),REAL(AF(1)),PHASZ,PHAW)
WRITE(3,305) (I,AF(1)),CA,CPU
305 FORMAT(1H * (I2.2,F16.6,F10.4)
RD CONTINUE
WRITE(3,275)
275 FORMAT(777.7 SCATTERING ANGLE = PHASZ,PHAW,CPRNATAN2(I,MAG(AF(1)),REAL(AF(1)),PHASZ,PHAW)
AN=0.0
P5=K(OR)
DO 320 J=1,30
CALL EXMTAN(OR)
M=0.0
DO 330 J=1,NH
MH=FPV(I)+AF(I)+MH
330 CONTINUE
CH=CARS(MH)
ECHD=K(OR)M*2/4.0
ECL=K(OR)M*1/4.0
PH=K(OR)M
ECL=10.0*ECL+K(OR)M
WRITE(3,335) (AN,C1)
335 FORMAT(1H * (D2.2,F10.6,F16.6)
AN=AN*P5
320 CONTINUE
STOP
END
DATA
85TTP
//
//

```

8.5 Listing of the program to compute scattering cross sections  
from characteristic currents.

```

//YUCHANG JOB 10639,FF,2,2,9001,'CHANGY',REGION=180K,CLASS=A
// EXEC WATFIV
//DD,PT02001 DD SYSDIT=8
//DD,SYSIN DD *
$JOB      CMANG
SUBROUTINE EXMXP(MI,OK)
COMPLEX CJ
COMPLEX PP
COMPLEX VNI
COMPLEX AE,AJ,AV
COMMON AJ(400),AF(130),VN(130),EV(130),CJ
COMMON P(1900),T(100),DX(132),DY(132),XM(132),YM(132),DL(132)
COMMON N2,N,NM,JM
ETA=374.7501
N=(N2-1)/2
CP=COS(PHI)
SP=SIN(PHI)
I=0
L=0
DO 200 I=3,N2,2
  I1=I+1
  J1=I+M
  I2=I-2
  I3=I-1
  I4=I+3
  EV(I1)=0.0
  EV(J1)=0.0
  DI 210 M=I1,I4
  LL=M+L
  PP=(XM(M)*CP+YM(M)*SP)*OK
  PP=(DX(M)*SP+DY(M)*CP)
  C=PP/COS(PHI)
  SP=SP/SIN(PHI)
  PP=(CP*P+SP*EPI)*ILL
  EV(I1)=PP*EV(I1)
  EV(I2)=PP*DL(I2)+EV(J1)
210 CONTINUE
  EV(I1)=ETA*EV(I1)
  EV(J1)=CJ*EV(J1)
L=L+2
200 CONTINUE
RETURN
*MI
COMPLEX FC(130)
COMPLEX CAMD(130),VA(130)
COMPLEX VNI,CJ,MPD
COMPLEX AE,AJ,AV
COMMON AJ(400),AF(130),VN(130),EV(130),CJ
COMMON P(1900),T(100),DX(132),DY(132),XM(132),YM(132),DL(132)
COMMON N2,N,NM,JM

```

```

DIMENSION T(160),AMD(130)
DIMENSION XP(133),YM(133)
AM=12.0
A10=10.0
P1=3.141593
P4=180.0/3.141593
NP=33
N1=NP-1
N2=NP-2
N3=(N1-2)/2
N1=4*N
ML=1.0
E1=374.7501
P1=3.141593/180.0
ANS=0.0
OK=2.0/3.141593/ML
WF=GR/ETA
A1=0.7
A10=A1/GR
W10=GR*ETA
NM=2*N
EM=2.56
UR=1.0
GR=CONJ(I)*GR*GR
WF=WF*GR
W10=W10*GR
C1=(0.,1.)
PA=4*OK*P1
P2=ANS*P1
IME=TA=0.0
DI 5 I=1,NP
XP(I)=R)*COS(THETA)*ML
YP(I)=R)*SIN(THETA)*ML
IME=TA*TA*P2
5 CONTINUE
DI 10 J=1,N1
  J1=J+1
  DI 1 J1=XP(J1)-XP(J)
  DY(J1)=YP(J1)-YP(J)
  DL(J1)=SQRT(DX(J1)**2+DY(J1)**2)
  XM(J1)=0.5*(XP(J1)+XP(J))
  YM(J1)=0.5*(YP(J1)+YP(J))
10 CONTINUE
L=0
DO 20 M=3,N2,2
  M1=M3-2
  M2=M3-1
  M3=M3-1
  I1=M1+L
  I2=M1+1
  I3=L+2+1
  I4=L+3+1
  L4=L+3+1
  T(L1)=.5*(DL(M1)/DI(M1)+DL(M2))
  T(L2)=DL(M1)+.5*(DL(M2)+DL(M1)+DL(M2))
  T(L3)=DL(M1)+.5*(DL(M2)+DL(M1)+DL(M1)+DL(M2))
  T(L4)=.5*(DL(M2)/DI(M2)+DL(M1))
  DI(L1)=.7/DI(M1)+DI(M2)
  DI(L2)=DI(L1)
  DI(L3)=1.0/DI(M1)+DI(M2)
  DI(L4)=DI(L1)

```

```

L=L+2
20 CONTINUE
101 FORMAT(9F15.7)
READ(1,201) JM
201 FORMAT(I3)
WRITE(4,201) JM
N1=JM*NM
READ(1,101) (AM(I),I=1,JM)
N=AD(1,101) (FC(I),I=1,JM)
READ(1,101) (FC(I),I=1,N1)
WRITE(4,202) (AM(I),I=1,JM)
WRITE(4,101) (FC(I),I=1,JM)
WRITE(4,203) (FC(I),I=1,N1)
202 FORMAT(10F16.4/10F16.4/16F16.7)
203 FORMAT(10F16.4/10F16.4/16F16.7)
DO 50 J=1, JM
  J1=(J-1)*NM
  DO 60 I=1, N
    I1=J1+I
    P(I1)=P(I1)/777.0
60 CONTINUE
90 CONTINUE
CALL EXMXP(ANS,OK)
LL=0
DI 100 I=1, JM
  VN(I)=0.0
  DI 110 J=1, NM
  L=L+L
  VN(I1)=EV(J1)+P(I1)+VN(I1)
110 CONTINUE
LL=LL+NM
100 CONTINUE
  DO 210 I=1, JM
  VA(I)=VN(I)+FC(I)
210 CONTINUE
  LL=NM
  DI 220 I=1, JM
  LL=LL+NM
  DI 225 J=1, NM
  L=L+L+J
  A(JL)=VA(I)*P(I)
225 CONTINUE
220 CONTINUE
  DI 230 I=1, NM
  AF(I)=0.0
  DI 235 J=1, JM
  K=(J-1)*NM+I
  AF(I)=AF(I)+A(K)
235 CONTINUE
230 CONTINUE
  WRITE(4,275)
275 FORMAT(//'/ SCATTERING ANGLE = PHI=(DY,1.00018N/DX)ARCTAN(1.00018N/DX)
  AN=0.0
  PPA(OKP)
  DI 320 I=1,36
  CALL EXMXP(ANS,OK)
  ME=0.0
  DI 330 I=1, NM
  ME=ME+V(I)*AF(I)+P(I)
330 CONTINUE
  STOP
  END

```

```

$DATA
18
$STOP
/0
//

```

## REFERENCES

1. R. J. Garbacz, "A Generalized Expansion for Radiated and Scattered Fields," Ph.D. Dissertation, Ohio State University, Columbus, 1968.
2. R. F. Harrington and J. R. Mautz, "Theory of Characteristic Modes for Conducting Bodies," IEEE Trans. on Antennas and Propagation, vol. AP-19, No. 5, September 1971.
3. R. F. Harrington and J. R. Mautz, "Computation of Characteristic Modes for Conducting Bodies," IEEE Trans. on Antennas and Propagation, vol. AP-19, No. 5, September 1971.
4. R. F. Harrington, J. R. Mautz, and Y. Chang, "Characteristic Modes for Dielectric and Magnetic Bodies," IEEE Trans. on Antennas and Propagation, vol. AP-20, No. 2, March 1972.
5. R. F. Harrington, Field Computation by Moment Methods, New York: Macmillan, 1968.
6. R. F. Harrington, Time-Harmonic Electromagnetic Fields, New York: McGraw-Hill, 1961.
7. G. T. Ruck, D. E. Barrick, W. D. Stuart, and C. K. Krichbaum, Radar Cross Section Handbook, vol. 1, New York: Plenum Press, 1970.
8. J. R. Mautz and R. F. Harrington, "Radiation and Scattering from Bodies of Revolution," Appl. Sci. Res., vol. 20, June 1969.
9. R. F. Harrington and J. R. Mautz, "Radiation and Scattering from Loaded Bodies of Revolution," Appl. Sci. Res., vol. 26, 1971.
10. R. F. Harrington and J. R. Mautz, "Control of Radar Scattering by Reactive Loading," IEEE Trans. on Antennas and Propagation, vol. AP-20, No. 4, July 1972.
11. R. F. Harrington and J. R. Mautz, "Modal Analysis of Loaded N-port Scatterers," Scientific Report No. 16 on Contract No. F19628-68-C-0180 between Syracuse University and Air Force Cambridge Research Laboratories, AFCRL-72-0179, March 1972.
12. R. F. Harrington and J. R. Mautz, "Synthesis of Loaded N-port Scatterers," Scientific Report No. 17 on Contract No. F19628-68-C-0180 between Syracuse University and Air Force Cambridge Research Laboratories, AFCRL-72-0665, October 1972.
13. R. F. Wallenberg and R. F. Harrington, "Radiation from Apertures in Conducting Cylinders of Arbitrary Cross Section," IEEE Trans. on Antennas and Propagation, vol. AP-17, No. 1, Jan. 1969